Norwegian University
of Life Sciences

Master's Thesis 2022 60 ECTS
Faculty of Chemistry, Biotechnology and Food Science

Development of a CRISPR/Cas9 Editing System for Antigen Knock-In in *Lactiplantibacillus plantarum* WCFS1

Lisa Kaasbøll Haugen
Master of Science in Biotechnology

Acknowledgment

The work presented in this thesis was carried out at the Faculty of Chemistry, Biotechnology and Food science of the Norwegian University of Life Sciences, supervised by Dr. Geir Mathiesen, Ph.D. candidate Kamilla Wiull and Professor Vincent Eijsink as supervisors.

First, I would like to thank my main supervisor Geir Mathiesen for all the good advice, patience and meaningful discussions. I am truly grateful for the opportunity to learn so much from you. Kamilla, it has meant so much to me that you have always been available, answering my questions, and not least, motivating me through this period. I would also like to thank Steffen for all the good times inside and outside the lab, it has been a pleasure. Further, I would like to thank everyone in the PEP-group, it has been a privilege to work with so many knowledgeable and inspiring people.

Lastly, I will be forever grateful to Mathias, my family and friends for uplifting me through this year, motivating and empowering me to do better.

Ås, May 2022

Lisa Kaasbøll Haugen

Abstract

Lactic acid bacteria (LAB) have been used in food products for hundreds of years and are commonly used in food fermentation, therapeutics, and for health promotion. They are "Generally Recognized as Safe", have excellent stress tolerance to harsh environments and have proven to provoke the innate and adaptive immune system. These traits make LAB promising candidates as adjuvants and vectors for antigen delivery at mucosal sites. Considering the significant potential LAB holds in the industrial and medical field, the CRISRP/Cas9 tool should be implemented for use in LAB to facilitate scarless genetic manipulation. Since its discovery in 1987, Clustered Regularly Interspaced Short Palindromic Repeat (CRISPR) loci and their associated Cas9 endonucleases have transitioned from a prokaryotic immune system to a revolutionary tool for genome editing in eukaryotes. However, due to challenges and lack of methods, the state-of-art CRISPR/Cas9 has limited use in bacteria today.

This study will try to solve some of the challenges encountered in CRISPR/Cas9 genome editing in bacteria and aims to develop a CRISPR/Cas9 knock-in system for use in *Lactiplantibacillus plantarum* WCFS1. The ultimate goal is to anchor the receptor binding domain (RBD) of SARS-CoV-2 to the cell surface of *L. plantarum* WCFS1, as a prototype for a SARS-CoV-2 mucosal vaccine. As a proof-of-concept, the goal was to insert the RBD fragment into the genome of *L. plantarum* WCFS1.

Four necessary components for establishing CRISPR/Cas9 knock-in in bacteria; sgRNA, SpCas9, a donor repair template and a recombinase machinery, were assembled on a two-plasmid system. The CRISPR/Cas9 knock-in system I successfully inserted RBD into the genome of *L. plantarum* WCFS1. Optimalization of the knock-in system was attempted to increase efficiency and insert larger fragments (>800 bp). Yet, the CRISPR/Cas9 knock-in system referred to as system II, failed to yield knock-ins. The production of cytoplasmatic antigen from the *L. plantarum* WCFS1 knock-in strain of RBD was confirmed by Western blot. To compare genomic and plasmid-based cytoplasmatic production of RBD a pSIP vector was constructed. Characterization of the genomic, inducible expression of RBD indicates low production of RBD compared to the plasmid.

Sammendrag

Melkesyrebakterier har blitt brukt i matprodukter i flere hundre år og blir anvendt i matfermentering og terapeutiske midler med helsefremmende effekter. De er generelt ansett som trygge, har utmerket stresstoleranse i ulike miljøer og kan stimulere det medfødte og adaptive immunforsvaret. Slike egenskaper gjør melkesyrebakterier til lovende kandidater som adjuvanter og vektorer for levering av antigener til slimhinner. Med tanke på potensialet til melkesyrebakterier innenfor industri og medisin, burde CRISPR/Cas9 verktøyet bli implementert i melkesyrebakteriefamilien for å muliggjøre genetisk manipulasjon uten avtrykk. Siden oppdagelsen av clustered regularly interspaced palindromic repeat (CRISPR) i 1987, har deres lokus og assosierte Cas9 endonukleaser gått fra å være et immunsystem i prokaryote organismer, til et revolusjonerende system for genmodifisering av eukaryoter. Likevel har mangel på metoder og andre hindringer ført til at CRISPR/Cas9 har begrenset bruk i bakterier i dag.

Målet med denne studien er å løse noen av utfordringene til CRISPR/Cas9 genmodifisering i bakterier, samt å utvikle et CRISPR/Cas9 knock-in system for bruk i *Lactiplantibacillus plantarum* WCFS1. Hovedmålet er å ankre det reseptor bindende domenet (RBD) til SARS-CoV-2 i cellemembranen til *L. plantarum* WCFS1 som en prototype for en SARS-CoV-2 slimhinnevaksine. For å bevise CRISPR/Cas9 mediert genomeditering, var målet å sette inn RBD fragmentet i genomet til *L. plantarum* WCFS1.

Fire nødvendige komponenter for å etablere CRISPR/Cas9 knock-in i bakterier ble satt sammen i et to-plasmid-system: sgRNA, SpCas9, et donor reparerings templat og et rekombinase maskineri. CRISPR/Cas9 knock-in system I førte til vellykket innsetting av RBD i genomet til *L. plantarum* WCFS1. For å øke effektiviteten og sette inn større fragmenter (>800 bp), ble det forsøkt å optimalisere system I. CRISPR/Cas9 system II klarte ikke å skape noen knock-in. Produksjonen av cytoplasmatisk antigen fra *L. plantarum* WCFS1 knock-in stammen med RBD ble bekreftet med Western blot. En pSIP vektor ble konstruert for å sammenlikne genomisk og plasmidbasert cytoplasmatisk produksjon av RBD. Karakterisering av induserbar genomisk uttrykk av RBD, indikerer lav produksjon av RBD sammenliknet med plasmidproduksjonen.

Abbrevations

ACE-2	Angiotensin-Converting Enzyme 2
BSA	Bovine Serum Albumin
CRISPR	Cluster Regulatory Interspaced Short Palindromic Repeats
crRNA	CRISPR RNA
DC	Dendritic Cell
dNTP	Deoxyribonucleotide Triphosphate
dsDNA	Double-stranded Deoxyribonucleic Acid
DSB	Double-Strand Break
GI	Gastrointestinal
GRAS	Generally Recognised As Safe
HDR	Homology Directed Repair
KI	Knock-In
LAB	Lactic Acid Bacteria
NHEJ	Non-Homologous End Joining Pathway
PAM	Protospacer Adjacent Motif
PCR	Polymerase Chain Reaction
RBD	Receptor Binding Domain
SARS-CoV-2	Severe Acute Respiratory Syndrome Coronavirus 2
SDS-PAGE	Sodium Dodecyl Sulphate Polyacrylamide gel
SgRNA	Single guide RNA
TALEN	Transcription Activator-Like Effector Nucleases
tracrRNA	Trans-activating crRNA
ZFN	Zinc-Finger Nucleases

Table of contents

Development of a CRISPR/Cas9 editing system for antigen knock-in in *Lactiplantibacillus plantarum* WCFS1

1 Introduction

Lactic acid bacteria (LAB) have been used in food products for thousands of years and commonly used in food fermentation, therapeutics, and health promotion. They are "Generally recognized as safe" (GRAS), have excellent stress tolerance to harsh environments and have proven to provoke the innate and adaptive immune system. This also makes the bacteria a promising candidate as an adjuvant and vector for antigen delivery at mucosal sites. When working with bacteria, genome editing is the core operation for developing a microbe that can express modulated biochemicals.

Over the last two decades, clustered regularly interspaced short palindromic repeat (CRISPR) loci and their associated Cas9 endonucleases have transitioned from a prokaryotic immune system to a revolutionary tool for genome editing in eukaryotes. CRISPR/Cas9 is easily guided to direct double stranded break (DSB) at the genome, thus allowing for genomic modifications such as mutations, knock-out of genes, and insertion of genes. However, due to lack of methods the state-of-art CRISPR/Cas9 has a limited use in prokaryotes. Considering the significant potential LAB holds in the industrial and medical field, the CRISRP/Cas9 tool should be implemented for use in LAB to facilitate scarless genetic manipulation.

1.1 Lactic acid bacteria

Lactic Acid Bacteria (LAB) is a superfamily of Gram-positive, non-sporing, facultative anaerobic bacteria that ferment carbohydrates into lactate (Kandler, 1983; Kwok, 2014). They are usually found in plants, meat, dairy, fermented foods and mucosal surfaces of mammals such as the small intestine, colon and vagina (Carr et al., 2002; Hammes & Tichaczek, 1994; König & Fröhlich, 2009; Kwok, 2014; Makarova et al., 2006; Sun et al., 2014).

For the last thousands of years, LAB have been used in food products (Gareau et al., 2010). Thus, they have accomplished the status GRAS by the European Food Safety Authority, except for a few pathogenic bacteria (Zhang & Zhang, 2014). Recent studies also uncover the

significance of LAB in disease genesis and behaviour (Lozupone et al., 2012; Milani et al., 2017). The bacteria produce vitamins, and prevent infections caused by intestinal pathogens (Markowiak & Ślizewska, 2017). LAB are a dominant probiotic used in food (Klaenhammer et al., 2008; Kleerebezem et al., 2010; Makarova et al., 2006; Markowiak & Ślizewska, 2017). Probiotics, stated by the World Health Organization (WHO), are living microorganisms which confer a health benefit to the host, when administered in adequate amounts. Some products of probiotic metabolism may even show antimicrobial, anti-carcinogenic and immunosuppressive properties

1.1.1 *Lactiplantibacillus plantarum*

Lactiplantibacillus plantarum (*L. plantarum*), formerly known as *Lactobacillus plantarum*, has been widely used as a model species for studies in lactobacilli. This specie is a versatile LAB known for surviving harsh environments in the gastrointestinal tract (GIT) such as acidic pH, bile salts and proteolytic enzymes (Hammes & Tichaczek, 1994). Recent studies also indicate excellent stress tolerance (Huang et al., 2019; Oozeer et al., 2006). Perhaps the most interesting potential of *L. plantarum* is the immunomodulatory effects. Different strains of *L. plantarum* have shown to skew either pro- or anti- inflammatory immune responses (Goldstein et al., 2015; Mohamadzadeh et al., 2005; Villena et al., 2021). All this makes *L. plantarum* an ideal candidate as an adjuvant and a delivery vector for immunogens to mucosal sites.

In 2003, the complete genome of *L. plantarum* WCFS1 was sequenced by Kleerebezem et al. (2003). The strain exhibits a large genome and many regulatory and transport functions, which explains the flexibility and adaptivity of *L. plantarum* (Kleerebezem et al., 2003). Due to the beneficial prospects of *L. plantarum*, development of feasible CRISPR/Cas9 knock-in of antigens is highly desirable and will contribute to uncover the potential of *L. plantarum*.

1.2 History and mechanisms of the CRISPR/Cas9 genome editing system

Ever since the DNA double helix was uncovered in the late 1950s, technologies to precisely edit the genomic material have been highly desired among scientists (Doudna & Charpentier, 2014). Discoveries in the last three decades have made effective genome editing feasible through techniques including mega nucleases, Zinc fingers (ZFN), transcription activator-like effector nucleases (TALEN), and most importantly, the Clustered Regularly Interspaced Short Palindromic Repeat (CRISPR) Cas9 complex.

In the beginning, rare endonucleases and mega nucleases were used to induce cuts in the genome of mammalian cells for genome editing (Adli, 2018; Paques & Duchateau, 2007).

Unfortunately, the mega nucleases are restricted to a few hundred naturally acquired endonucleases, meaning that the likelihood of finding a mega nuclease targeting the desired locus is low (Adli, 2018). The discovery of the Clustered Regularly Interspaced Short Palindromic Repeat (CRISPR) and its associated nucleases, Cas9, in 1987 was a revolution. CRISPR/Cas9 led to easy genomic modification in eukaryotes and widespread adaptation of the tool to science communities because of its fast, efficient and accurate genetic modifications such as insertion and deletion at particular locations in the genome.

The CRISPR system was discovered to be an adaptive immune system in bacteria and archaea, against intruding plasmids and RNA/DNA from bacteriophages (Doudna & Charpentier, 2014; Leenay & Beisel, 2017). The system consists of two components: The Cas9 effector protein and the CRISPR array. The CRISPR array is a short stretch of DNA composed of alternating conserved repeats and target-specific spacers (Leenay & Beisel, 2017), and can uniquely recognize foreign sequences. Each spacer is acquired from a fraction of the foreign genetic material, allowing the CRISPR array to hold a heritable memory of the infection (Mojica et al., 2005). The system works by recognizing and cutting foreign nucleotides. This adaptive immune system is achieved through i) adaptation, ii) expression and iii) interference (Zhang et al., 2020, Figure 1.1).

i) First, adaptation leads to insertions of new sequences, called spacers, into the CRISPR array.

ii) In the second stage, expression occurs by transcription of the CRISPR array into long precursor CRISPR RNAs (pre-crRNA), followed by processing of the pre-crRNA by accessory proteins and Cas9, into mature crRNA (Rath et al., 2015). These crRNA associate with the Cas9 effector protein to form a ribonucleoprotein surveillance complex used to search the genome for protospacer adjacent motifs (PAM) (Leenay & Beisel, 2017). PAM is essential for the attachment of Cas9 to the genome, as the effector molecule rapidly detached from the DNA without the PAM sequence (Doudna & Charpentier, 2014; Ghavami & Pandi, 2021; Lone et al., 2018). (Adli, 2018). The sequence varies from different species-derived effector proteins, and more than 10 CRISPR/Cas9 proteins have been found (Adli, 2018). E.g., the Cas9 protein from *Streptococcus pyogenes*, SpCas9 has a 5`-NGG-3` PAM

iii) Lastly, in the interference stage, targeted nucleic acid is recognized and destroyed by the combined action of crRNA and Cas proteins (Rath et al., 2015). Upon binding, the complex interrogated the extent of base pairing between the

downstream sequence and the spacer sequence of the crRNA. Extensive base pairing results in a conformational change in Cas9 that cleaves the target sequence, causing a cleavage of the foreign DNA (Leenay & Beisel, 2017).

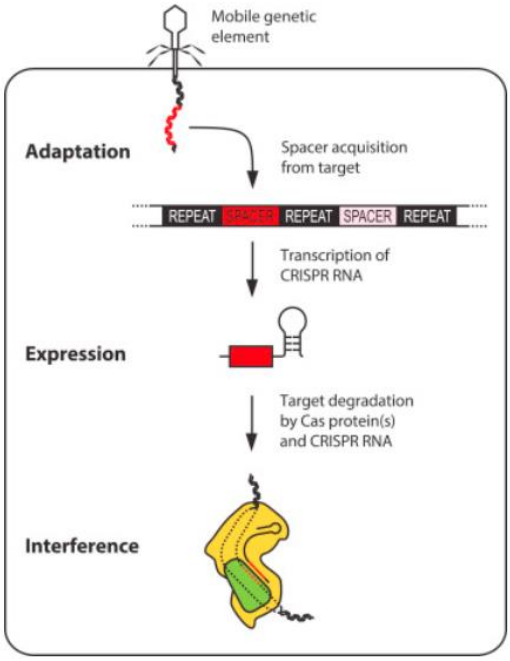

Figure 1.1 The CRISPR/Cas9 is a defence system. Adaptive immunity is acquired by three steps: i) adaptation, ii) expression and iii) interference (D. Zhang et al., 2020). i) Adaptation is achieved via the insertion of nucleotides, called the spacer, into the CRISPR locus. ii) Expression occurs by transcription of the CRISPR locus into long precursor CRISPR RNA (pre-crRNA) and then processing of the pre-crRNA by accessory proteins and Cas9 into mature crRNA (Rath et al., 2015). iii) Interference is detection and degradation of the intruding nucleotide sequence by the mature crRNA which is attached to the Cas9 protein. The Cas9 protein undergoes a conformational change and cleaves the intruder strand (Rath et al., 2015). The figure is taken from Rath et al., (2015).

The most used scheme divides the system into two classes, six types and 19 subtypes (Leenay & Beisel, 2017; Zhang et al., 2020). The two classes are differentiated by the effector protein (the enzyme used for interference, Figure 1.2). Class 1 consists of effector proteins working in a cascade, while the class 2 systems only contain one protein. The six types (I-VI) are defined by a signature protein responsible for nucleic-acid cleavage (e.g., Cas3 for type I, Cas9 for type II). Class 1 has the subtypes I, III and IV, while class 2 consists of subtype II, V and VI. Type I, II and V targets DNA, type VI targets RNA, and type III cuts both DNA and RNA (D. Zhang et al., 2020). Due to the function of DNA cleavage and the simplicity of one effector molecule, Cas9 is the most and best studied effector protein to date (Zhang et al., 2020). That is why class 2, type II, have become the desirable choice for the development of novel genome editing

technology.

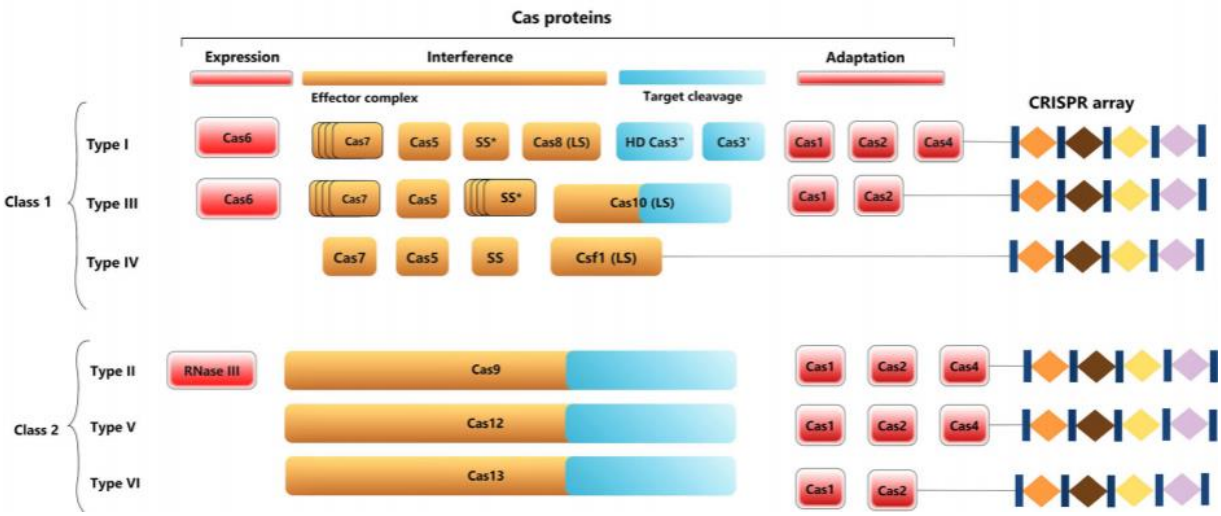

Figure 1.2 Classification and subtypes of the CRISPR/Cas9 system. The CRISPR/Cas9 systems are divided into two classes. Class 1 consists of a set of effector proteins working in a cascade, whilst class 2 systems only contain one protein. Each class contains three subtypes, class 1 has the subtypes I, III and IV, while class 2 has subtype II, V and VI. Type I, II and V targets DNA, while type VI targets RNA, and type III cuts both DNA and RNA (D. Zhang et al., 2020). The cuts are preformed blunt, but interestingly, the Cpf1 effector protein, from subtype IV, cuts ds DNA in a staggered way (Adli, 2018). The figure is taken from D. Zhang et al., (2020).

1.2.1 The use of CRISPR/Cas9 for genome editing

The defense system of the bacteria has been adapted by scientists for DNA editing. By creating a small piece of RNA with a "guide" sequence which anneals to a specific target sequence in the genome, scientists can easily design the single guide RNA (sgRNA) to target any place in the genome. Once the DNA is cut, one can use the cell's own DNA repair machinery to insert (knock-in), delete (knock-out) or create indels in the genome.

Cas9 is guided by an approximately 20- nucleotide long guide sequence within an RNA tracrRNA-crRNA duplex, referred to as sgRNA (Jinek et al., 2012; D. Zhang et al., 2020). The 5`-end of the sgRNA determinates the DNA target site, by Watson-crick base pairing, and the 3`-end forms a stabilizing interaction with the Cas9 enzyme (Doudna & Charpentier, 2014, Figure 1.3). Changes in the sgRNA sequence leads the Cas9 to target any DNA sequence of interest. At the target site, the two catalytic centers in the Cas9 enzyme, the HNH and RuvC-like nuclease domains, will cut the target and non-target DNA strand, respectively (Jinek et al., 2012; Rath et al., 2015; Zhang et al., 2020), resulting in a DSB (Figure 1.3). Easy synthesis and manipulations of the sgRNA (Jinek et al., 2012) makes the CRISPR/Cas9 complex a great tool for generating a DSB in the DNA, thus also an initiator for genome editing.

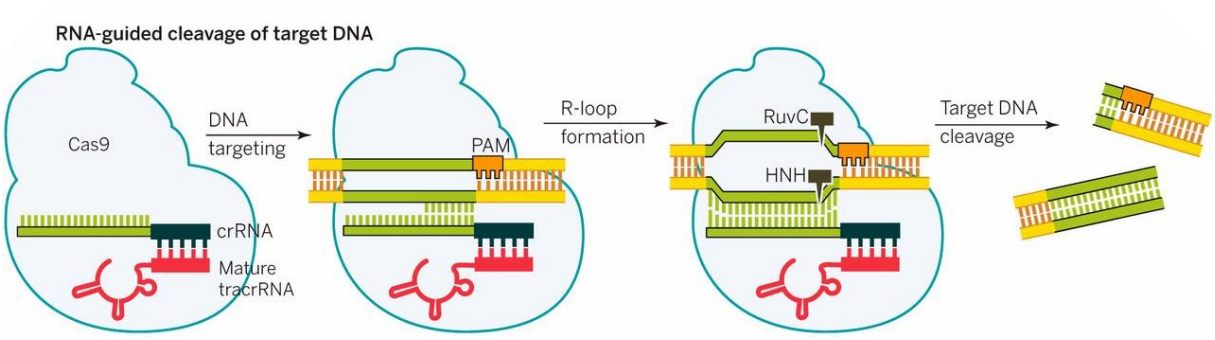

Figure 1.3 Function of the type II, CRISPR/Cas9 complex. The figure shows RNA-guided cleavage of target DNA. The Cas9 enzyme associates with the sgRNA (tracrRNA:crRNA duplex) and is led to a matching complement target sequence. Recognizing of matching sequence and PAM site will generate a conformational change in the HNH and RuvC-like catalytic domains of the Cas9, generating a blunt DSB 3 bp upstream of PAM site, resulting in cleavage of intruding DNA (Doudna & Charpentier, 2014). The figure is taken from Doudna & Charpentier, (2014).

A DSB in the DNA is lethal for any cell and will therefore trigger cellular repair pathways. The DNA repair machinery can either initiate error prone non-homologous end joining (NHEJ) or homology-directed repair (HDR, Figure 1.4). NHEJ is the predominant pathway in eucaryotic cells, and results in random indels and gene disruptions at the target site. Because the indels may lead to frameshift mutations, this pathway can be utilized to knock out genes. The HDR pathway can insert a gene at the target site and is the preferred pathway in bacteria. The insert of a gene of interest at a specific site relies on HDR and uses a homologous template to repair DSBs (Figure 1.4). Consequently, efforts have been made to inhibit NHEJ or enhance HDR to favor site-specific insertion of new genetic information by HDR.

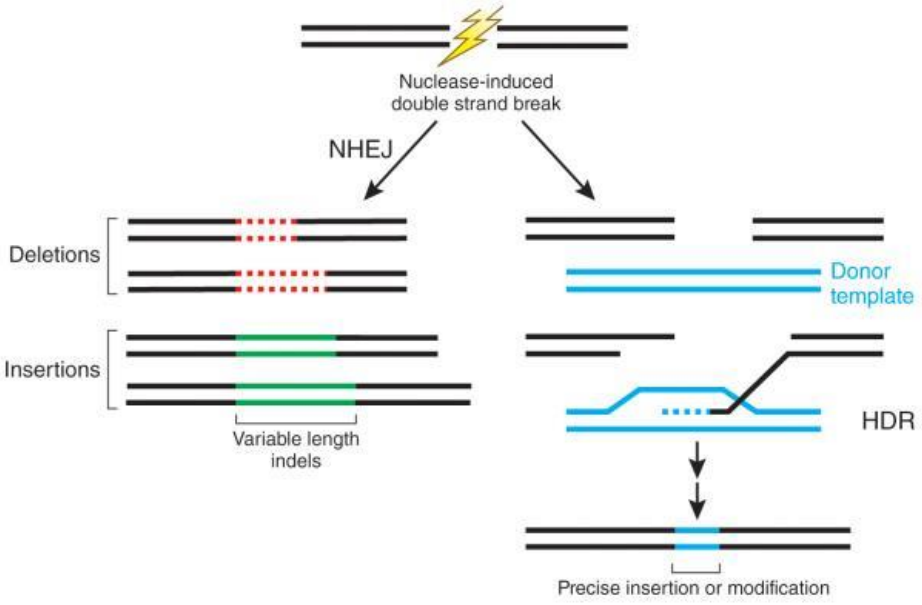

Figure 1.4. Cellular repair pathways. Cas9 is a nuclease used in biotechnology to cleave DNA and induce genome manipulation. When genomic DNA undergoes a DSB, the cell stops dividing. An organism is dependent on cell division for growth and survival; thus, the cell must be repaired. Two repair pathways for DSBs are known, the NHEJ and the HDR. NHEJ repair can generate random variable-length insertions (shown in green) or deletions (shown in red) at DSB site, whilst HDR- mediated repair pathway can insert precise point mutations or insertions from a donor ds or ss template (shown in blue) (Sander & Keith Joung, 2014). The figure is taken from Sander & Joung, (2014).

Today, the CRISPR/Cas9 system is a revolutionary tool for genome editing in the fields of biomolecular research, agriculture, biotechnology, and medicine (Adli, 2018; Barrangou et al., 2007; Doudna & Charpentier, 2014; Hsu et al., 2014; Jinek et al., 2012; Leenay & Beisel, 2017). Yet, the current state-of-the-art CRISPR/Cas9 editing tool is less explored in prokaryotes and are facing a lot of challenges when used in bacteria.

1.3 CRISPR/Cas9 genome editing in bacteria

CRISPR/Cas9 is heavily used in eukaryotes, but raises challenges and difficulties in prokaryotes. When working with bacteria, genome editing is one of the core operations. This enables scientists to study the genetic basis of their physiological and metabolic traits or to develop a next generation microbe expressing modulated biochemicals or even a wide array of synthetic genes (Arroyo-Olarte et al., 2021a). Even though genome editing is beneficial for enhancing chemical production in industrial bacteria, CRISPR/Cas9 has been slow to extend to the multitude of industrially relevant bacteria (Vento et al., 2019). Traditional genome-editing approaches do exist (Berg et al., 2011; Li et al., 2013; Liu et al., 2003). However, genome editing without introducing a scar or antibiotic markers makes genome editing with CRISPR

advantageous over previous methods. Currently, no standard protocol for CRISPR/Cas9 knock-in exists (Vento et al., 2019), and its utilization in bacteria remains limited and ineffective for most bacteria.

CRISPR/Cas9 systems have been used to achieve highly efficient genome editing in some stains. CRISPR/Cas9 editing in the gram-negative *Escherichia coli* have successfully yielded gene deletions, mutations, and insertions. D. Zhao et al. (2016) provided a recombination strategy based on the coupling of the CRISPR/Ca9 and the lambda-red (λ) system (D. Zhao et al., 2016). The λ-red system includes three phage-derived proteins, Exo, Beta and Gam, that are necessary for carrying out dsDNA recombination in *E. coli* (Mosberg et al., 2010). J. Zhao et al. (2020) co-transformed one plasmid containing Cas9, a donor repair template and a second plasmid containing the λ-red system into *E. coli*. The findings demonstrated that Cas9 works with λ-red recombinase in *E. coli* to efficient generate small insertions or deletions through HDR (J. Zhao et al., 2020). The study indicates that the CRISPR/Cas9 editing in bacteria can depend on upregulation of a recombinase in order to edit the genome of the bacteria.

To perform precise knock-in through HDR, an insertion sequence, e.g., a template containing mutations or a heterologous gene, must have a sequence homologous to the genome (HA) upstream and downstream of the sgRNA target sequence. HA is used as a template for homologous recombination. Followed by a successful repair attempt, anything between the HA will consequently be inserted in the genome, although this is size limiting. After knock-in of the gene of interest into the genome, the PAM sequence is altered, thus preventing DSB by Cas. The cleavage of unedited cells will serve as a strong beneficial counterselection, but for most prokaryotes the system is cytotoxic and often fails to yield mutants.

There are many reasons for an ineffective CRISPR/Cas9 system in prokaryotes. Firstly, the system displays toxicity in many prokaryotes (Ramachandran & Bikard, 2019). The CRISPR/Cas9 genome editing relies on repair mechanisms in the cell. In eukaryotes the cell repairs their break by HDR or NHEJ, thus enabling the cell to survive. In bacteria, the CRISPR/Cas9 DSB tends to be lethal, resulting in mass distinction instead of genome editing. The reason is that most bacteria do not express an efficient repair system like most eukaryotes. Recombinases, that are essential for HDR, are usually fairly expressed and NHEJ are not prevalent in prokaryotes (Lieber, 2010). In addition, the Cas9 enzyme has shown cytotoxicity. The toxicity leads to fatal chromosome breaks, low transformation efficiency and failure in gene editing. Both endogenous and exogenous CRISPR/Cas9 system targeting the chromosome

have been shown to be lethal for the bacteria. Another reason why CRISPR/Cas9 is not implemented as a genomic editing tool in prokaryotes, is that once a method for CRISPR/Cas9 genome editing is established for a specific specie, the method is mainly restricted to that species. There have been reported wide differences among the prokaryotes, even within the same species. CRISPR/Cas9 editing efficiency varies among the strains, this means that the editing system needs to be modified between strains.

Recently, Huang et al. (2019) found that by overexpressing *L. plantarum* homologous recombinases, as well as providing a homology repair template the bacteria can perform HDR (Huang et al., 2019). Yang et al. (2015) identified an exonuclease encoded by the gene *lp_0642* and a host nuclease inhibitor, encoded by *lp_0640* in *L. plantarum* WCFS1. They discovered that these two proteins alongside a single stranded annealing protein encoded by lp_0641 could perform homologous recombination between a heterologous dsDNA substrate and host genomic DNA. Thus, this system is homologous to the three lambda proteins, Exo, Beta and Gam. Huang, Song and Yang (2019) implemented these three proteins for assisted recombination repair and found that the implementation of the recombinases can rescue the lethality caused by CRISPR/Cas9-induced DSBs in *L. plantarum* WCFS1.

1.4 Gene expression systems in *L. plantarum*

For applications *in vivo*, or in biotechnological processes, the antigen expression level is crucial, as expression should be of a certain level, but without causing too much stress to the bacteria. Some of the key factors for control of gene expression are choice of promoter, promoter strength and copy number for the plasmid-based systems (Tauer et al., 2014).

Protein production can be controlled via inducible or constitutive promoters. Both have their advantages and disadvantages., an inducible system can be beneficial for overproduction of heterologous proteins if the target proteins are toxic to the host (Tauer et al., 2014). An inducible expression system will allow initial growth of the bacteria before activation of the expressed protein, which can decrease toxicity. Genes that are expressed with an inducible system allows for regulation by additives, such as various carbohydrates, pH or temperature (Kuipers et al., 1997). In recent years, vectors have been developed for high inducible gene expression in *L. plantarum*, so-called “pSIP” vectors (Mathiesen et al., 2004; Sørvig et al., 2003).

The pSIP expression system is a one-plasmid inducible system based on the autoregulatory properties (quorum-sensing) for production of bacteriocins in LAB (Axelsson et al., 2003; Sørvig et al., 2003, Figure 1.5). The constructed plasmids consist of a histidine kinase receptor

(SppK), which is activated by an inducer pheromone (SppIP) and a cognate response regulator (SppR). The original genes encoding the SppIP have been deleted in the expression cassettes, thus SppK can only be switched on by an externally added SppIP. The vector has been modulated, permitting easy exchange of all parts of the cassette through restriction-enzyme digestion and ligation. A gene of interest is easily fused to the inducible P_{sppA} promoter, which also is controlled by adding SppIP. The pSIP-system has further been modified for secretion and anchoring of heterologous proteins to the cell surface of *L. plantarum* (Fredriksen et al., 2012a; Mathiesen et al., 2009).

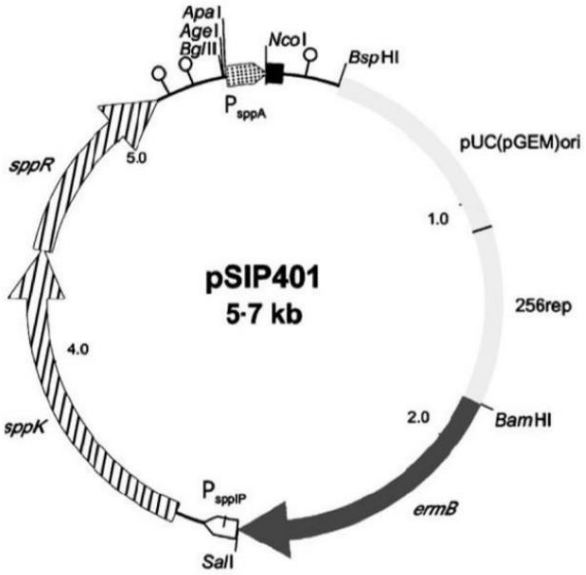

Figure 1.5.Inducible pSIP401 one plasmid system. Histidine protein kinase (sppR) and response regulator genes (sppK) are marked in vertically hatched regions and the inducible SppIP promoter is white. The dark grey region is the erythromycin (ermB) resistance gene. Inducible bacteriocin promoter (PsppA) is marked as a dotted region. Downstream PsppA a multicloning site marked as a black box is used for cloning of target genes. The pUC(pGEM)ori is the replicon used in E. coli and is marked in light grey. In this experiment the 256-replicon for *L. plantarum*, marked in light grey, is changed to a broad SH71 replicon (pSIP411). Figure taken from (Sørvig et al., 2005)

A drawback with choosing an inducible promoter is the fact that a knock-in gene on the chromosome, which is controlled by an inducible promoter would often need helper genes. This would make the expression of knock-in genes more tedious. In addition, vaccine applications with the pSIP system would be more complicated. Expression cassettes have a selection marker which usually is based on an antibiotic resistance gene which would be very unfavorable to insert in a live *L. plantarum* vaccine. One of the big advantages of CRISPR/Cas9 genome

knock-in of antigens is that the bacteria can be modified without using antibiotic resistant genes as selective markers.

A constitutive promoter is not dependent on other genes for activation, making the expression less intricate and faster to work with. It is also assumed that constitutive promoter leads to stable expression throughout varying conditions, whereas inducible ones will drastically change in expression levels in response to environmental stimuli (Xiong et al., 2018). A strong constitutive promoter can also be preferable for ensuring high gene expression (Tauer et al., 2014). Several promoters, both natural and synthetic, have been exploited for heterologous gene expression in *L. plantarum*, where some of the strongest constitutive promoters showed higher activities than those from the inducible pSIP system (Rud et al., 2006). In this case of toxicity from the heterologous gene a weaker constitutive promoter may be chosen.

1.5 Secretion and anchoring of proteins in gram positive bacteria

As mentioned, LAB are recognized as safe for consumption, they are promising vectors for molecule delivery to mucosal sites and some strains even have probiotic effects. The superfamily has a wide range of potential applications, proper display of the expressed proteins are therefore of high value.

Gram positive bacteria have one cytoplasmic cell membrane surrounded by a thick peptidoglycan cell wall (Schneewind & Missiakas, 2014). Proteins in gram positive bacteria are synthesized on the ribosomes, but not all proteins function inside the cell and therefore need to be transported over the cell membrane (Schneewind & Missiakas, 2014). If the protein is exported out of the cytosol, it is tagged by an N-terminal peptide sequence that guides the protein to its end location through several mechanisms (Kleerebezem et al., 2010).

Seven main protein secretion mechanisms have been characterized in Gram positive bacteria, they are called the secretion (Sec), twin-arginine translocation (Tat), flagella export apparatus (FEA), fimbrilin-protein exporter (FPE), holin (pore-forming), peptide-efflux ABC and the WXG100 secretion system (Wss) pathways (Michon et al., 2016). In Gram positive bacteria, secreted proteins are mainly transported across the plasma membrane via the Sec pathway (Schneewind & Missiakas, 2014; Tjalsma et al., 2004). Proteins with a Sec-type N-terminal signal peptide are recognized intracellularly, guided to the translocation machinery that transports the proteins over the cell membrane. However, not all secreted proteins are released into the extracellular milieu. Other subcellular locations are; 1) lipid anchored to the cytoplasmatic membrane. 2) attached to the cell wall either covalently (LPxTG) or non-

covalently (LysM). 3) anchored to cytoplasmic membrane via N or C-terminal transmembrane helix (Kleerebezem et al., 2010), Figure 1.6)

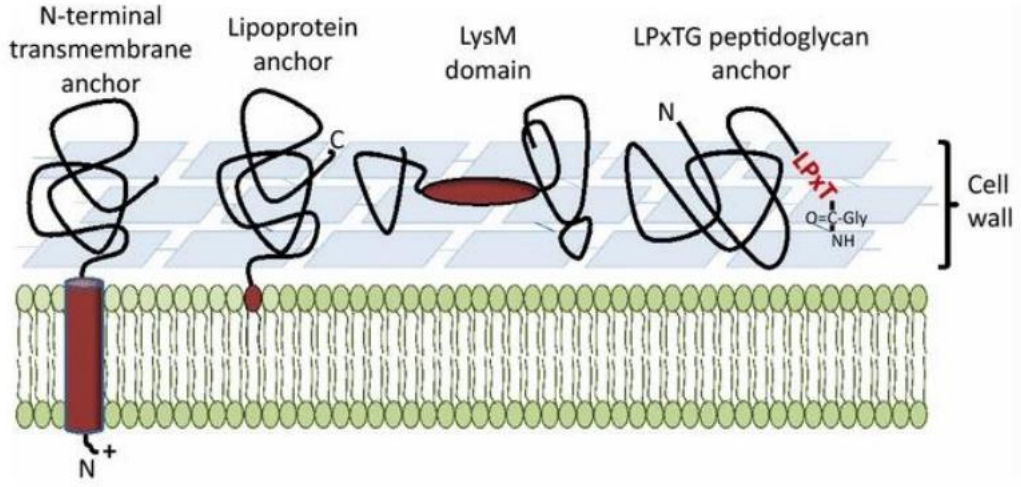

Figure 1.6. Schematic overview of the different anchoring mechanisms in gram positive bacteria. The figure shows the most exploited anchoring methods for display in gram positive bacteria that are based on covalent or non-covalent interaction with the cell membrane (green) or cell wall (grey). Recombinant proteins can be attached to the membrane layer by using a transmembrane anchor or a lipoprotein-anchor, or to the cell wall by covalent binding via the LPXTG motif, or by non-covalent LysM binding domains. The dark red part coupled to the protein is the anchor domains/motifs. The figure is taken from Michon et al., (2016).

For anchoring to the cell membrane, heterologous protein sequence should be fused to a lipoprotein, downstream the L-X-X-C motif (lipobox) (Michon et al., 2016). A protein sequence containing a lipobox in the signal peptide leads to anchoring f the protein to the plasma membrane. After secretion via the Sec pathway, the enzyme diacylglycerol transferase catalyses a coupling reaction between a conserved cysteine in the lipobox and a phospholipid in the membrane. The signal peptide is shortly cleaved off by signal peptidase II and the modified cysteine then forms the N-terminus of the mature lipoprotein, which covalently bind to phospholipids in cell membrane via thioether linkages (Kleerebezem et al., 2010; Tjalsma et al., 2004).

The known anchoring methods of the bacteria makes it possible to exploit the anchoring of proteins in the development of bacterial vectors for antigen delivery by translationally fusing antigens with anchoring motifs (Desvaux et al., 2006). The choice of anchor should be carefully validated, as full exposure of immunogens may be beneficial for a better interaction with the mucosal immune system. At the same time, it may be better to protect the

immunogen from the harsh environments by embedding it in the cell wall (Michon et al., 2016). In *Lactobacillus*, the 547-residue oligopeptide ABC transporter Lp_1261 have successfully been used as a lipoprotein anchor (Fredriksen et al., 2012a), thus this anchor is implemented for antigen display in this thesis.

1.6 COVID-19

L. plantarum holds a great potential as a vector for antigen delivery to mucosal sites (Kuczkowska et al., 2016). By development of a CRISPR/Cas9 knock-in protocol, in theory any antigen of interest can be inserted and expressed from the genome without the introduction of antibiotic resistant genes. With the use of an anchor, the antigen is displayed at the cell surface. By CRISPR/Cas9 mediated knock-in of an antigen of choice, may therefore provide immunity against any pathogen.

Recently, the world has been facing a serious health threat, the severe acute respiratory syndrome coronavirus 2 (SARS-CoV-2). The novel coronavirus was first detected in Wuhan City of China December 2019 and was readily declared a pandemic. SARS-CoV-2 is causing coronavirus disease 2019 (COVID-19) (Dhar et al., 2020), which mainly results in pneumonia, but severely affected patients are experiencing progressive respiratory failure and death due to alveolar damage (Zhou et al., 2020). The WHO states that over 460 million have been affected by the virus, and 6 million have died.

The SARS-CoV-2 virus is an enveloped single stranded positive-sense RNA virus related to SARS-CoV. The virus consists of spike proteins that interact with the ACE-2 receptors on human mucosal cells. These cells are found on the nasal-, intestinal epithelium and on the lung parenchyma. The spike protein of the virus beholds a smaller (~600 bp) receptor binding domain (RBD), which is the fusion part to ACE-2 (Figure 1.7). RBD mediates endocytosis into the mucosal cells where the virus replicates and finally destroys the cell. Because RBD interacts with ACE-2, it is commonly used in vaccines to trigger immunity. When RBD is used as the antigen in vaccines, the neutralization antibodies will bind to the RBD and block entry of the host cells.

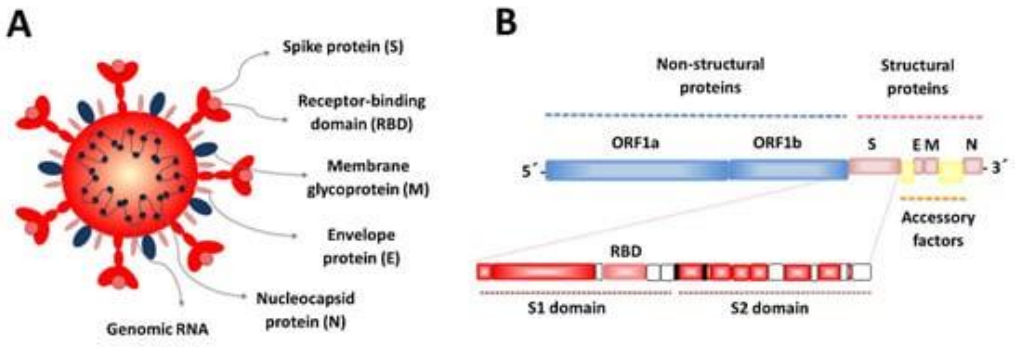

Figure 1.7. SARS-CoV-2 virion (A) and genome structures (B). SARS-CoV-2 virion (A) and genome (B) structures. The SARS-CoV-2 virus consists of genomic RNA enclosed by nucleocapsid proteins (N) forming a nucleocapsid shelter. Approximately two thirds of the RNA genome encode for a large polyprotein, ORF1a/b, while the last part proximal to the 3′-end encodes four structural proteins: spike (S), envelope (E), membrane (M) and nucleocapsid (N). The structure of the S-protein shows the S1 and S2 domains, and the receptor-binding domain (RBD). Figure from Villena et al., (2021)

Currently, several COVID-19 vaccines have either finished trial phase III or been granted an emergency use authorization; Pfizer, Moderna, Sputnik-V and Sinovac (Villena et al., 2021), in hope to stop the pandemic. However, these vaccines are parenteral, meaning that the vaccines will only elicit systemic immunity despite the fact that SARS-CoV-2 infects mucosal tissues (Xu et al., 2020). Mucosal immune responses are most effectively induced by mucosal immunization, while injected vaccines are generally poor inducers of mucosal immunity (Neutra & Kozlowski, 2006). The virus initiates its replication in the mucosal tissue, hence in order to efficiently prevent respiratory infections, the activation of the mucosal immune system is essential (Medina et al., 2010).

1.7 The aim of this study

This study aims to develop a method for CRISPR/Cas9 knock-in in *L. plantarum* WCFS1, where the purpose is to expand the gene-editing toolbox for this strain. To establish proof-of-concept, the receptor binding domain (RBD) of SARS-CoV-2 was chosen as the insertion sequence. RBD was chosen due to its relatively small size (~600bp), since CRISPR/Cas9 studies from the model strain, *E. coli*, shows that insertion of smaller fragments is more efficient. The ultimate goal for this study was to anchor the RBD to the cell surface of *L. plantarum* WCFS1, as a prototype for a SARS-CoV-2 mucosal vaccine. Consequently, several donor repair templates were constructed as vectors for CRISPR/Cas9 knock-in, including a template for constitutive expression of RBD.

In order to develop an operational CRISPR/Cas9 knock-in method, four necessary components; single guide RNA, *Streptococcus pyogenes* Cas9, donor repair template and a recombinase machinery, were assembled on an inducible two-plasmid system for thorough control of the expression. Throughout the study, the CRISPR/Cas9 system was attempted to be optimized to increase knock-in efficiency.

As the main goal was to exploit the lactic acid bacteria as a promising candidate for antigen delivery (Section 1.1.1), a subgoal was to characterize genomic expression of the heterologous knocked-in genes and compare it to the expression from plasmid. The knock-in of RBD was characterized by growth curves and Western Blot analysis. In addition, a novel in-house knock-in strain expressing a red fluorescent reporter gene, mCherry, was used in fluorescence assays to analyse dose-response.

2 Methods

2.1 Bacterial Strains, Media, and Culture Conditions

All bacterial strains and plasmids used in this study are listed in Table 3.1. *L. plantarum* WCFS1 was cultivated in Man, Rogosa, and Sharpe (MRS) broth (Oxoid, Hampshire, England) under static conditions at 37°C, in both liquid media and agar plates. *L. lactis* was used for pSIP411-based plasmid amplification and was cultivated in (M17) broth (Oxoid) supplemented with 0.5% glucose under static conditions, in liquid media and agar plates, at 30°C. *E. coli* Top10 (Invitrogen, Massachusetts, USA) and MAX Efficiency™ Stbl2™ Competent Cells (Thermo Fisher Scientific, Massachusetts, USA) were used as a host for molecular cloning, cultivated under shaking at 225 rpm in Brain Heart Infusion (BHI) (Oxoid) at 37°C and 30°C, respectively. The *E. coli* Stbl2.0 was selected as host for cloning of plasmid that contains SpCas9 enzyme because these cells are suitable for cloning of unstable DNA. To minimize stress, which correlates to mutation rate, the Stbl2.0 cells were grown on 30°C degrees. Erythromycin (Merck, Darmstadt, Germany) and chloramphenicol (Merck) were supplemented for selection, see Table 2.1.

Table 2.1. Overview of strains and antibiotic concentration with appropriate growth medium.

Antibiotic	***Agar plates (µg/mL)***	***Liquid medium (µg/mL)***	***Agar plates (µg/mL)***	***Liquid medium (µg/mL)***
	E. coli		*L. plantarum/ L. Lactis*	
Erythromycin	200-300	200	5-10	5-10
Chloramphenicol	34	34	5-10	5-10

2.2 Primers

Table 2.2 Primers used in this study

Primers	Sequence*	Description	Restriction enzyme
HL_2071-2074_SapI_rev	GCTCTTCTTATGGGC TAATAACAAGC	In-Fusion primer for insertion of HL into pSgRNA_KI.	SapI
HL-pSgRNA-SmaI_F	TTTTTAAGTGGTACCC CCTACAAGATCCACCA ACTTTATTGC	In-Fusion primer for insertion of HL into pSgRNA_KI	Acc65I
H-2071-2074-R_fwd	CACAGCGTCCATAGA AGCTTGCTCTTCATAA TCCTACTTGGTTAGACTG	In-Fusion primer for insertion of HR into pSgRNA_KI	SapI
HR-pEdit2-SmaI_R	GGCGCCTTCGAACCCAC GAGCCAGACAGTTTTAAGTGC	In-Fusion primer for insertion of HR to smaI cutting site	
RBD_F	TAGGAGTATGATTCAT ATGCCAAACATCACGAACTT	In-Fusion primer 15 nt homologous to sppA	NdeI
RBD_R	CTGTAATTTGAAGCTT CTATGGACGCTGTGGGGT	In-Fusion primer 15 nt homologues to pSgRNA_KI at HindIII	HindIII
SgRNA-LpRec_F	CCTCCAGTAACTCGA GACCGGTGGGCCCATATTA	In_fuison primer that binds to sppA for insertion into pSgRNA_KI	
Sg-Cas9_R	CGCCTTCGAACCCGG GTCAGTCACCTCCTAGCTGA	In_fuison primer that binds to SpCas9 for insertion into pSgRNA_KI	
HL-pSgRNA-SmaI_F	TTTTTAAGTGGTACCCCCT ACAAGATCCACCAACTTTATTGC	In-Fusion primer that binds to HL with a 15 nt overhang to pSgRNA	
HR-pEdit2-SmaI_R	GGCGCCTTCGAACCCA CGAGCCAGACAGTTTTAAGTGC	In-Fusion primer that binds to HR with a 15 nt overhang to pSgRNA	
SgRNA-LpRec_F	CCTCCAGTAACTCGAG ACCGGTGGGCCCATATTA	In_fusion binds to sppA, overhang to pSgRNA	
SgRNAKI-1-HA_cas9_R	TCTTGTAGGGGGTACC GTCAGTCACCTCCTAGCTGAC	In_fusion binds to SpCas9, overhang to pSgRNA	
2071-2074_SekF	ATGAAAACCATGAGTCTTGT	Binds to the genome of *L. plantarum* WCFS1 for screening after insertion at DSB site.	

2071-2074_SekR	TGATGAAGCTAAGGCTGAT	Binds to the genome of *L. plantarum* WCFS1 for screening after insertion at DSB site.	
HL_2071-2074_SapI_rev	GCTCTTCTTATGGGCTA ATAACAAGC	Primer with SapI cutting site to generate editable donor repair template	SapI
pSgKI1-HL_XhoI_F	CCTCCAGTAACTCGAGCT ACAAGATCCACCAACT	In-Fusion primer, binds to SgRNA plasmid	XhoI
pSgKI1-HR_AgeI_R	ATATGGGCCCACCGGT ACGAGCCAGACAGTTTTAAGT	In-Fusion primer, binds to SpCas9	AgeI
HL_SlpA_RBD_fwd	TGCTTGTTATTAGCCCA TAAGAAGAGCAGATCTA TAAAGTTGTTTGATAAATGC	In-Fusion primer binds to SlpA for insertion to HL	
Cas9-LpRec_F	AGGTGACTGACTCGAG ACCGGTGGGCCCATATT	In-Fusion primer, binds to P_{sppA}	XhoI
Cas9-LpRec_R	CGCCTTCGAACCCGGGTC AATCTATGAGTAAGTCGTCTG	Binds to recombinases	XmaI
Psppa-RBD_fwd	GCTTGTTATTAGCCCA TAAGAAGAGCACCGG TGGGCCCATATTAAC	Primer used to amplify RBD. Overhang to HL Contains SapI cutting site.	
RBD_rev	AAGCTTCTATGGA CGCTGTGGCTCTTC	Amplify RBD. Overhang to HR. Contains SapI cutting site.	
KI1_HR_RBD_R	AGTCTAACCAAGTAG GATTATGAAGAGCAA GCTTCTATGGACGCTG	In-Fusion primer for insertion of knock-in sequence in the pSgRNA_KI plasmid.	SapI
HL_SlpA_RBD_F	TGCTTGTTATTAGCCCAT AAGAAGAGCAGATCTATA AAGTTGTTTGATAAATGC	In-Fusion primer for inserting the knock-in sequence in the pSgRNA_KI plasmid.	SapI
SgRNA_KI	ATAAACGACTTCGGT GGAA	SgRNA for SpCas9 mediated DSB between *lp_2071* and *lp_2074* in *L plantarum* WCFS1	

*Underline indicates restriction sites

2.3 Longtime storage of bacteria

For long-term storage of bacteria, glycerol stocks were made and kept at -80°C. The addition of glycerol stabilizes the frozen bacteria and prevents damage of the cell membrane. This keeps the cells viable.

Procedure

A single colony from a clone is picked with a toothpick, in sterile conditions, and cultured overnight in 10 mL of the appropriate growth medium supplied with appropriate antibiotics, (Table 2.1). 1 mL of the culture was transferred to a 1.5 mL cryovial (Sarstedt, Trollasen, Norway). Next, 300 µL of sterile 87% glycerol (Merck) was added to the cryovial, and the tube was inverted 6 times for homogenization of the mixture. The stock was kept at -80°C.

2.4 Bacterial plasmid isolation and purification.

Isolation of plasmid DNA from bacteria allows for molecular biology procedures such as cloning, transfection, digestion, PCR, and sequencing. For plasmid isolation the NucleoSpin® Plasmid Kit (MACHEREY-NAGEL, Düren, Germany) was used. Following agitation, precipitation, centrifugation, and the removal of supernatant, cellular debris are removed, and the plasmid was isolated and purified.

Depending on the replicon of the plasmid, NucleoSpin® Plasmid Kit protocol 5.1 was followed for high plasmid copy number, and 5.2 for low plasmid copy number. *L. lactis* required an additional lysis step and was lysed with A1 buffer and additional 25 µL of 100 mg/mL lysozyme, for 1 hour at 37°C before continued as described in the NucleoSpin® Plasmid Kit protocol.

2.5 Isolation of microbial DNA

Genomic DNA can be isolated from a variety of microorganisms. Microbes such as gram-positive bacteria are harder to lyse due to their thick peptidoglycan wall. FastPrep-24 instrumental (MP Biomedicals) is used for mechanical lysis for easy disruption of the cell wall. The samples were lysed at 6.5 m/s^2 for 30 seconds in the NucleoSpin® BeadsTube type B, by using ~1g glass beads. For isolation of microbial DNA from the gram-positive bacteria *L. plantarum*, the NucleoSpin® Microbial DNA kit (MACHEREY-NAGEL) is used. Isolation was performed following the manufacturer's Standard protocol for gram-positive and gram-negative bacteria.

2.6 Restriction enzyme digestion of DNA

Restriction enzymes recognize short DNA sequences and cleave dsDNA at specific sites within or adjacent to the recognition sequences. Hundreds of different restriction enzymes are known, allowing a variety of molecular cloning techniques.

Digestion with restriction enzymes was used to prepare DNA fragments for ligation. Both the DNA fragment for insert and a vector must be double digested. The doubled digestion results in compatible ends between the DNA fragments so they can be ligated. Restriction enzymes digest DNA asymmetrically across their recognition sequence, which results in a single stranded overhang on the digested end of the DNA fragment, referred to as sticky ends. When these ends are compatible, meaning that the overhang base pairs on the vector and insert are complementary, the vector and insert can bind together in a ligation reaction.

Procedure

1. The digest was set-up at room temperature in the corresponding order (Table 2.3). For enzymes supplied from New England Biolabs, the catalogue from (https://nebcloner.neb.com/#!/redigest) was used to find corresponding digestion buffer (rCutSmart/r1.1/r2.1/r3.1) and digestion temperature. For FastDigest® Restriction enzymes, the 10x Restriction buffer was used (Thermo Fisher Scientific and New England Biolabs (NEB), Massachusetts, USA).

Table 2.3. Components for restriction enzyme digestion of DNA

Component	**Volume**
dH2O up to	50 µL
10x Restriction buffer	5 µL (1x)
DNA	1 µg
Restriction enzyme	1 µL*

**Maximum 10% of the restriction enzymes were added in the reaction

2. The mixture was gently mixed and spun down.

3. The reaction was incubated at 37°C for 2.5 hours. In blunt digesting, Calf Intestinal Alkaline Phosphatase (CIAP) (Thermo fisher scientific) was added and incubated for 15 minutes. And the CIAP was inactivated at 65°C for 15 minutes. This was done to prevent re-circularization/self-ligation of the vector in the cloning process.

4. After the digest, the mixture was directly loaded onto an agarose (2.8).

2.7 Ligation

The final step for construction a recombinant plasmid is to connect the insert the fragment of interest into the compatible digested vector backbone. This is accomplished by covalently

connecting the sugar backbone of the two DNA fragments with a ligase. The reaction requires ATP and cofactor Mg^{+}, which is supplied in the ligation buffer.

2.7.1 Quick Ligation

For fast ligation of DNA fragments, the Quick Ligation ™ Kit (NEB) was used. The kit contains a Quick T4 DNA Ligase, which is an enzyme that can ligate both sticky- and blunt-ends.

Procedure

1. In a 1.5 mL eppendorf tube, 50 ng of the vector with a 3-fold molar excess of the insert was mixed. The volume was adjusted to 10 µL with dH2O.

2. 10 µL 2x Quick Ligation Reaction Buffer (NEB) was added and vortexed.

3. 1 µL Quick T4 DNA Ligase (NEB) was added and mixed by pipetting up and down 7 times.

4. The Eppendorf tube was briefly centrifugated and incubated at 25°C for 15 minutes.

5. After incubation, the ligation mixture was cooled on ice, and then transformed within a few hours to competent cells, or stored at -20°C.

2.7.2 In-Fusion Cloning

In-Fusion are designed for directional cloning of one or more fragments. The In-Fusion enzyme fuses DNA fragments by the recognition or a 15-bp overlap. The inserts can be PCR generated and the 15-bp overlaps are engineered by designed primers that are homolog to the ends of the linearized vector. For in-fusion cloning the in-Fusion HD Cloning kit (Takara Bio USA, Inc) was used.

Figure 2.1. In-Fusion cloning. A linearized vector is generated by restriction digest. Gene specific primers with a 15 bp overhang homologous to the vector are designed (Red and yellow blocks) The insert (green) is PCR amplified with the In-Fusion primers. The reaction mix with the linearized vector and the amplified insert is

incubated at 50°C for 15 minutes before being transformed to a host. The illustration is a modified version from the In-Fusion® HD Cloning Kit User Manual.

Procedure

1. The insert sequence was added in a 2-fold excess to the digested vector. To determine the amount of purified PCR product and linearized vector needed for each reaction, the ligation calculator from NEBioCalculator® (https://nebiocalculator.neb.com/#!/ligation) was used.

2. The components in Table 2.4 were transferred to a 1.5 mL eppendorf tube and mixed gently. 5x In-Fusion HD Enzyme Premix (NEB) was added last to the mixture.

Table 2.4. In-Fusion Cloning Procedure

Components	**Volum (µL)**
dH2O up to	10
Purified PCR fragment	10-200 ng*
Linearized vector	50-200**
5x In-Fusion HD Enzyme Premix	2

*<0.5 kb: 10–50 ng, 0.5 to 10 kb: 50–100 ng, >10 kb: 50–200 ng

**<10 kb: 50–100 ng, >10 kb: 50–200 ng

3. The reaction was incubated at 50°C for 15 minutes and then placed on ice.

4. After incubation, the reaction mix was either transformed into competent cells or stored at -20°C.

2.7.3 Ligation with ElectroLigase

Ligation using Electro ligases is directly compatible with electrocompetent cells used for transformation with electroporation. For electro ligation the ElectroLigase ® (NEB) was used together with the 2x electro ligation reaction buffer (NEB).

Procedure

1. 20-100 ng of vector was combined with a 3-fold molar excess of insert and the volume was adjusted with dH_2O to 5 µL.

2. 5 µL of 2x ElectroLigase Reaction Buffer (NEB) and 1 µL of ElectroLigase (NEB) was added to the reaction and mixed by pipetting up and down 7 times.

3. The ligation reaction was incubated at 25°C for 60 minutes.

4. The ligase was then heat inactivated at 65°C for 15 minutes.

5. After inactivation, the ligation mix was cooled on ice and transformed within a few hours or stored at -20°C for later use.

2.8 Preparation of electrocompetent *L. plantarum* WCFS1

When bacteria are competent, they can take up free, extracellular DNA, this is called transformation. In the laboratory the host is artificially made competent by weakening the cell wall. *L plantarum* are grown in medium supplemented with extra glycine, which replaces the L-alanine in the cell wall resulting in a permeable cell wall. For transformation a current is applied to make the cell membrane permeable so the DNA can move into the cell. The procedure was executed according to the protocol described in Aukrust et al., (1995).

Procedure

1. *L. plantarum* WCFS1 was cultured overnight from a glycerol stock in 10 mL MRS with appropriate antibiotics at 37°C.

2. 1 mL of the overnight culture was used to make a serial dilution of 10^{-1} to 10^{-10} in MRS containing 1 % glycine.

3. 1 mL of the overnight culture with an OD_{600} of 2.5 ± 0.5 was further diluted in 20 mL MRS + 1% glycine.

4. The culture was then grown until it reached the logarithmic phase of OD_{600} of 0.7± 0.07, and then placed on ice for 10 minutes to stop further growth. (NB. If induction of a vector is necessary the culture is induced at this step with 25 ng/mL SppIP at OD_{600}~0.3).

5. The culture was centrifuged at 5000x g for 7 minutes at 4°C, and the supernatant was discarded.

6. The pellet was resuspended in 5 mL ice cold fresh 30% PEG_{1450}. Additional 20 mL of the PEG_{1450} (Thermo Fisher Scientific) was added, and the tube was inverted gently and placed on ice for 10 more minutes.

7. The cells were collected by centrifugation at 5000x g at 4°C for 7 minutes.

8. The pellet was resuspended in 400 µL 30% PEG_{1450} and portions of 40 µL were pipetted into ice cold eppendorf tubes and immediately frozen at -80°C.

2.9 Transformation of competent cells

Transformation is the process by which foreign DNA is introduced into a cell. Newly constructed plasmids are transformed to bacterial hosts for propagation. The transformation can be proceeded electrically or chemically.

2.9.1 Transformation of Electrocompetent Competent Cells

Procedure

1. Electrocompetent cells were thawed on ice.

2. 5 µL plasmid or electro-ligation-mix was transferred to a tube containing 40 µl electrocompetent cells.

3. The mixture was then transferred to the GenePulser® electroporation cuvette 0.2 cm (Bio-Rad)

4. The cuvette was placed in the GenePulser® II electroporator (Bio-Rad) and subjected to optimal current (Table 2.5) adjusted by the Pulse controller plus (Bio-Rad).

5. Addition of media was added according to Table 2.5. Immediately after addition of the media to the cuvette, the transformed cells were transferred to a sterile Eppendorf tube.

6. The cells were incubated at the appropriate temperature, without shaking, for 2-4 hours 7. After incubation, 100 µL of the cells were spread out on either MRS or GM17 agar plates with appropriate antibiotics and incubated overnight.

Table 2.5. The setup on the GenePulser, media and incubation for transformation of electrocompetent cells. The conditions vary among strains.

Strain	Cuvette (cm)	Capacitance (µF)	Volt (kV)	Resistance (Ω)	Media (µL)	Incubation (°C)	Incubation (h)
L. plantarum	0.2	25	1.5	400	950 MRSSM	37	2-4
L. lactis	0.2	25	2.0	200	700 SGM17	30	2-4

2.9.2 Transformation of Chemically Competent *E. coli*

Chemically competent cells are heated in a water bath, which opens pores of the cell membrane to facilitate plasmid entry. Plasmids were propagated in OneShot™ TOP 10 chemically competent *E. coli* (Invitrogen) or MAX Efficiency™ Stbl2™ Competent *E. coli* (Thermo Fisher Scientific)

Procedure

1. One vial for each transformation of OneShot™ TOP 10 chemically competent cells (Invitrogen) were thawed on ice and transformed to a pre-chilled Falcon 2059 Polypropylene Round Bottom tube 14 mL (Becton Dickinson, New Jersey, USA).

2. 1-5 µL of DNA was added into a vial of OneShot™ TOP10 cells (Invitrogen), and gently stirred.

3. The vials were incubated on ice for 30 minutes.

4. The cells were heat-shocked for 30 seconds at 42°C without shaking.

5. After the heat-shock, the cells were placed on ice for 2 minutes.

6.250 µL pre-warmed Super Optimal broth with Catabolite repression (S.O.C) medium (Invitrogen) was then aseptically added to each of the vials and placed in 225 rpm shaking-incubator at 37°C for 1 hour.

7. 100 µL of the incubated transformation mix was spread out on BHI agar plates with appropriate antibiotics and incubated at 37°C overnight.

2.10 Polymerase Chain Reaction

Polymerase Chain Reaction (PCR) is a method used for in vitro amplification of a specific DNA fragment by a heat stable polymerase. The PCR rely on a series of heating and cooling that allow DNA to be synthesized. The basic steps are denaturation, annealing and extensions. The denaturation step requires heat to separate the DNA strands and provide a ssDNA strand as a template. The annealing step cools the reaction so that the primers are allowed to bind to the complementary sequence on the ssDNA template. The temperature is next raised to the optimum temperature of the polymerase so that the polymerase can extend the primers and synthetize the area between the forward and revers primer, thus amplifying the specific region. Alongside the DNA template and specific forward and revers primers, the reaction requires free

nucleotides (dNTPs): Adenine, cytosine, guanine, thymine. Each cycle of heating and cooling exponentially synthetizes the DNA and cycles between 25-35 is commonly used.

2.10.1 PCR using Q5® Hot Start High-Fidelity 2x Master Mix

Q5® High-Fidelity DNA Polymerase (NEB) was used for amplification of inserts used in cloning, or for amplify genes in *L. plantarum* for Sanger sequencingm the enzyme has better a proof-reading mechanism than the Red Taq Polymerase (VWR, Pennsylvania, USA). The PCR reactions were carried out following the manufacturer's suggestions of the Q5® Hot Start High-Fidelity 2x Master Mix (NEB).

Procedure

1. The reactions were kept on ice. The components (Table 2.6) were gently mixed in 0.2 ml PCR tubes (Axygen, California, USA) and spun.

2. The PCR tubes containing the reaction mix were put in the Mastercycler gradient PCR machine (Eppendorf, Hamburg, Germany) and the cycling program (Table 2.7) was applied.

Table 2.6. Components for PCR using Q5® Hot Start High-Fidelity DNA polymerase.

Components	**Volume (µL)**	**Final concentration**
dH2O up to	50	-
10 µM Forward primer	2.5	0.5 µM
10 µM Reverse primer	2.5	0.5 µM
Template	variable	< 1µg
Q5® Hot Start High-Fidelity 2x Master Mix	25	1x

Table 2.7. Thermocycle conditions for Q5 PCR

Steps	**Temperature (°C)**	**Time**	**Cycles**
Initial denaturation	98	30 seconds	1
Denaturation	98	10 seconds	25-35
Annealing	50-72*	30 seconds	25-35

Elongation	72	20-30 seconds/kb**	25-35
Final elongation	72	2 minutes	1

*Annealing temperature is primer dependent.

**Annealing duration depends on the length of the DNA fragment being synthesized. The duration of this step is 20-30 seconds per 1000 bp DNA.

2.10.2 PCR using Taq Polymerase

VWR® Red Taq DNA polymerase (VWR) has a higher error rate than the Q5 polymerase, thus PCR with Red Taq DNA polymerase was mainly used to investigate if successful transformation was accomplished. In this case, a toothpick was used to transfer colonies from the agar plates to the PCR tubes. To ensure lysis of the thick peptidoglycan cell wall in the gram-positive bacteria, the PCR tubes was microwaved on full effect for 1 minute before the rest of the components were added to the PCR reaction.

1. The PCR reactions were carried out as suggested by the manufacturer of the Red Taq DNA Polymerase 2x Master Mix. The reaction was setup at ice in the order shown in Table 2.8 in sterile PCR tubes.

Table 2.8. Components for PCR using Taq DNA polymerase

Components	Volume (µL)	Final concentration
dH2O	Up to 50	-
10 µM Forward primer	1	0.2 µM
10 µM Reverse primer	1	0.2 µM
Template	variable	< 1000 µg
Red Taq DNA Polymerase 2x Master Mix	25	1x

2. The PCR tubes containing the reactions were placed in a thermal cycler, and the cycling program (Table 2.9) was applied.

Table 2.9 Thermocycling set-up for PCR using Taq DNA polymerase

Step	Temperature (°C)	Time	Cycles
Initial denaturation	95	2 minutes	1
Denaturation	95	10 seconds	25-35
Annealing	50-65*	30 seconds	25-35
Elongation	72	1 minute/kb**	25-35
Final elongation	72	5 minutes	1

*The temperature varied depending on the primers. The annealing temperature was 3-5 °C lower than Tm of the primers.

**The duration of the annealing step depended on the length of the DNA fragment being copied. The duration of the step is one minute per 1000 bp DNA.

2.11 Agarose gel electrophoresis

Agarose gel electrophoresis is a technique that uses electrical current to separate linearized DNA fragments based on their physical properties: size and charge. Since the nucleic acid is negatively charged it migrates through the pores in the agarose gel, toward the positively charged end of the gel when electrical current is applied. The speed of the migration is size dependent, as smaller fragments require less resistance, it migrates faster in the gel thus separating the DNA fragments after size.

Procedure

1. 6.5 g of SeaKem® LE Agarose (Lonza, Basel, Switzerland) was dissolved in 0.5 L of 1 x TAE buffer (Thermo Fisher Scientific) to make a 1.2% agarose gel.

2. The solution was sterilized in the CertoClav (OneMed, Skedsmokorset, Norway) at 115°C for 15 minutes. The 0,5 L stock solution of 1.2% agarose gel was kept at 60°C for short time storage.

3. Gels was prepared by blending 50 mL of the 0,5 L stock solution and 2.5 µL peqGREEN (Peqlab, Wilmington, USA) in a beaker. The mix was poured into a gel tray with 8 or 15 combs.

4. The gel was solidified for 30 minutes before the combs were removed, before it was transferred to an electrophoresis chamber and covered with 1x TAE buffer (Thermo Fisher Scientific).

6. Loading dye was added to the samples, and the samples were loaded into the wells in the gel.

7. The gel was run at 90V for up to 60 minutes, depending on the fragment sizes.

6. The GelDoc EZ imager (Bio-Rad) was used to take pictures of the gels.

7. If some DNA fragments were to be used later, the DNA-fragments were visualized under UV-light and excised using a scalpel. The gel pieces were stored in -20°C.

2.12 Purification of DNA and extraction of DNA fragments from the agarose gel

The NucleoSpin® Gel and PCR Clean-up (MACHEREY-NAGEL, Duren, Germany) was used to purify the DNA amplified with PCR and the DNA extracted from agarose gels. The purification and extraction steps were carried out according to the relevant protocol supplied by the manufacturer.

2.13 Determination of DNA concentration

The Qubit Fluorometer (Thermo Fisher Scientfic) with the Invitrogen™ Qubit™ dsDNA Broad Range Assay kit was used to quantify the DNA concentration to calculate the amount of vector and insert for ligation reactions and in-fusion.

Procedure

1. A working solution was made where Qubit Reagent was diluted 1:200 in Qubit Broad Range Buffer (Thermo Fisher Scientific). The working solution was vortexed.

2. 2 µL DNA was added to the 198 µL working solution in an Assay Tube. The solution was vortexed and incubated for 1 minute before the DNA concentration was determined by the Qubit Fluorometer (Thermo Fisher Scientific).

2.14 DNA sequencing of plasmids and PCR fragments

DNA fragments were sent for Sanger sequencing for plasmid and PCR fragments to confirm correct cloning. In an Eppendorf tube (Axygen USA) purified 400-500 ng plasmid or 100-400 ng PCR template was mixed with 2.5 µL of 10µM primer and dH_2O up to 11 µL. The tube was labeled with a unique barcode and sent to Eurofins Genomics. The results were analyzed with CLC DNA Main Workbench 7 (Qiagen, Hilden, Germany).

2.15 Plasmid curing by using negative selection with replica plating

Negative selection was conducted by replica plating in order to select a plasmid cured colony. Appropriate dilutions of each overnight culture were made and 100 µL was plated out on MRS plates lacking antibiotics (Figure 2.2). A sterile stamp with velvet touches the original plate and is stamped onto Ery, Cm and Ery/Cm MRS agar plates, for antibiotic concentrations see Table

2.1. The colonies that do not grow on ERY/CM are most likely plasmid cured colonies and are chosen from MRS plates without antibiotics for further characterization.

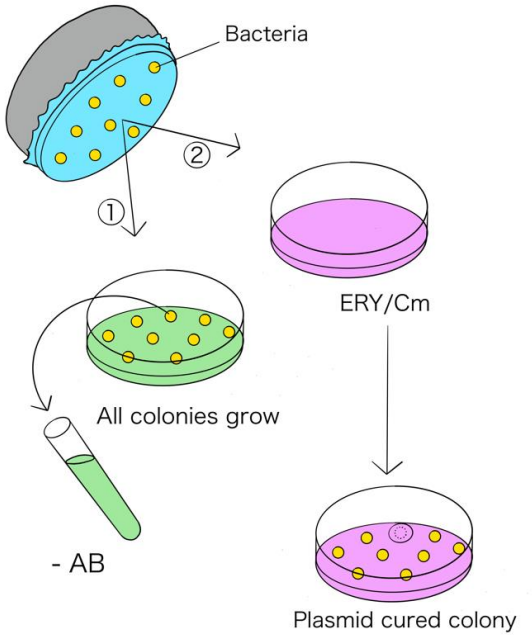

Figure 2.2. Negative selection using replica plating. First the bacterial suspension is grown on medium lacking antibiotics (green plate), then a sterile velvet stemple (blue) is used to transfer the colonies to an agar plate containing antibiotics (purple plate). If the antibiotics inhibit the growth of a colony, the colony now lacks the plasmid containing the resistance gene and have therefore been plasmid cured. The corresponding replica on the agar plate lacking antibiotics is chosen for downstream applications. Illustration by Sigrid Helena Bue (2022).

2.16 Growth curve

Procedure

1. ONC of *L. plantarum* containing the gene of interest were grown with appropriate antibiotics under static incubation at 37°C.

2. Overnight cultures were diluted in 10 ml prewarmed MRS with appropriate antibiotics to OD_{600} 0.10 - 0.15. These cultures were further incubated at 37 °C until OD_{600} reached 0.27-0.33. At this point, three technical replicas of 200 µL uninduced cultures were transferred to its own well in the sterile 96 well Microwell plate (Thermo Fisher Scientific) as a control. The rest of the cultures were induced with 25 ng/µL SppIP, inverted and 3 x 200 µL times three technical parallels of the induced culture were transferred to the sterile 96 well Microwell plate.

3. The plate was sealed with a sealing film for microplates (VWR) before placing it in the Multiscan FC (Thermo Fisher Scientific) for measurement every 20 minutes at OD_{595}.

4. The growth curve was measured by the SkanIt Software 2.5.1 (Thermo Fisher Scientific).

2.17 Cultivation and harvesting of *L. plantarum*

Procedure

1. Overnight cultures of the *L. plantarum* containing the plasmid of interest were grown.

2. The overnight cultures were diluted in 10 mL prewarmed MRS medium to an OD_{600} of 0.13-0.15.

3. The cultures were incubated at 37°C until it reached an $OD6_{600}$ of 0.3, then 25 ng/mL unducer peptide SppIP (CASLO, Copenhagen, Denmark) was added to the tube and the tube was inverted.

4. The induced cells were further incubated for 3 hours, and harvested by centrifugation at 5000x g for 10 minutes at 4°C.

5. The supernatant was decanted and the pellet was washed with 10 mL cold Phosphate Buffered Saline (PBS).

6. The cells were collected by centrifugation at 5000x g for 10 minutes at 4°C, and the pellet was lysed according to section 2.18, or stored at -20°C for later use.

2.18 Preparation of cell lysate

Procedure

1. Harvested bacteria were resuspended in 1 ml PBS, and the suspension was transferred to a FastPrep® tube (Thermo Fisher Scientific) containing approximately 0.5 g glass beads (Sigma, Missouri, USA).

2. The FastPrep® tubes were placed in a FastPrep® - 24 Tissues and Cell homogenizer (Thermo Fisher Scientific) and ran three times at 6.5 m/s for 45 seconds. In between runs, the tubes were chilled on ice for 5 minutes.

3. The tube was centrifuged at 16.100 x g and 4 °C for 1 minute.

4. The supernatant was transferred to an eppendorf tube and centrifuged at 16.100 x g and 4 °C for 1 minute.

5. The protein extract was transferred to a new eppendorf tube and either denaturated for SDS-PAGE following protocol 2.16 or stored at -20 °C.

2.19 Gel electrophoresis of proteins

Sodium dodecyl-sulfate polyacrylamide gel electrophoresis (SDS-PAGE) is commonly used to obtain high resolution separation of complex mixtures of proteins. The method initially denatures the proteins that underwent electrophoresis by specific detergents. Anionic detergent lithium dodecyl sulphate (LDS) breaks noncovalent bindings and reducing agent dithiothreitol (DTT) breaks disulphide bands. This denatures the proteins and gives them a uniform negative charge, thus by applying current, the proteins are separated as they migrate towards the positive electrode. A protein standard (ladder) with known molecular weights is used to determine the weight of the proteins.

Procedure

1. 7.5 µL NuPAGE® LDS Sample Buffer (4X) (Invitrogen) and 3 µL NuPAGE® Reducing agent (10X) (Invitrogen) were mixed. 10 µL of this mix was added to 20 µL protein extract.

2. The samples were incubated in a boiling water bath for 10 minutes.

3. A NuPAGE® Novex Bis-Tris gel (8 cm x 8 cm x 1 mm, 10 wells) (Invitrogen) was placed in an electrophoresis chamber, and Tris-Glycine-SDS (TGS) (Bio-Rad) buffer was added to the chamber.

4. The boiled samples and ladder was loaded onto the gel. In the first well 7.5 µL of the MagicMark™ XP Western Protein Standard (Invitrogen) was added.

5. The gel was run for 30 minutes at 200 V.

2.20 Western blotting analysis

Blotting refers to the transfer of biological samples from the SDS-PAGE to a nitrocellulose membrane and their subsequent detection on the membrane. Western blotting, also called immunoblotting, was introduced in 1979 by Towbin et al. and is now a routine technique for protein analysis. The specificity of the antigen-antibody interaction allows a targeted protein to be detected from a complex protein mixture and offers qualitative and semi-quantitativedata about the protein of interest.

An applied current enables protein transfer from the gel to the nitrocellulose membrane where the proteins are immobilized. Unbound areas of the membrane are blocked with bovine serum albumin (BSA) to hinder nonspecific antibody binding. Primary antibodies bind to the epitopes of the target protein, and abundant antibodies are washed away. To visualize the protein, a

secondary antibody conjugated to horseradish peroxidase (HRP) binds to the primary antibodies. The bound HRP oxidizes luminol and emit light upon reaction in a luminol substrate.

2.20.1 Blotting with the iBlot™ Dry Blot System

Proteins were blotted from the SDS-PAGE on to the nitrocellulose membrane by using the iBlot™ Dry Blot System. The transfer stock was arranged as shown in Figure 2.3.

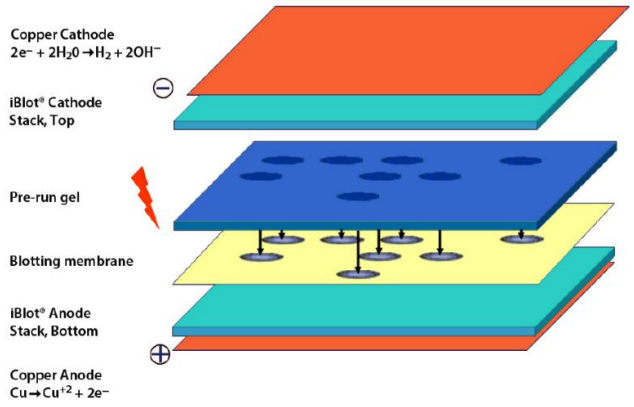

Figure 2.3. Schematic of the iBlot™ transfer stock. The stack consists of the protein-containing polyacrylamide gel which is in direct contact with the nitrocellulose paper. These are surrounded by two electrodes. For facilitated transfer pads and pre-wetted filter paper are used. When the current was applied the proteins moved from the pre-run gel to the blotting membrane. The figure is taken from the iBlot ™ Dry Blotting System manual.

Procedure

1.The iBlot® Anode bottom stack (Invitrogen), containing the anode and the Pure Nitrocellulose Membrane (0.45 µm) (Bio-Rad), was placed directly in the iBlot® Dry Blotting blotting apparatus System (Invitrogen)

2. The pre run gel was soaked in dH_2O and transferred to the nitrocellulose membrane. Any air bubbles were removed using a blotting roller (Invitrogen).

3. A iBlot® filter paper (Invitrogen) pre-wetted in dH_2O was placed on top of the gel, and any air bubbles were removed.

4. The iBlot® Cathode stack (Invitrogen) was placed on top of the filter paper, with the copper electrode facing up.

5. A iBlot® Disposable sponge (Invitrogen)was placed on the top of the cathode and the lid was closed.

6. The blotting was carried out at 20 V for 7 minutes.

2.20.2 SNAP i.d.® immunodetection

The SNAP i.d.® immunodetection system (Millipore, Massachusetts, USA) is used to hybridize antibodies to the proteins. The nitrocellulose membrane is placed in a blot holder, that is placed on top of the SNAP i.d.® immunodetection device. The device uses vacuum to pull the reagents through the membrane.

Procedure

1. The SNAP i.d ® Single Well Blot Holder (Millipore, Massachusetts, USA) was wetted with dH_2O before the nitrocellulose membrane was placed in the blot holder with the protein side facing down.

2. A wetted filter paper was placed on top of the membrane. Bubbles were removed with a SNAP i.d ® Blot roller (Millipore), and the blot holder was closed.

3. The blot holder was placed in the SNAP i.d.® Protein detection system device (Millipore).

4. 30 mL of the blocking solution was poured on to the blot holder, 10 mL at a time, and the vacuum was applied until all the solution had gone through the membrane.

5. 5 mL of TTBS/ 5% BSA (blocking solution) with 1 µl Primary antibody SARS-CoV/SARS-CoV-2 Spike RBD Polyclonal (MyBioSource, California, USA) was added to the membrane and incubated for 10 minutes.

6. The membrane was washed three times with TTBS, with continuously running vacuum. When the washing was done, the vacuum was switched off.

7. 5 mL of TTBS/5 % BSA with 0.2 µl Secondary antibody HRP-Goat Anti-Rabbit IgG (Invitrogen) was added and incubated for 10 minutes.

8. Step 6 was repeated, but with 4 washing steps.

9. The membrane was removed from the blot holder and was ready for chemiluminescent detection of the protein.

2.20.3 Chemiluminescent detection of proteins

Procedure

1. 5 ml of SuperSignal® Luminol/Enhancer (Thermo Fisher Scientific) and 5 ml of Stable Peroxide Buffer (Thermo Fisher Scientific) was mixed to a substrate solution.

2. The nitrocellulose membrane was incubated in the substrate solution for 5 minutes without light exposure.

3. Azure c400 (Azure biosystems, California, USA) was used for visualization and imaging of the membrane.

3 Results

The antigen used in the present study is the receptor binding domain (RBD) from the SARS-CoV-2 virus (Section 1.6), a small domain commonly used for immunization (Dalvie et al., 2021). In addition, the RBD include a dendritic cell binding peptide (DC) fused to the C-terminus of RBD. The DC binding sequence is included in all constructs. Dendritic cells are major contributors to the initiation of an immune response, thus by using the fusion antigen, RBD_DC, a higher affinity to the dendritic cell is thought to enhance the immune response for the mucosal vaccines(Cohn & Delamarre, 2014; Morel & Butterfield, 2015).

Plasmid-based antigen production usually carries antibiotic resistant genes and other heterologous genes which is a drawback regarding horizontal gene transfer. It is therefore an advantage to insert the antigen in the genome without the use of antibiotic resistant genes. In this thesis the goal was to make a system for CRISPR/Cas9 mediated insertion (knock-in) in *L. plantarum* as a proof-of-concept, and to characterize genomic antigen production.

RBD was chosen because it is a relatively small domain (~600bp), and earlier CRISPR/Cas9 studies have shown that insertion of smaller fragments is more efficient (Paix et al., 2017). To compare genomic and plasmid-based RBD production, vectors for plasmid-based expression were constructed using the pSIP system (Section 1.4) by using the pLp1261_RBD_DC as the template for all RBD_DC constructs (Table 3.1). However, genomic expression of RBD by using the pSIP system would be complicated because the system is dependent on two regulatory genes and additives for expression of the target gene. To solve this, a constitutive expression system, that is not dependent on additives nor helper genes, was constructed under the P_{SlpA} promoter.

In total, eight plasmids were constructed (Table 3.1). Two pSIP vectors expressing RBD, and six vectors expressing parts of, or the whole CRISPR/Cas9 knock-in system. The plasmids were assembled in *E. coli* or *L. lactis* and electroporated into *L. plantarum*.

Table 3.1 Plasmids and strains used in this study.

Plasmid	Description	Source
pSIP_RBD_DC	Inducible plasmid-based expression of RBD	This work
pSIP_SlpA_RBD_DC	Constitutive plasmid-based expression of RBD	This work
pLp1261_RBD_DC	Inducible plasmid-based expression of RBD with lipoprotein anchoring	(Trondsen, 2021)
pSIP_SlpA1261_AG85B_ESAT6_DC	Constitutive expression of tuberculosis fusion antigen. The vector is used as a backbone for constitutive expression	Unpublished*
pSIP_mCherry	Inducible expression of mCherry	(Wiig, 2020)
pEV	Empty vector. pSIP401 derivative without target genes	(Fredriksen et al., 2012b)
pSIP_411_LpRec	Vector for overexpression of the of the recombinase machinery from the *lp_0640-lp_0642* genes	Unpublished*
pSgRNA_KI_Cas9_RBD_DC	CRISPR/Cas9 knock-in vector for insertion of inducible RBD in genome of *L. plantarum*. Applied in system I	This work
pSgRNA_KI_RBD_DC_Cas9	CRISPR/Cas9 vector for knock-in of inducible RBD. Applied in system I	This work
pSgRNA_KI_1261_RBD_DC_Cas9	CRISPR/Cas9 vector for knock-in of lipoprotein anchoring of RBD. Applied in system I	This work
pSgRNA_KI_SlpA_RBD_DC_Cas9	CRISPR/Cas9 vector for knock-in of constitutive RBD. Applied in system I	This work
pSgRNA_KI_Cas9	Vector with the sgRNA_KI and inducible Cas9	This work
pSgRNA_KI	Vector containing sgRNA for DSB mediated by SpCas9 in between *lp_2071* and *lp_2074*	Unpublished*
pSIP_Cas9_LpRec_SH71	Broad-host-range vector for the CRISPR/Cas9 system II containing Rep_{SH71}	This work
pSgRNA_KI_RBD_DC	Vector containing SgRNA and inducible RBD flanked with homologous arms. Applied in system II	This work
pSgRNA_KI_1261_RBD_DC	Vector containing SgRNA and inducible RBD flanked with homologous arms. Applied in system II	This work

pSgRNA_KI_SlpA_RBD_DC	Vector containing SgRNA and constitutive RBD flanked with homologous arms. Applied in system II	This work
pSIP_403_pCas	Inducible expression of SpCas9	(Wiull, 2018)
pCas_SH71	SpCas9 with SH71 replicon	(Wiull, 2018)
Strain	**Description**	**Source**
***L. plantarum* WCFS1::RBD**	Knock-in of RBD with inducible promotor	This work
***L. plantarum* WCFS1::RBD + pEV**	Knock-in of RBD with expression cassette for protein expression	This work
***L. plantarum* WCFS1::mCherry**	Knock-in of mCherry with inducible promotor	Unpublished*
***L. plantarum* WCFS1::mCherry + pEV**	Knock-in of mCherry with expression cassette for protein expression	Unpublished*

*Previously made by K. Wiull

3.1 Construction of control plasmids for plasmid-based expression of RBD

Vectors for plasmid-based expression of RBD were constructed to compare plasmid- and genomic-based expression in *L. plantarum*. In previous studies, RBD_DC has been codon optimized for *L. plantarum* and tagged for lipoprotein anchoring by *lp_1261*, in a pSIP vector, named pLp1261_RBD_DC (Trondsen, 2021, Table 3.1). This vector was used as a template to construct inducible and constitutive expression of cytoplasmatic RBD, which later were exploited as templates for the assembly of the vectors used for CRISPR/Cas9 knock-in.

The first step in constructing the inducible vector was to isolate the pLp1261_RBD_DC plasmid from an *E. coli* culture. For construction of pSIP_RBD_DC (Figure 3.1), primers RBD_F and RBD_R (Table 2.2) were used to amplify the RBD_DC from the isolated pLp1261_RBD_DC. In addition, the template-plasmid was digested with NdeI and HindIII to excise the lipoprotein anchor and RBD_DC. Next, the PCR amplified RBD_DC was cloned into the pLp1261_RBD_DC NdeI/HindIII digested backbone by In-Fusion (Section 2.7.2) to yield the pSIP_RBD_DC.

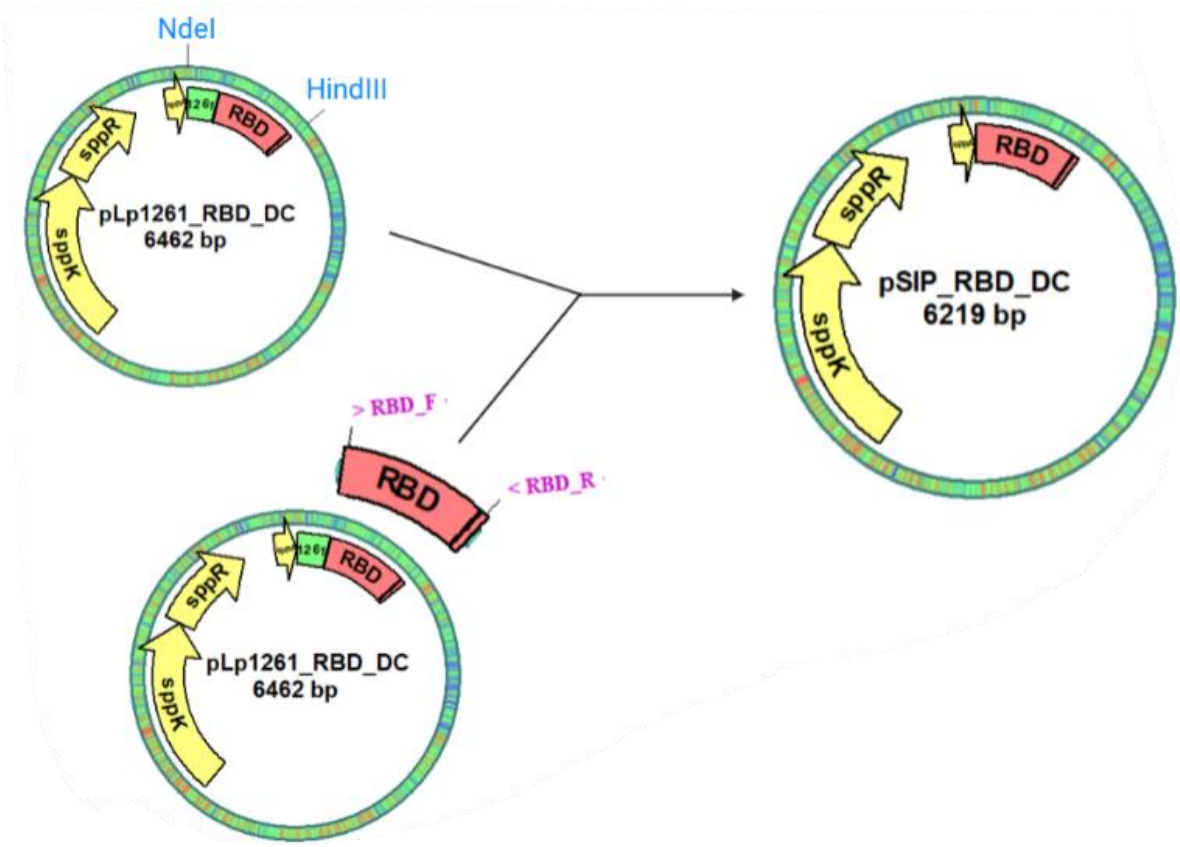

Figure 3.1 Strategy to construct the pSIP_RBD_DC vector. The RBD was amplified by PCR with primers RBD_F and RBD_R, whilst the pLp1261_RBD_DC backbone was digested with restriction enzyme NdeI and HindIII. Then, the inducible pSIP_RBD_DC vector was obtained using In-Fusion ligation of the fragments. The vector contained an *E. coli* replicon for subcloning (pUC ori) and a replicon for replication in *L. plantarum* (Rep_{256}).

To construct the pSIP_SlpA_RBD_DC vector (Figure 3.2) for constitutive expression of RBD, the pSIP_SlpA1261_AG85B_ESAT6_DC vector (Table 3.1) was isolated from *E. coli* and used as the backbone for constitutive expression of RBD_DC. pSIP_SlpA1261_AG85B_ESTAT6_DC was digested with restriction enzymes NdeI and HindIII to remove the *lp_1261* lipoprotein anchor along with the AG85B_ESAT6_DC fusion antigen. The pSIP_RBD_DC vector, on the other hand, was digested with the same restriction enzymes to excise RBD_DC. In the end, the fragments were ligated by using Quick ligase.

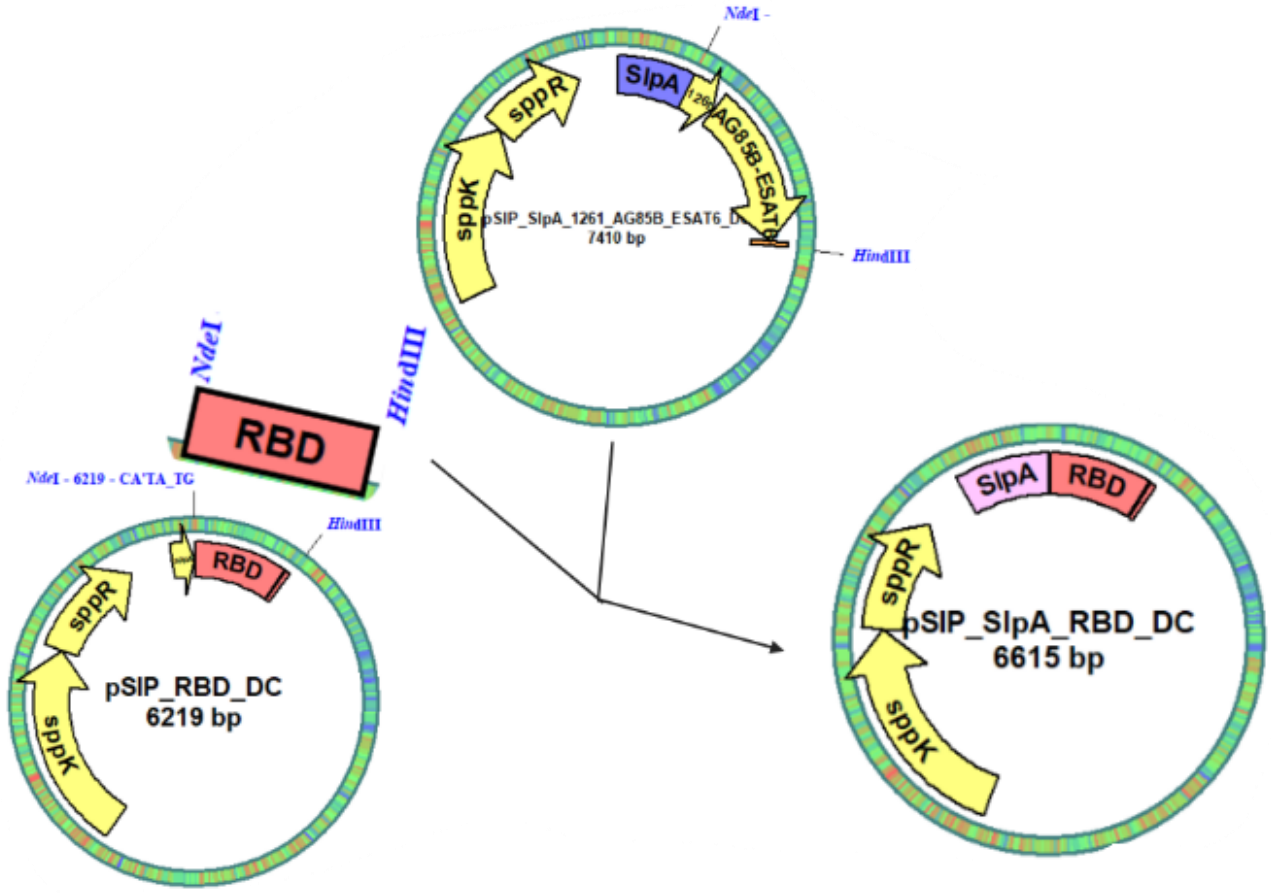

Figure 3.2. Strategy for constructing the pSIP_SlpA_RBD_DC vector. pSIP_RBD_DC was digested with NdeI and HindIII to excise RBD_DC. The plasmid pSIP_SlpA_1261_ AG85B_ESAT6_DC was digested with NdeI and HindIII to serve as the backbone for Quick ligation of the fragments. The vector contained the replicon pUC ori and a Rep_{256}.

The constructed pSIP_RBD_DC and pSIP_SlpA_RBD_DC were transformed into OneShot® TOP10 chemically competent *E. coli* cells. Correct clones were verified by colony PCR (Section 2.10.2) and verified by Sanger DNA sequencing (data not shown), before they were transformed into *L. plantarum* in order to characterize plasmid-based expression.

As one of the main goals of this study was to create a knock-in strain with constitutive expression of cell-membrane anchored RBD_DC in *L. plantarum*, construction of a pSIP_SlpA_1261_RBD_DC vector was attempted (Figure 3.3).

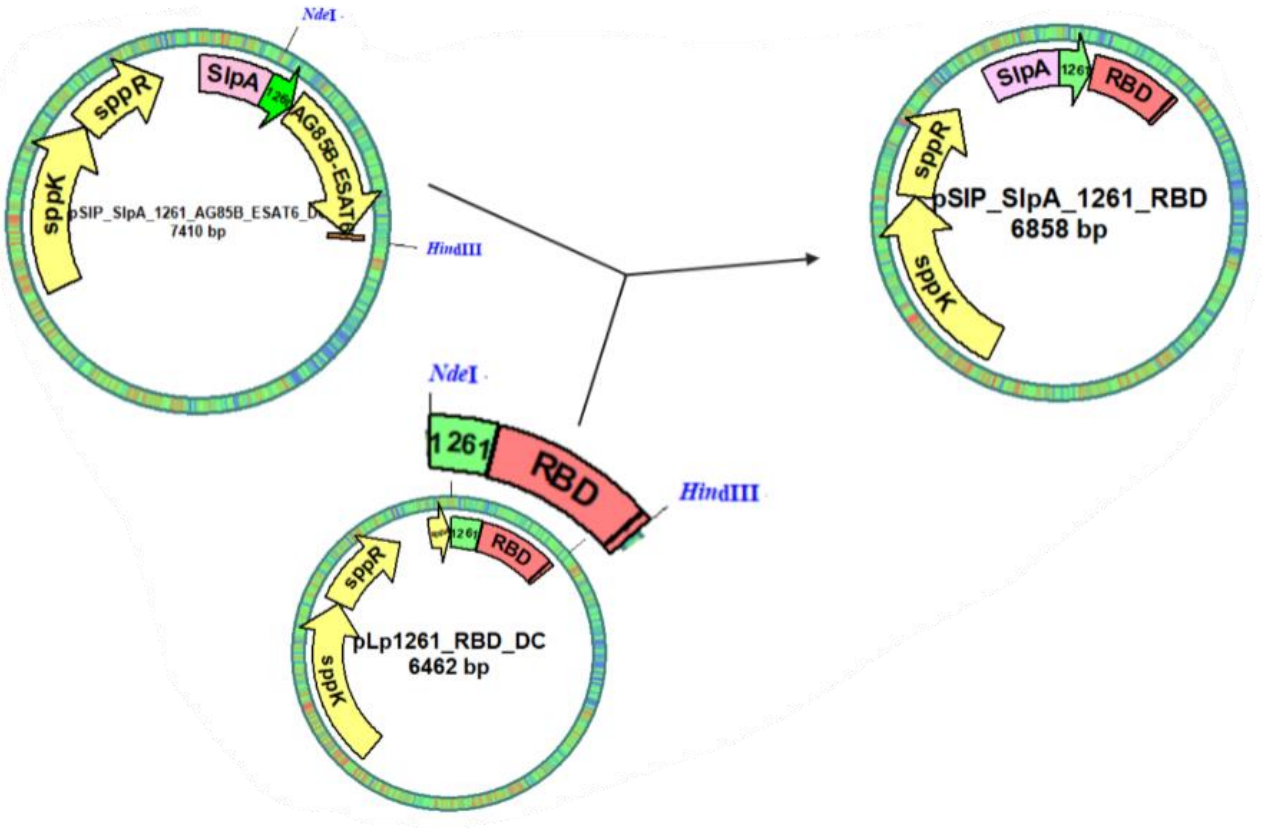

Figure 3.3. Strategy for constructing pSIP_SlpA_1261_RBD. pSIP_SlpA_1261_ AG85B_ESAT6_DC was digested with NdeI and HindIII to remove the lipoprotein anchor *lp1261* and the AG85B_ESAT6_DC fusion antigen. pLp1261_RBD_DC was also digested with NdeI and HindIII to excise *lp_1261* and the RBD_DC. Next, the fragments were ligated by Quick ligase for cloning in *E. coli* or electro-ligase for cloning in *L. plantarum*.

In pSIP_SlpA_1261_RBD_DC, RBD is fused to the lipoprotein anchor Lp_1261 (Figure 1.6) and under the control of the constitutive promoter SlpA (P_{SlpA}). Because P_{SlpA} is considered to be very active in bacteria (Verdú et al., 2019), subcloning the pSIP_SlpA_1261_RBD_DC could be challenging due to plasmid instability and negative effects produced by toxicity of exogenous proteins. To overcome this challenge, several strategies varying incubation temperature, plasmid concentration, ratio of insert compared to vector and subcloning host were attempted in order to construct the vector with P_{SlpA}, *lp_1261* and RBD_DC (Table 3.2). Nonetheless, no transformants emerged.

Table 3.2. Various strategies for constructing the pSIP_SlpA_1261_RBD_DC vector. pSIP_SlpA_1261_RBD_DC vector was subcloned in *E. coli* and *L. plantarum* at 30 and 37 °C using varying plasmid concentrations and insert:vector ratios.

Experimental rounds	Subcloning host	Vector (ng)	Ratio (Insert: Vector)	Incubation temperature (°C)
2	*E. coli* OneShot® TOP10	50	3:1	37
1	*E. coli* OneShot® TOP10	50	4:1	37
1	*E. coli* OneShot® TOP10	50	3:1	30
1	*E. coli* Stellar	50	3:1	37
2	*L. plantarum*	20	3:1	37
1	*L. plantarum*	50	3:1	37
1	*L. plantarum*	50	3:1	30

3.2 The development of a CRISPR/Cas9 knock-in system for *L. plantarum* WCFS1

The CRISPR/Cas9 knock-in system was developed as a two-plasmid system. In total, two CRISPR/Cas9 two-plasmid systems were developed, named system I (Figure 3.8) and system II (Figure 3.15). Both systems contained all components necessary for knock-in; the single guide RNA (sgRNA), *Streptococcus pyogenes* Cas9 (SpCas9), donor repair template and the recombinase machinery.

3.2.1 Assembly of the single guide RNA and SpCas9 to target the genome of *L. plantarum* WCFS1

For the SpCas9 to achieve nuclease activity, the enzyme must assemble with the sgRNA. In this study, the sgRNA was constitutively expressed by using the P_3 promoter. The sgRNA, named sgRNA_KI, (Table 2.2) assembled with SpCas9 to guide the nuclease to the target site. At the target site the sgRNA:SpCas9 complex introduced a double-stranded break (DSB) in the genome. The target site was directed to be between two genes, the glycosyltransferase *lp_2071* and the transposase fragment *lp_2074*, with reading frames in opposite directions (Figure 3.4)

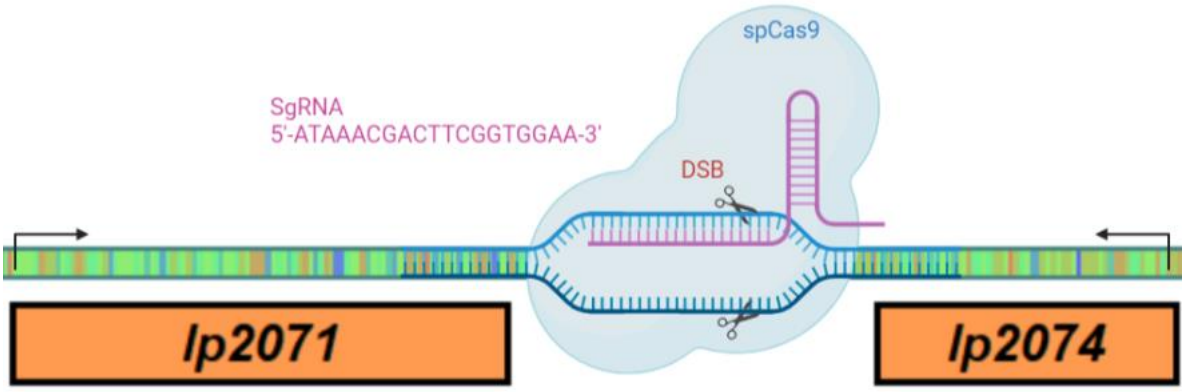

Figure 3.4. A 20-nucleotide sgRNA sequence targeting the genome of *L. plantarum*. The SgRNA_KI (pink), was designed to target the genome of the *L. plantarum* WCFS1 between the *lp2071* and *lp2074* genes (orange boxes). A DSB (red) is mediated three nucleotides downstream the PAM.

The pSgRNA_KI_Cas9 vector (Table 3.1), was constructed for expression of SpCas9 and sgRNA_KI to mediate the double-strand break (DSB) at the target site. In addition, the SpCas9 and the sgRNA were used for negative selection of unedited cells. To construct the pSgRNA_KI_Cas9 vector, the gene encoding SpCas9, fused downstream of a P_{sppA} inducible promotor, was PCR amplified from the pSIP_403_Cas9 vector (Table 3.1) by using In-Fusion primer pair SgRNA_lpRec_F and Sg_Cas9_R (Table 2.2, Figure 3.5). Next, the pSgRNA_KI vector (Table 3.1), containing the sgRNA_KI (Figure 3.4) was digested with restriction enzymes XhoI and XmaI. The digestion opened the pSgRNA_KI vector and allowed for insertion of the PCR product, which contained the inducible promoter P_{sppA} and the gene encoding SpCas9, by using In-Fusion (Section 2.7.2).

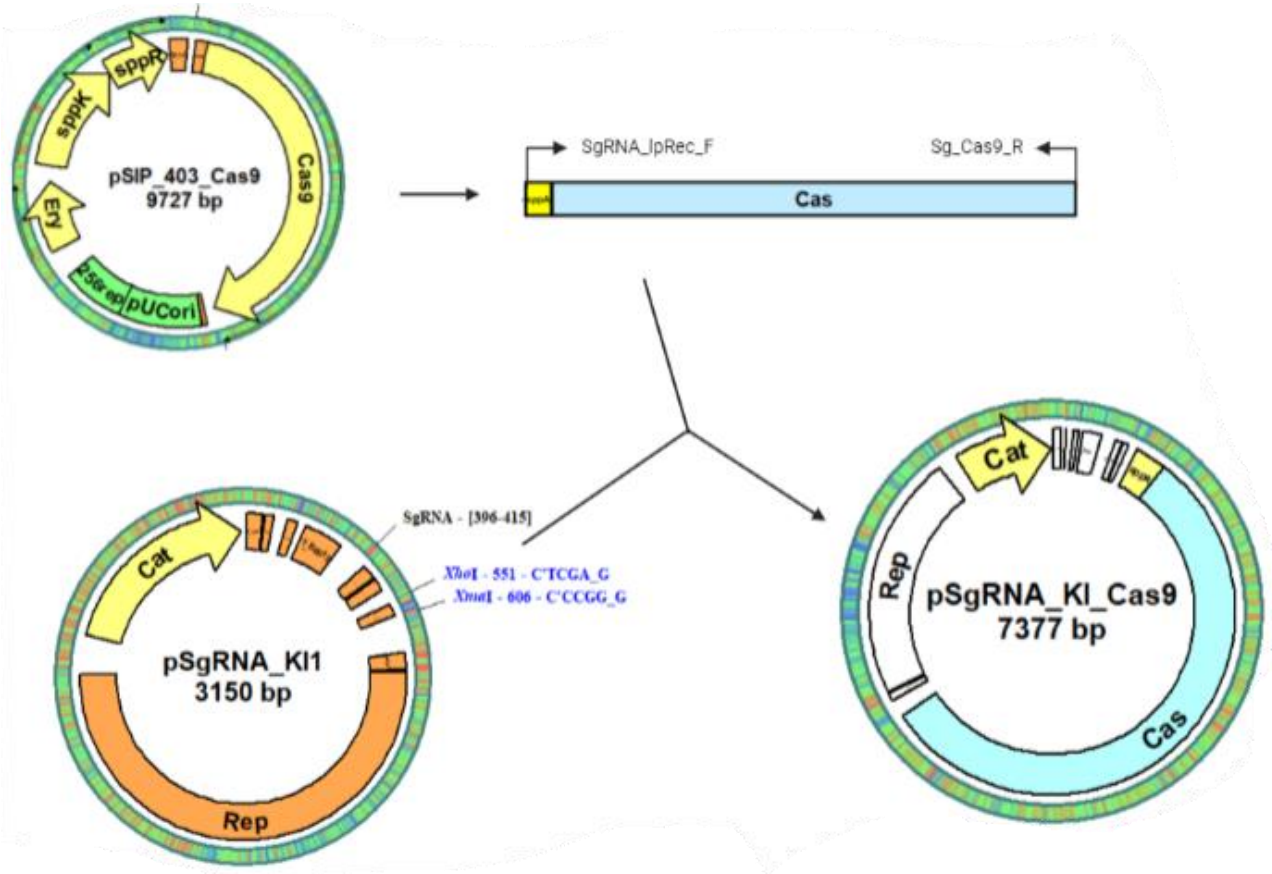

Figure 3.5. Strategy for constructing pSgRNA_Cas9. In-fusion primers sgRNA_LpRec_F and Sg_Cas9_R were used to PCR amplify the inducible SpCas9 from the pSIP_403_Cas9 vector. The insert was translocated to the pSgRNA_KI vector digested with XhoI and XmaI, by In-Fusion. pSgRNA_KI_Cas9 contained SpCas9-coding gene under the control of the inducible promoter P_{SppA}. All pSgRNA_KI vectors contained sgRNA_KI under the control of the constitutive promoter P3, the Rep_{256} replicon and an antibiotic selection marker for chloramphenicol.

As a precaution for cloning unstable inserts, all vectors containing the gene encoding SpCas9 were subcloned in *E. coli* Stbl2™ Competent cells. While vectors lacking the *spCas9* gene were subcloned in competent *E. coli* one shot TOP10™ cells.

3.2.2 Implementation of a recombinase machinery to rescue cell lethality

Unfortunately, CRISPR/Cas9 mediated DSBs in bacteria usually cause cell death(Choudhury et al., 2020). This is thought to be due to cytotoxicity of the nuclease or inefficient cell repair mechanism for DSB (Arroyo-Olarte et al., 2021b; Lone et al., 2018; Vento et al., 2019; Zhao et al., 2020). To overcome the lethality and mediate for homology directed repair pathway (HDR), a recombinase machinery was implemented in the development of the CRISPR/Cas9 knock-in systems. *L. plantarum* homologous genes *lp_0640-lp_0642*, under the control of the inducible promotor P_{sppA} were used to overexpress the recombinase to mediate knock-in. In system I, overexpression of the recombinase machinery was provided by the pSIP_411_LpRec

plasmid (Table 3.1) In system II, the recombinase machinery was expressed from pSIP_411_Cas9_LpRec (Table 3.1). For construction of the pSIP_411_Cas9_LpRec, see Figure 3.14.

3.2.3 Construction of the donor repair template

The chromosomal break can be repaired with the HDR (mediated by the recombinase machinery, see above) if a donor repair template is present (Section 1.3). The donor repair template should consist of two sequences homologous to the genomic sequence upstream and downstream of the DSB site in order to mediate allelic recombineering. Hence, primer pairs HL_2071-2074_SapI_rev and HL-pSgRNA-SmaI_F (Table 2.2) were used to PCR amplify a 1 kb sequence from genomic DNA of *L. plantarum* WCFS1 WT upstream of the DSB, referred to as homology left (HL) (Figure 3.6). Similarly, primer pairs H-2071-2074-R_fwd and HR-pEdit2-SmaI_R (Table 2.2) were used to PCR amplify a 1 kb sequence from the genomic WT DNA downstream of the DSB, referred to as homology right (HR). HL and HR, referred to as homologous arms (HA), make up the template for allelic recombineering. Anything between the HA has the potential to be inserted into the genome (knock-in), consequently P_{sppA} and RBD_DC were inserted between HL and HR in a PCR reaction. This was accomplished by PCR amplification of the pSIP_RBD_DC plasmid with primer pairs Psppa-RBD_fwd and KI1_HR_RBD_R (Table 2.2) which amplified P_{sppA} and RBD_DC with incorporation of 15 bp overhangs complementary to HL and HR. As a result, the insert was incorporated between HL and HR in a second PCR amplification using only the forward primer of HL and the reverse primer of HR (outer primers; HL-pSgRNA-SmaI_F and HR-pEdit2-SmaI_R, Table 2.2).

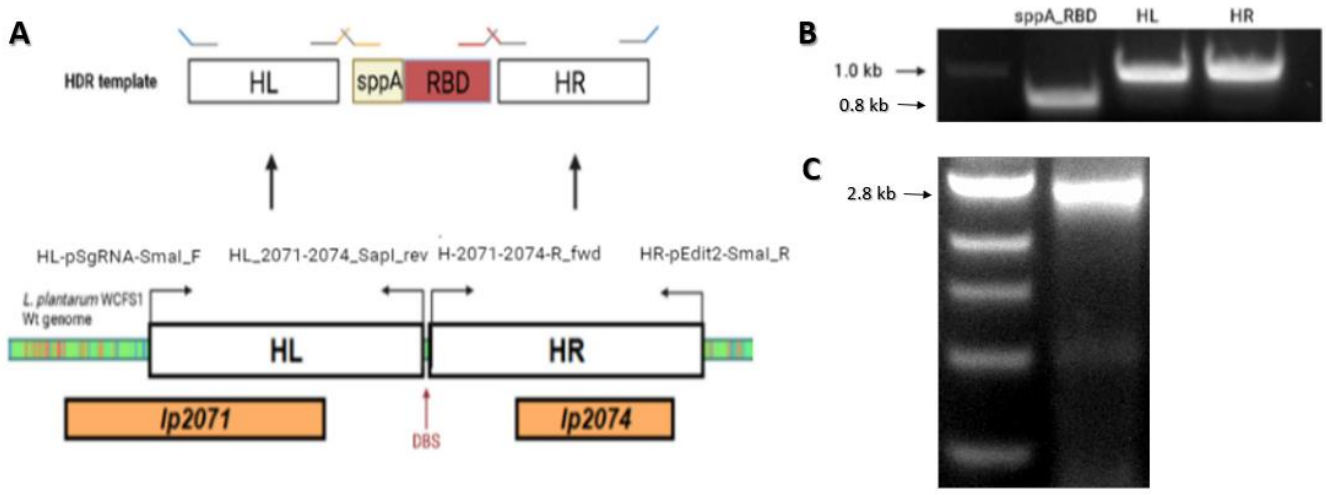

Figure 3.6. Strategy for constructing the ds donor repair template. A) Schematic overview of the donor repair template. The red arrow indicates the genomic site in *L. plantarum* WCFS1 WT where sgRNA_KI aligns and

mediate CRISPR/Cas9 induced DSB. Primers with a 15-nucleotide overlapping region to the HL and HR is used to amplify the insertion sequence. In-Fusion primers HL-pSgRNA-SmaI_F and HR-pEdit2-SmaI_R are used in a second PCR to assemble the donor repair template B) Agarose gel pictures from PCR amplification of HL, P_{sppA} upstream of RBD_DC and HR. The size of the insert is ~800 bp, and each HA are ~1000 bp. C) The three fragments are aligned in the second PCR, visualized as the band at ~2.8 kb, making up the donor repair template.

3.2.4 Knock-in of cytoplasmatic RBD

To insert the RBD_DC on the genome of *L. plantarum* WCFS1 between *lp_2071* and *lp_2074,* 5 µg PCR product of the donor repair template together with 1 µg pSgRNA_KI_Cas9 were electroporated into *L. plantarum* WCFS1 harbouring pSIP_411_LpRec. 5 µg PCR product of the donor repair template was also electroporated to *L. plantarum* WCFS1 harbouring pSIP_411_Cas9_LpRec. Nonetheless, no transformants emerged.

As an attempt to improve recombination efficiency the PCR product of the donor repair template was constructed as a plasmid donor in the pSgRNA_KI_RBD vector (Table 3.1, Figure 3.7) and implemented in the CRISPR/Cas9 knock-in system I (Section 3.2.5). pSgRNA_KI was digested with SmaI and used as the backbone for insertion of the PCR amplified donor repair template by using In-Fusion.

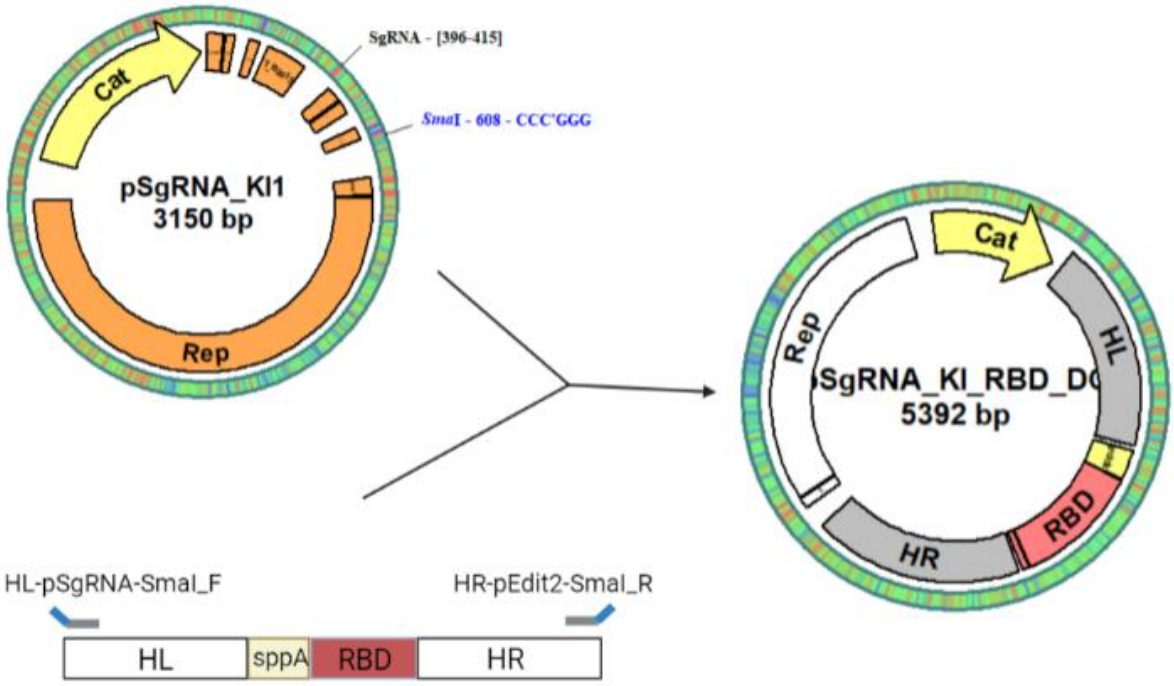

Figure 3.7. Strategy for constructing pSgRNA_KI_RBD. The donor repair template was amplified with In-fusion primers HL_pSgRNA_SmaI_F and HR_pEdit_2_SmaI_R. Next, the pSgRNA_KI was digested with restriction enzyme SmaI for In-Fusion of the vector and the PCR amplified donor repair template.

3.2.5 Development of CRISPR/Cas9 knock-in system I for knock-in of cytoplasmatic RBD

First, the CRISPR/Cas9 knock-in system I was developed (Figure 3.8). In this system, *L. plantarum* WCFS1 harboring the pSIP_411_LpRec (Table 3.1) plasmid was made electrocompetent and induced before storage of the cells. Overexpression of the recombinase machinery was induced by supplying 25 ng/mL inducer pheromone, SppIP to the culture at OD_{600}~0.3 at step 4 in the protocol for "preparation of electrocompetent *L. plantarum*" (Section 2.8). The CRISPR/Cas9 knock-in vector pSgRNA_KI_Cas9_RBD_DC (Table 3.1, Figure 3.9), consisting of SpCas9, sgRNA_KI and the donor repair template was electroporated into *L. plantarum* WCFS1 harboring and overexpressing the recombinase machinery (Figure 3.8).

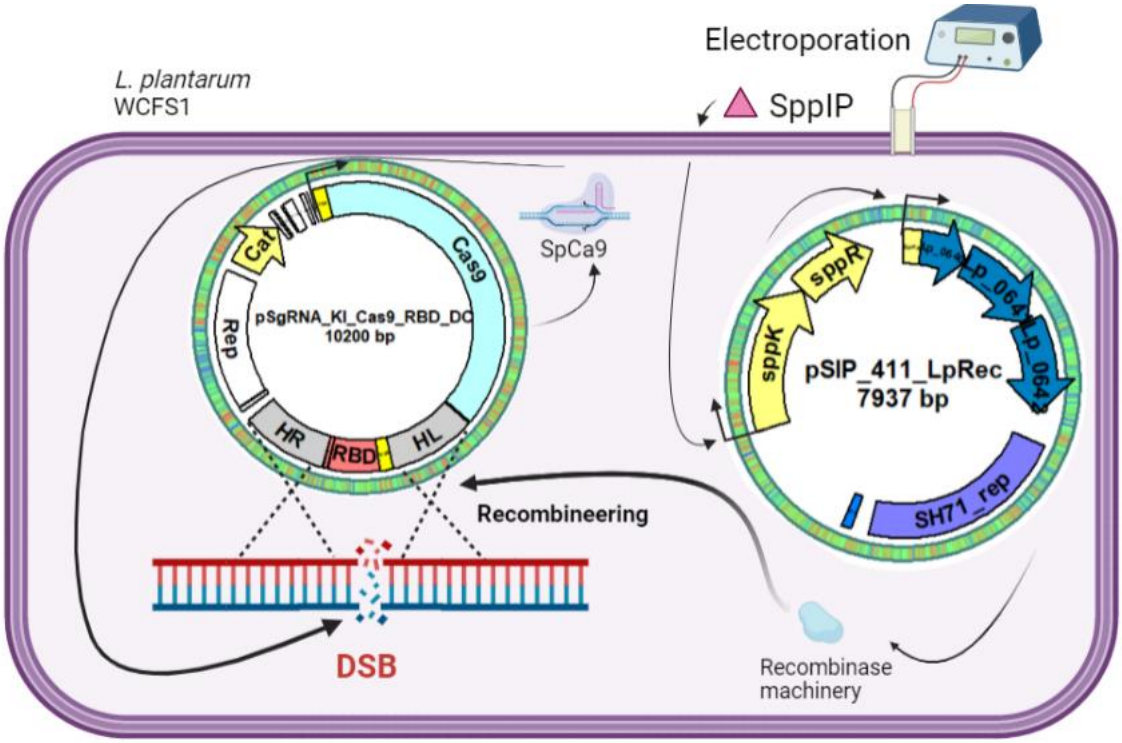

Figure 3.8. The CRISPR/Cas9 two-plasmid knock-in system I in *L. plantarum* WCFS1. *L. plantarum* WCFS1 harbouring the recombinase machinery under the inducible promotor P_{sppA} is induced before transformation of the CRISPR/Cas9 plasmids. This makes the recombinase machinery being expressed prior to introducing CRISPR/Cas9 DSB. Next, the vector responsible for constitutive expression of the sgRNA, inducible expression of SpCas9 and the donor repair template is electro transformed into the *L. plantarum* overexpressing the recombinase machinery. SpCas9 is immediately expressed due to the structural genes (section 1.4) from the pSIP_411_LpRec plasmid, sgRNA and SpCas9 assembles, and induces a DSB in the genome. The recombinase machinery then facilities HDR for incorporation of RBD into the genome (knock-in).

For construction of the pSgRNA_KI_Cas9_RBD_DC, used in the CRISPR/Cas9 knock-in system I, In-Fusion primer SgRNA_LpRec_F and SgRNAKI1_HA_Cas9_R (Table 2.2) were used to PCR amplify the gene encoding SpCas9, and promoter P_{sppA} from pSIP_403_pCas (Figure 3.9). Subsequently, the pSgRNA_KI_RBD_DC was digested with XhoI and Acc65I. Next, the P_{sppA} and SpCas9 were inserted in pSgRNA_KI_RBD_DC XhoI/Acc65I vector by In-Fusion, yielding the pSgRNA_KI_Cas9_RBD_DC. The plasmid was cloned in *E. coli* Stbl2™ Competent cells and grown at 30 °C.

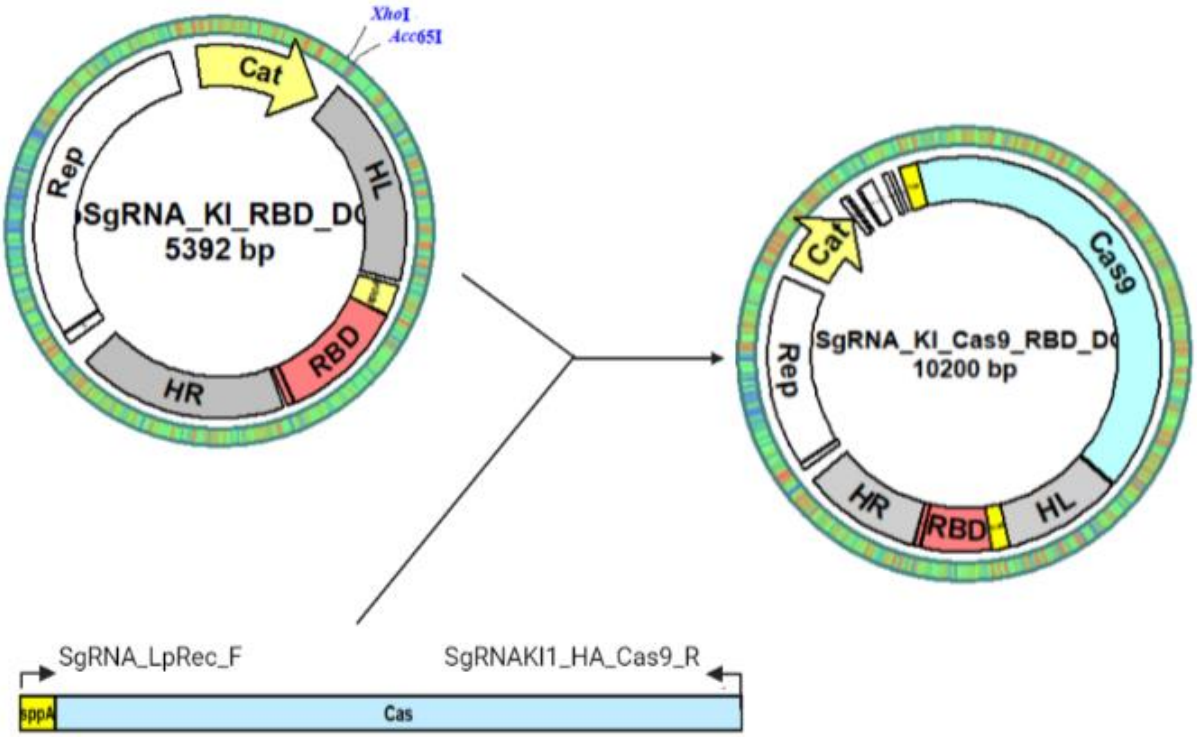

Figure 3.9. Strategy for constructing pSgRNA_KI_Cas9_RBD_DC. pSgRNA_KI_RBD_DC was used as the backbone for insertion of inducible SpCas9 by In-Fusion. The P_{sppA} promoter and SpCas9 encoding gene were PCR amplified from the pSIP_403_pCas vector. The vector contained *cat* gene, responsible for chloramphenicol resistance and the replicon pUC ori and a Rep_{256}.

To test the CRISPR/Cas9 knock-in system I, 1 µg of pSgRNA_KI_Cas9_RBD_DC was electroporated to *L. plantarum* WCFS1 harbouring pSIP_411_Lp_Rec. The transformation mix was incubated for 0-, 1-, 2-, 3-, 4-, 6-, 8-, and 18 hours before 100µL was spread on MRS agar plates containing chloramphenicol (Cm) and erythromycin (Ery). One colony appeared on the plate spread with transformation mix three hours after transformation, while no colonies grew on the plates spread at any of the other seven time-points. The experiment was replicated three

times, with the same result. The three transformants, one transformant from each experimental round, were screened with colony PCR with primer pair 2071-2074_F and 2071-2074_R (Table 2.2). One of the transformants was confirmed to be a RBD_DC knock-in (WCFS1::RBD) under the control of the inducible promoter P_{sppA} (WCFS1::RBD) (Figure 3.10). *L. plantarum* WCFS1 (WT) was used as a control of unsuccessful knock-in, and shows a band at ~2500 bp. The total length of RBD_DC with the inducible promoter P_{sppA} is ~800 bp, meaning the band at ~3350 bp indicates a knock-in of RBD_DC with P_{sppA}.

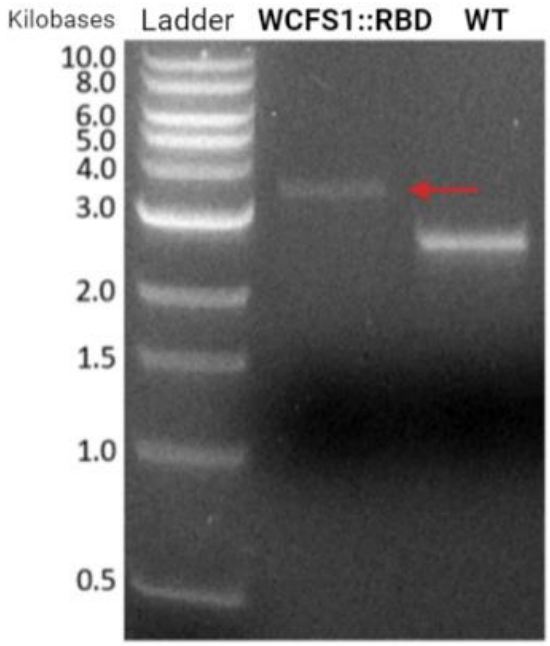

Figure 3.10. Colony PCR verification of knock-in of RBD in the genome of *L. plantarum* WCFS1. Well number 1) GeneRuler™ 1 kb DNA ladder. Well 2) Transformant after transformation with the CRISPR/Cas9 knock-in system I (~3350 bp). Well 3) *L. plantarum* WCFS1 wildtype strain (WT) (~2500 bp).

One of three transformants was validated as knock-in. The successful knock-in of RBD was sent to Sanger sequencing which revealed precise insertion of the RBD and the inducible promoter P_{sppA} exactly at the site of DSB. However, knock-in efficiency was low.

To increase transformation efficiency, as this was thought to correlate with knock-in efficiency, a pre-study was conducted. 0.5-, 1.5-, 3.5-, and 4.5 µg of pSIP_RBD_DC was electro-transformed to *L. plantarum* WCFS1. The experiment revealed a linear increasement of transformants with increased plasmid quantity (Figure 3.11). The experiment was not replicated, since it was only meant to be an indicator of plasmid transformation efficiency. In regards to the findings, 5µg pSgRNA_KI_Cas9_RBD_DC was electroporated to *L. plantarum*

WCFS1 harbouring pSIP_411_Lp_Rec (CRISPR/Cas9 knock-in system I). The transformation mix was incubated for 3 hours and 250µL mix was plated on MRS/Ery/Cm agar. However, zero transformants emerged.

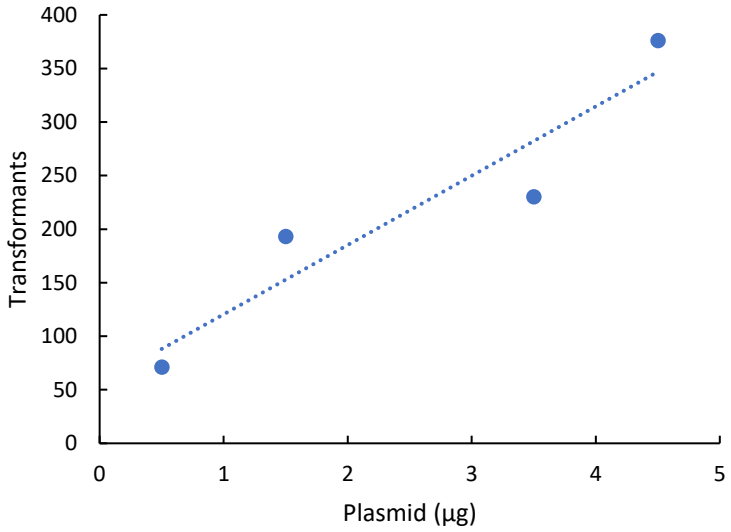

Figure 3.11. Transformation efficiency in *L. plantarum* according to plasmid quantity. 0.5-, 1.5-, 3.5-, and 4.5 µg of pSIP_RBD_DC was electro-transformed to *L. plantarum* WCFS1. The transformation mix was incubated for 3 hours before 50 µL was spread on MRS agar containing Cm.

The pSgRNA_KI_Cas9_RBD_DC vector was electroporated in various quantities to find the optimum transformation quantity for the CRISPR/Cas9 knock-in system I. 0.3-, 0.5-, 1-, 1.5-, 3- and 5 µg of the pSgRNA_KI_Cas9_RBD_DC was transformed to *L. plantarum* WCFS1 harbouring the pSIP_411_Lp_Rec vector. The transformation mix was incubated for 3 hours before it was spread on MRS/Ery/Cm agar plates. This time, one transformant emerged from each transformation. All colonies were screened with colony PCR, but only the transformant transformed with 1.5µg pSgRNA_KI_Cas9_RBD_DC was PCR verified to be knock-in of RBD. In total two knock-ins were constructed using transformation with 1 and 1.5 µg plasmid and 3 hours incubation of the transformation mix at 37 °C. All colonies appeared after 48 hours.

Since SpCas9, has previously shown cytotoxicity in bacteria(Arroyo-Olarte et al., 2021), induction of the inducible CRISPR/Cas9 knock-in system I was induced with SppIP after transformation to increase the number of transformants (Figure 3.12). Previously, the inducible CRISPR/Cas9 knock-in system I had been induced at step 1 (in the making of electrocompetent *L. plantarum* harbouring pSIP_411_LpRec). This time, the cells were induced after incubation

of the transformation mix at step 2, 3, 4 or 5 (Figure 3.12). To verify proper induction a control strain *L. plantarum* WCFS1 harbouring plasmid-based expression of the fluorescent mCherry, pSIP_mCherry (Table 3.1) was used. Red colonies from the *L. plantarum* pSIP_mCherry strain would appear on the agar plates to indicate proper induction of the pSIP expression system with SppIP. All steps except step 2 and 5b were validated for proper induction of the pSIP system. Step 2 was constructed to induce the transformation mix when spread directly on MRS/Ery/Cm agar containing 25 and 50 ng/mL SppIP. However, this resulted in a complete lack of transformants. Step 3 allowed the transformants to grow, before the *L. plantarum* harbouring the CRISPR/Cas9 knock-in system I was induced by transferring the transformants to MRS/Ery/Cm/SppIP agar, using a stamp. During step 3 all transferred transformants grew, 32 transformants were screened, but the induction failed to insert RBD. Step 4 was created to prevent stress from the pSIP expression system, by allowing the culture to be grown to OD_{600}~0.3 before induction with SppIP. The culture was either spread on a) MRS/Ery/Cm agar containing 25 or 50 ng/mL SppIP or b) MRS/Ery/Cm lacking SppIP. >300 colonies grew on a and b, 14 colonies from each plate were screened, yet no colonies could be verified as knock-ins.

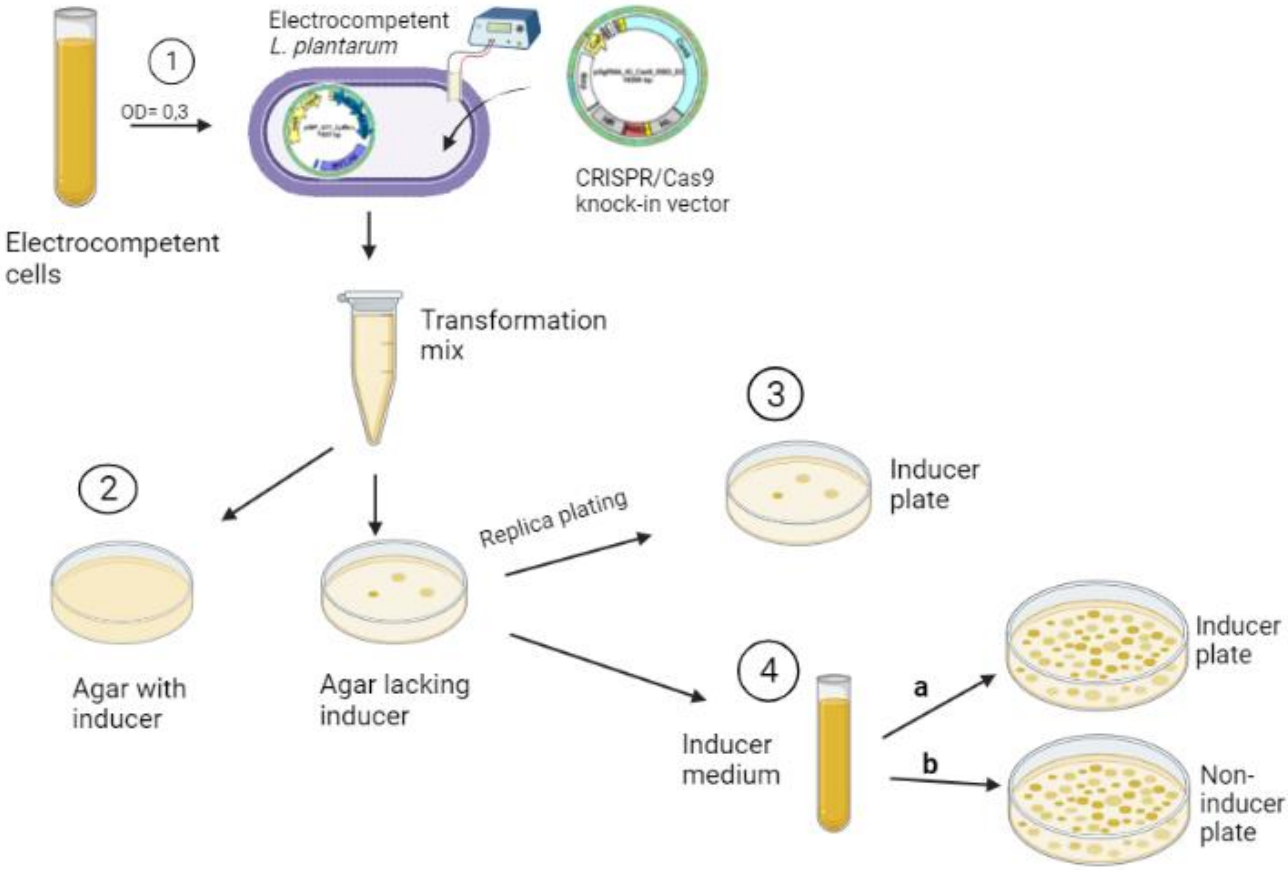

Figure 3.12. Inducing the CRISPR/Cas9 knock-in system at various steps. The CRISPR/Cas9 system was induced with 25 ng/mL inducer pheromone, SppIP, either at step 1,2,3,4 or 5. Step 1: *L plantarum* WCFS1 was induced with 25 ng/mL SppIP in the making of the electrocompetent cells. Step 2: 100µL transformation mix was plated after 0-, 1-, 2-, 3-, 4-, 8- and 18 hours on MRS/Ery/Cm agar plates containing 25 and 50 ng/mL SppIP. Step3: Uninduced transformants were transferred to MRS/Ery/Cm agar containing 50 ng/mL SppIP. Step 4: The uninduced transformant was picked with a toothpick and transferred to a tube containing liquid MRS/Ery/Cm. The culture was grown for 18 hours, then diluted to OD_{600}~0.1 and induced with 25 or 50 ng/mL SppIP before plated on MRS/Ery/Cm agar lacing or containing SppIP. Step 4 was also conducted by cultivation of an uninduced transformant for 48 hours in liquid MRS/Ery/Cm containing 25 ng/mL sppIP. In step 4 the culture was spread on either a) agar with 25 and 50 ng/mL SppIP or b) agar lacking SppIP After plating, the colonies were screened with colony PCR using the primer pairs 2071-2074_Sek_F and 2071-2074_Sek_R.

By not inducing the CRISPR/Cas9 knock-in system I at any point, the system was still expressed and two knock-in appeared. Transforming 1 µg pSgRNA_KI_Cas9_RBD_DC to *L. plantarum* WCFS1 harboring pSIP411_LpRec which were not induced before transformation of pSgRNA_KI_Cas9_RBD_DC. Two out of 32 transformants were verified by colony PCR as knock-ins of RBD (Figure 3.13). Out of the 32 transformants (figure does not show all 30 negative transformant) the two knock-ins were from transformation mix spread after 3 hours

(Figure 3.13 A). None of the transformant spread after 18 hours were found to be knock-ins (Figure 3.13 B).

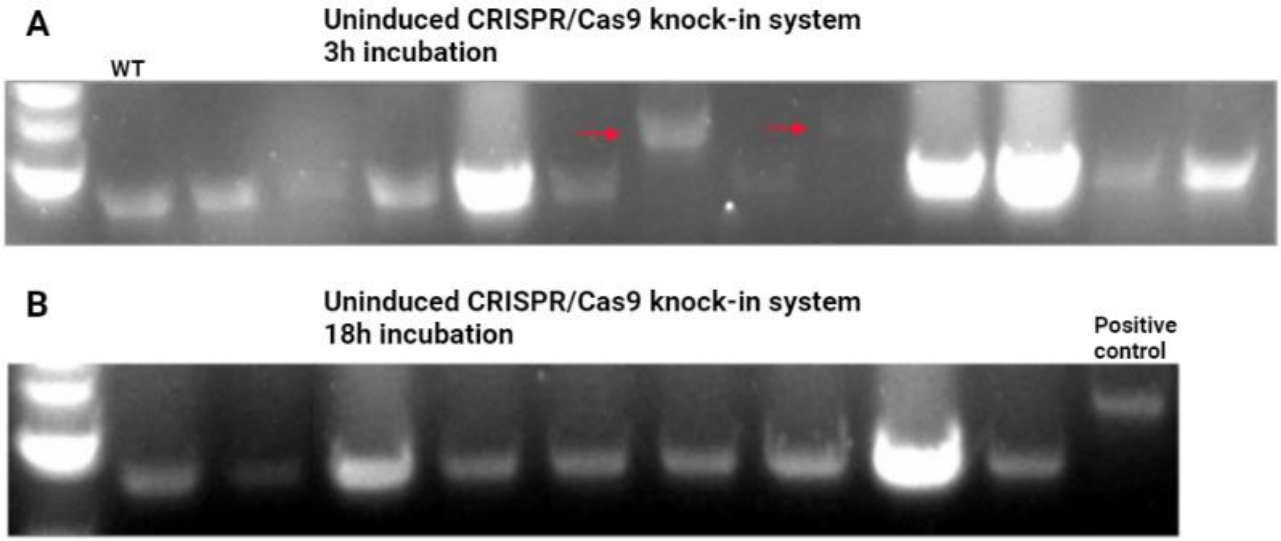

Figure 3.13. Colony PCR of uninduced *L. plantarum* WCFS1 harbouring the CRISPR/Cas9 knock-in system I. (A) Shows uninduced *L. plantarum* WCFS1 harbouring the CRISPR/Cas9 knock-in system I spread 3 hours post transformation. Verifications of two knock-ins of RBD_DC are shown with a red arrow (B) Shows uninduced *L. plantarum* WCFS1 harbouring the CRISPR/Cas9 knock-in system I spread 18 hours post transformation.

3.2.6 Knock-in of lipoprotein anchored RBD and constitutive expression of RBD

The CRISPR/Cas9 two-plasmid knock-in system I was successful, and after proof-of-concept, the goal was to achieve constitutive expression of RBD_DC and to anchor the RBD_DC to the cell membrane of *L. plantarum* WCFS1. Restriction enzyme SapI was used to digest the CRISPR/Cas9 knock-in vector (pSgRNA_KI_RBD_Cas9) to remove the inducible promoter P_{sppA} and RBD_DC (supplementary A-1). At the same time, pLp1261_RBD_DC and pSIP_SlpA_RBD_DC were used as templates with primer pairs pSppA_RBD_fwd and KI1_HR_RBD_R, and HL_SlpA_RBD_F and KI1_HR_RBD_R (Table 2.2), respectively, to obtain two new knock-in sequences. In-Fusion cloning was utilized to insert the PCR knock-in fragments into the digested pSgRNA_KI_RBD_Cas9 to obtain the vectors pSgRNA_KI_1261_RBD_Cas9 and pSgRNA_KI_SlpARBD_Cas9 (Table 3.3). For construction see supplementary A-1. Both vectors were transformed into *E. coli* and then transformed into induced (stage 1, Figure 3.12) and non-induced *L. plantarum* WCFS1 harboring the pSIP_411_LpRec vector (Table 3.3). 116 transformants were screened, no transformants were verified as knock-ins.

Table 3.3. Induced and uninduced CRISPR/Cas9 knock-in system I for knock-in of 1261_RBD_DC and SlpA_RBD. 1 mL are spread on agar plates from the transformation mix of the induced cells, and 100 µL are spread from the non-induced cells.

Experimental rounds	Induced	Insert	Screened[a] / colonies[b]
3	Yes	1261_RBD	49/70
1	No	1261_RBD	46/46
1	Yes	SlpA_RBD	4/4
1	No	SlpA_RBD	17/17

[a] Total number of transformants screened with colony PCR

[b] Total number of transformants appearing after transformation of the CRISPR/Cas9 knock-in system

3.3 Development of CRISPR/Cas9 knock-in system II

The CRISPR/Cas9 knock-in system I in *L. plantarum* WCFS1 was proven to be successful, nevertheless the system was inefficient and failed to knock-in larger inserts like lipoprotein anchored RBD_DC and constitutive RBD_DC. Optimization of the CRISPR/Cas9 knock-in system was proceeded by constructing a new two-plasmid CRISPR/Cas9 knock-in system, referred to as system II (Figure 3.15). To increase the elimination of unedited cells by SpCas9, the nuclease was inserted to the high-copy, broad-host-range vector pSIP_411_SH71 (Table 3.1), yielding the pSIP_411_Cas9_LpRec vector (Table 3.1, Figure 3.14)

pSIP_411_Cas9_LpRec was constructed by restriction cutting of the pCas9_SH71 vector with restriction enzymes XhoI and XmaI. Next, the *L. plantarum* homologous *lp_0640-lp_0642* genes, were PCR amplified from the pSIP_411_LpRec with primer pairs Cas9-LpRec_F and Cas9-LpRec_R (Table 2.2). The PCR product was then digested with XhoI and XmaI before the insert and the vector were ligated by ElectroLigase (Section 2.7.3) to gain pSIP_411_Cas9_LpRec. The plasmid was subcloned into *Lactococcus lactis* before transformed to *L. plantarum* WCFS1.

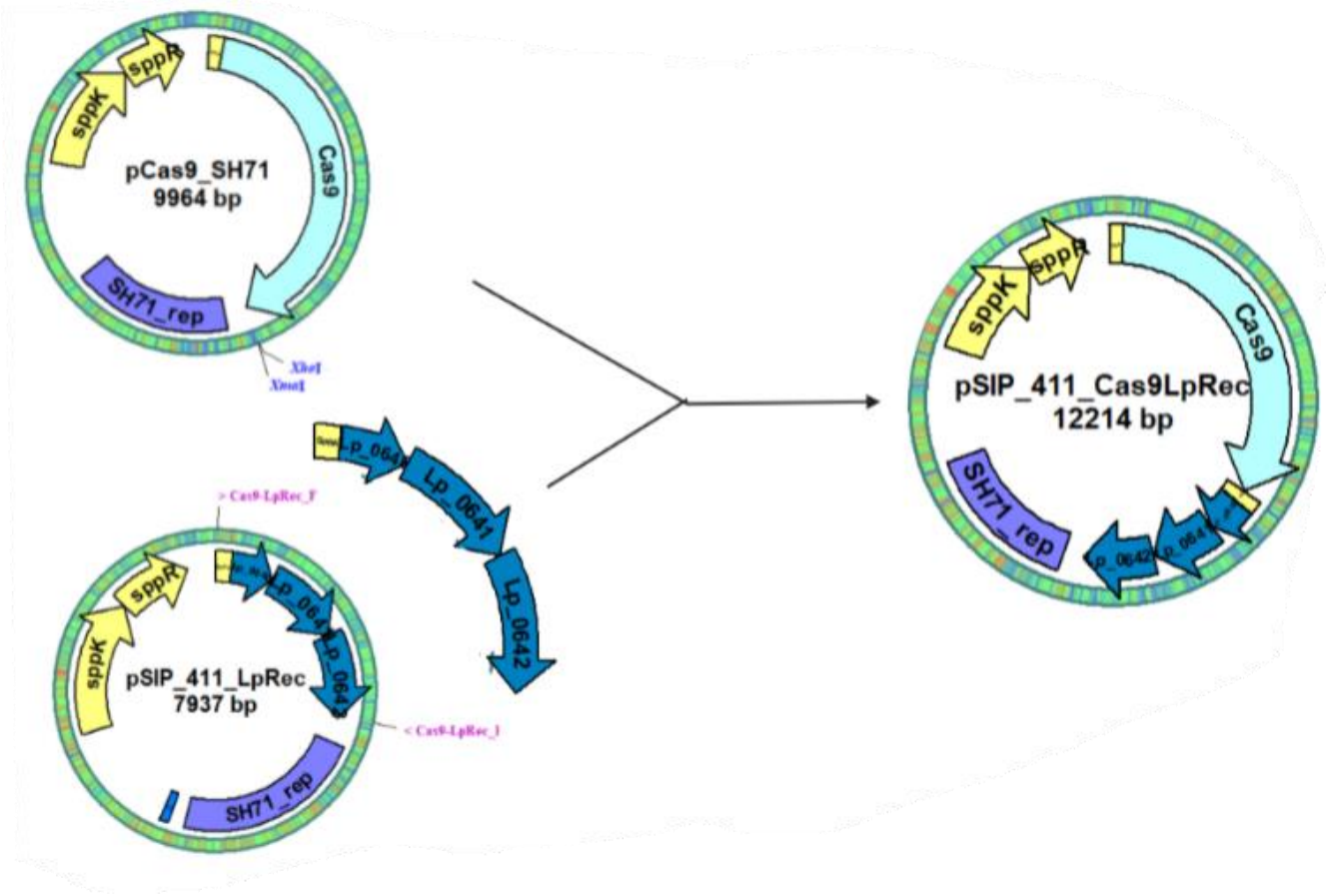

Figure 3.14. Strategy to construct the pSIP_411_Cas9_LpRec. The recombinase machinery encoded from the lp_0640-lp_0642 genes, was PCR amplified with primer pair Cas9_LpRec_F and Cas9_LpRec_R. Next, both the PCR product and the pCas9_SH71 vector were digested with XhoI and XmaI. ElectroLigase was used to ligate the fragments, yielding pSIP_411_Cas9_LpRec. The vector contains the broad-host-range, high copy number replicon Rep_{SH71} and selection marker Ery.

The pSIP_411_Cas9_LpRec vector was transformed to *L. plantarum* WCFS1. The gene encoding SpCas9 and the inducible promoter was Sanger sequenced after transformation to *L. plantarum*, and no mutations were discovered. The *L. plantarum* WCFS1 harboring SpCas9 and the recombinase machinery were made electrocompetent with (step 1, Figure 3.12) with and without induction of the cells. Targeting repair vectors (Figure 3.15), containing gRNA and a donor repair template (pSgRNA_KI_RBD_DC, pSgRNA_KI_RBD_DC and pSgRNA_KI_RBD_DC, Table 3.1) were electro-transformed to the competent cells (Figure 3.15), to obtain knock-ins of RBD_DC, lipoprotein anchored RBD_DC and constitutive expression of RBD_DC.

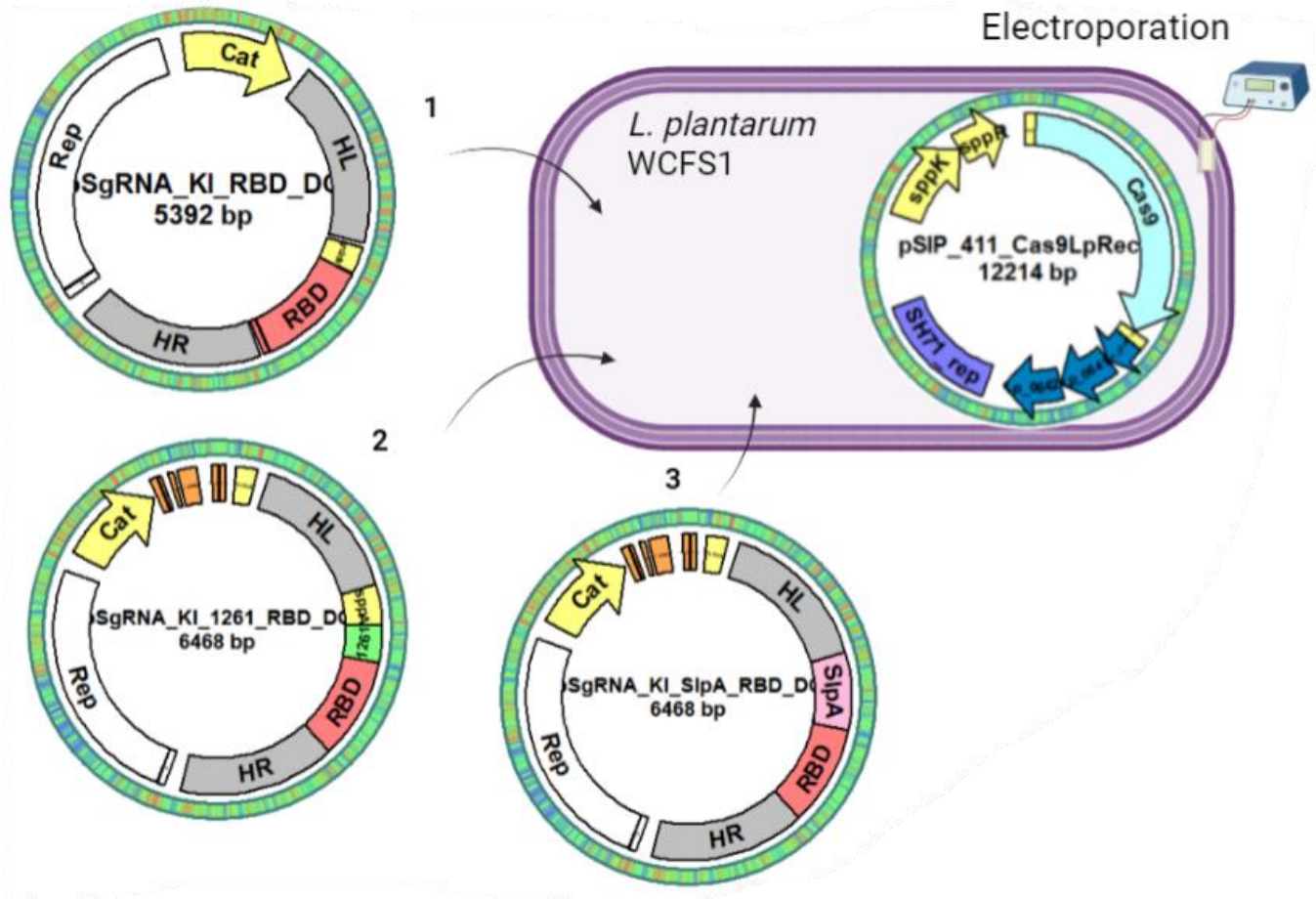

Figure 3.15. CRISPR/Cas9 knock-in system II. Targeting repair vectors 1, 2, and 3 were individually transformed to *L. plantarum* WCFS1 harbouring the high-copy-number, broad-host-range vector pSIP_411_Cas9_LpRec. The cells had 1) already been induced with 25 ng/mL inducer pheromone, SppIP, upon the making of the electrocompetent cells (Figure 3.12, step 1) or 2) not induced. Transformation mix was incubated for 3 hours before plating on MRS/Ery/Cm agar.

CRISPR/Cas9 knock-in system II (Figure 3.15) was tested for all three inserts, with variating plasmid concentration, incubation time and with a induced and non-induced system (Table 3.4) >70 transformants were screened with colony PCR, but no knock-in were detected.

Table 3.4. CRISPR/Cas9 knock-in system II. CRISPR/Cas9 knock-in system II was electro-transformed with vectors containing sgRNA, donor repair template (pSgRNA_KI_RBD_DC, pSgRNA_KI_1261_RBD_DC and pSgRNA_KI_SlpA_RBD_DC) and/or additional SpCas9 (pSgRNA_KI_Cas9 RBD_DC, pSgRNA_KI_1261 RBD_DC_Cas9 and pSgRNA_KI_SlpA_RBD_DC_Cas9).

Experi-mental rounds	CRISPR/Cas9 knock-in vector	Plasmid (µg)	Incubation (h)	Induced (Yes/No)	Plated (µL)	Screened[a] /colonies[b]
1	pSgRNA_KI_RBD_DC	0.5	3	Yes	250	14/32
1	pSgRNA_KI_RBD_DC	1	3	Yes	250	8/8
1	pSgRNA_KI_1261_RBD_DC	0.5	3	Yes	250 x 4	24/24
1	pSgRNA_KI_1261_RBD_DC	1	3	Yes	250 x 4	1/1
1	pSgRNA_KI_1261_RBD_DC	3	3	Yes	250 x 4	0
1	pSgRNA_KI_1261_RBD_DC	5	3	Yes	250 x 4	6/18
1	pSgRNA_KI_1261_RBD_DC	1	3	No	100	2/2
1	pSgRNA_KI_1261_RBD_DC	1	18	No	100	10/10
1	pSgRNA_KI_1261_RBD_DC	5	3	No	100	6/18
1	pSgRNA_KI_SlpA_RBD_DC	1	3	Yes	250	10/10
2	pSgRNA_KI_Cas9_RBD_DC	1	3	Yes	250 x 4	0

[a] Total number of transformants screened with colony PCR

[b] Total number of transformants appearing after transformation of the CRISPR/Cas9 knock-in system

3.4 Plasmid curing

Plasmids are extrachromosomal pieces of double-stranded circular DNA which have the capability to replicate independently of the host chromosome. Some plasmids are stable and can be maintained through successive generations (Ruiz-Barba et al., 1991). After knock-in on the genome, it is necessary to remove the editing plasmid. Plasmid curing agents are chemical or physical agents that inhibit the replication of the plasmid resulting in elimination of such plasmids from host population after several replication cycles.

For curing of the erythromycin and chloramphenicol plasmids in *L. plantarum* WCFS1, four different curing strategies were used. All overnight cultures were incubated statically at 37°C without antibiotics. 10 µL was transferred to fresh MRS to avoid the death phase of the growth curve. Each day 100 µL of the new overnight culture was spread on BHI agar plates containing erythromycin (Ery), chloramphenicol (Cm) and Ery/Cm agar to check for loss of plasmids.

The first method was based on an overnight culture lacking curing agents. The second method was based on an overnight culture which was induced with 25 ng/mL SppIP. The third method included an overnight culture supplied with fresh medium every 2-3 days. The fourth method included an overnight culture which was supplied with sodium dodecyl sulphate (SDS) with concentration ranging from 0.1-100 mg/mL SDS and incubated for 72 hours. The fourth method was based on the method in Ruiz-Barba et al., (1991). After inoculation of the culture with SDS, the culture with the highest concentration of SDS with visible growth, was spread on MRS agar plate without antibiotics. Next, replica plating was performed according to section 2.15. for negative selection of the plasmid cured bacteria.

Plasmid curing according to the method used in Ruiz-Barba et al., (1991) was time consuming and not very effective. Inoculation of the knock-in strain in 10 mL MRS lacking antibiotics (-AB) followed by negative selection by replica plating, was found to be the most time saving curing method. Within three days, 15% of the plated colonies were plasmid cured of both plasmids. One of the plasmid-cured colonies were chosen for further characterizations.

3.5 Growth curve analysis of recombinant *L. plantarum*

The growth curve analysis was performed to examine how expression of the RBD antigen, either expressed from plasmid and/or from the genome, influenced the growth of *L. plantarum* WCFS1. After induction of the bacteria (Section 2.16), 200 µL of culture were transferred to a 96 well microwell plate and OD595 was measured for 20 hours. The growth of the recombinant strains expressing RBD both from plasmids and from the genome were plotted in a graphical representation (Figure 3.16). The analysis included *L. plantarum* WCFS1 wildtype (WT) and *L. plantarum* WCFS1 harbouring the pEV as controls, *L. plantarum* knock-in of RBD (KI::RBD) with and without pEV, *L. plantarum* WCFS1 harbouring the plasmids of cytoplasmic expression of RBD ,pSIP_RBD_DC and pSIP_SlpA_RBD_DC. In addition to *L. plantarum* WCFS1 harbouring pLp1261_RBD_DC. The growth curve analysis was repeated with similar results. As expected, lipo-protein anchoring shows a significant reduction in

growth. Compared to the wildtype *L. plantarum* WCFS1, none of the recombinant strains with cytoplasmatic expression of RBD showed a reduction in growth.

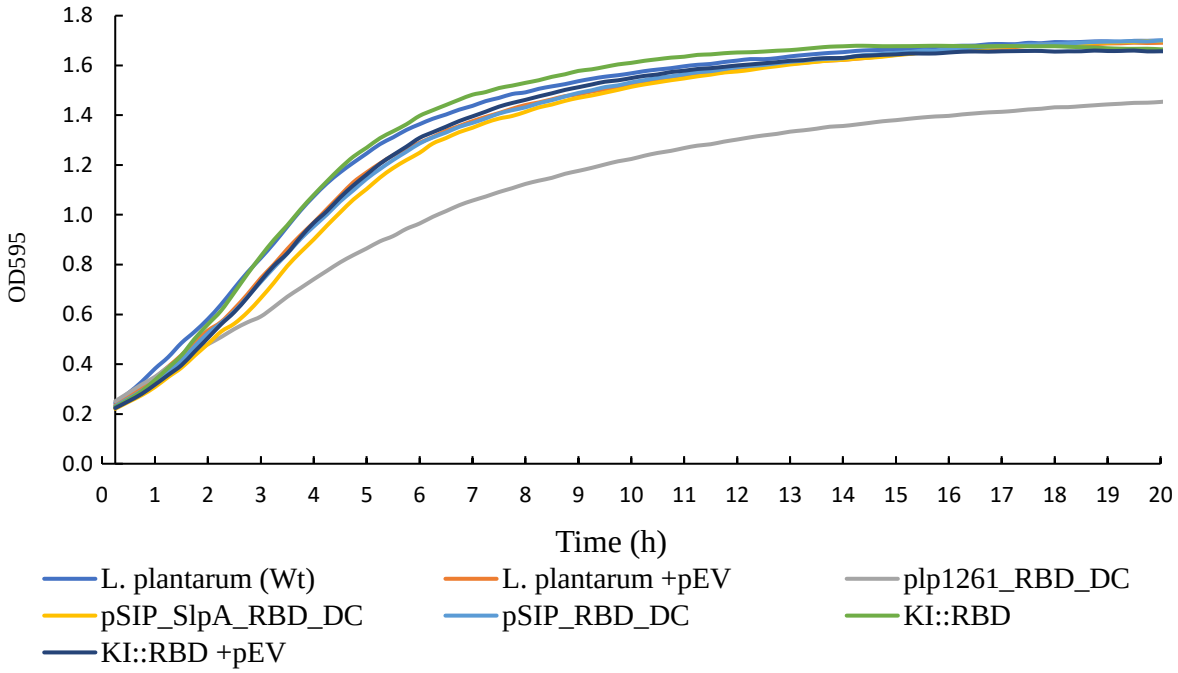

Figure 3.16. Growth curve of recombinant *L. plantarum* expressing RBD from the genome and plasmids. The growth of the recombinant strains were monitored by OD_{595} every fifth minutes for 20 hours. The presented results are an average of two independent experiments with three technical replicas each.

3.6 Detection of RBD antigen expressed from the genome by Western Blot analysis

Western blot analysis was used to verify the production of RBD from the genome located *RBD* gene (Figure 3.17). *L. plantarum* WCFS1 harboring plasmid-based cytoplasmatic expression of RBD were included as controls. The samples were harvested three hours post induction with 25 ng/mL SppIP (Section 2.17) and cell lysis using glass beads (Section 2.18). Next, the cell free protein extract was run on an SDS-PAGE (Section 2.19), before blotting the proteins onto a nitrocellulose-membrane (Section 2.20.1). The proteins were hybridized with specific antibodies using the SNAP i.d. immunodetection system (Section 2.20.2). Lastly, the proteins were visualized by chemiluminescence (Section 2.20.3, Figure 3.17). *L. plantarum* WCFS1 harbouring pEV was included as a negative control and as expected, it was not detected any band correlating to correct size of RBD. Compared to plasmid-based expression of RBD (pLp1261_RBD_DC, pSIP_SlpA_RBD_DC and pSIP_RBD_DC), genomic based expression of RBD showed a very faint, but detectable band. The theoretical molecular weights of the

proteins were 33 kDa (pLp1261_RBD_DC) and 25 kDa (SlpA_RBD_DC, pSIP_RBD_DC and KI::RBD + pEV), which correlated with the detected bands (Figure 3.17).

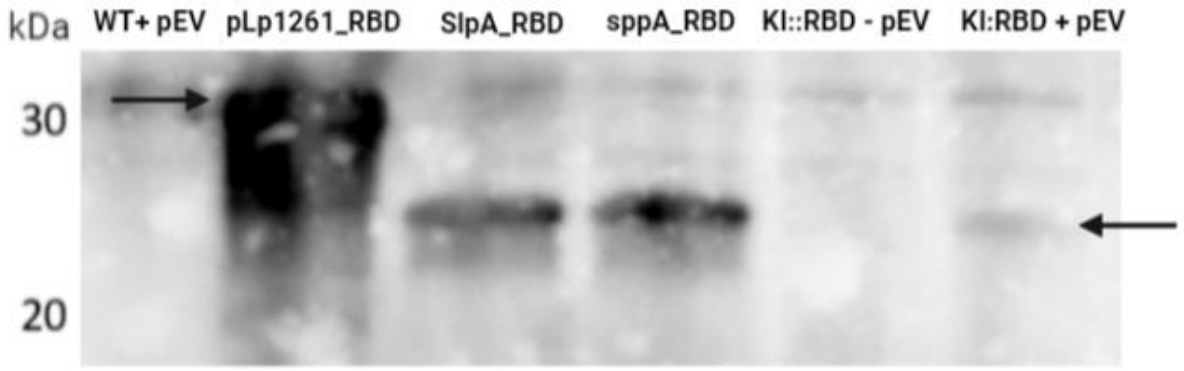

Figure 3.17. Verification of RBD expressed from the genome of *L. plantarum* WCFS1 by Western blotting 1) *L. plantarum* WCFS1 wild type strain harbouring the expression cassette pEV. 2) plasmid-based expression of lipoprotein anchored RBD (pLp1261_RBD_DC) 3) Plasmid based expression of RBD downstream the constitutive promoter (pSIP_Slpa_RBD_DC) 4) Plasmid-based cytoplasmatic expression of RBD pSIP_RBD_DC. 5) KI::RBD lacking expression cassette pEV. 6) Cytoplasmatic RBD expressed from the genome (KI::RBD_DC + pEV) The RBD band at about 25 kDa is indicated by an arrow.

To characterize RBD expression from the genome over time, a second Western blot analysis was performed (Figure 3.18). Samples of the knock-in strain of RBD harboring pEV (KI_RBD + pEV) and *L. plantarum* WCFS1 harboring plasmid-based expression of RBD (pSIP_RBD_DC) were harvested at different time points (from 2 to 18 hours) after induction. This was done to compare genomic-based antigen production from the knock-in of RBD over time, compared to plasmid-based antigen production in *L. plantarum*. The Western blot analysis showed strong bands of the cytoplasmatic RBD expressed from the plassmid 2 to 6 hours post induction, and faint bands from the bacteria harvested 8 and 18 hours after induction (Figure 3.18). KI::RBD harbouring the pEV revealed faint bands 2 to 4 hours after induction, and the strongest band from genomic expression was from the one harvested 3 hours after induction.

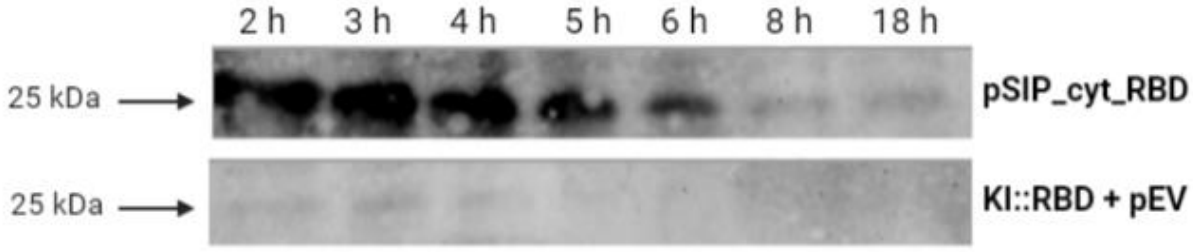

Figure 3.18. Genomic expression of RBD from *L. plantarum* WCFS1 over time. Plasmid based expression of RBD (at the top) and genomic expression of RBD (at the bottom). Well number 1) Samples harvested 2 hours past induction. 2) Samples harvested 3 hours past induction. 3) Samples harvested 4 hours past induction. 4) Samples harvested 5 hours past induction. 5) Samples harvested 6 hours past induction. 6) Samples harvested 8 hours past induction. 7) Samples harvested 18 hours past induction. The RBD band at about 25 kDa is indicated by an arrow.

To test dose-response the inducer pheromone was added to the cultures to a final concentration of 8- 100 ng/mL (Figure 3.19). All samples were harvested 3 hours after induction. Genomic expression did not show a clear dose response, only faint bands from all induced samples were detected. RBD expressed from the plasmid showed a clear dose-response. Plasmid-based expression showed a faint band from the sample induced with 8 ng/mL SppIP, and stronger bands in the samples induced with 25 and 50 ng/mL SppIP.

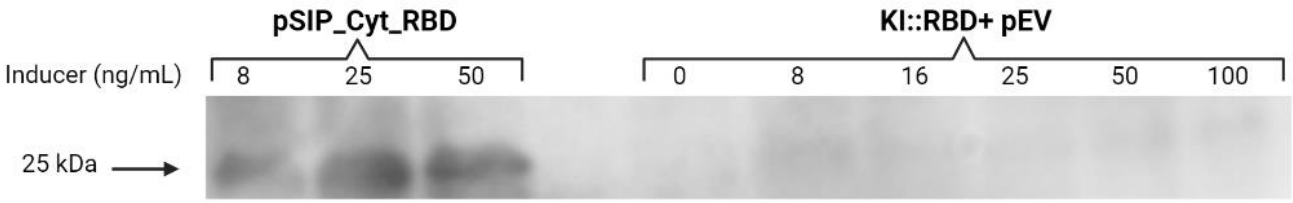

Figure 3.19. Dose-response of genomic expressed RBD. Well number 1) Plasmid-based expression induced with 8 ng/mL SppIP. 2) Plasmid-based expression induced with 25 ng/mL SppIP. 3) Plasmid-based expression induced with 50 ng/mL SppIP. 4) empty well. 5) RBD expressed from the genome induced with 0 ng/mL SppIP. 6) RBD expressed from the genome induced with 8 ng/mL SppIP. 7) RBD expressed from the genome induced with 16 ng/mL SppIP. 8) RBD expressed from the genome induced with 25 ng/mL SppIP. 9) RBD expressed from the genome induced with 50 ng/mL SppIP 10) RBD expressed from the genome induced with 100 ng/mL SppIP.

3.7 Fluorescence analysis with genomic expression of mCherry for characterization of genomic expression

L. plantarum WCFS1 knock-in of the fluorescent reporter gene, mCherry (Table 3.1) was used in a quantitative dose-response analysis of protein expression to quantify genomic expression, due to low expression by using Western blotting with the RBD knock-in (Figure 3.20). The knock-in of mCherry was made in-house by using CRISPR/Cas9 system I (Wiull unpublished). The overnight culture of the knock-in strain of mCherry was diluted to OD_{600}=0.15 and grown to OD_{600}~0.3, and induced with either 0, 1, 2, 4, 8, 16, and 25 ng/mL SppIP. 200µL sample was transferred to a microtiter plate and fluorescence was measured every 15 minutes for 17 hours, in a plate reader. The samples were measured in triplicates and the experiment was performed with two parallels. The graph was plotted from the measurements taken 3 hours post induction

and normalized according to growth. *L. plantarum* WCFS1 harboring pEV was used as a negative control. Uninduced expression of mCherry from knock-in strain of mCherry harboring the pEV were measured at the same value as the negative control, meaning that the expression of mCherry by P_{sppA} was thoroughly controlled. The fluorescent measurements showed a clear dose-response, with a positive correlation between the concentration of 1-25 ng/mL SppIP and the expression of mCherry.

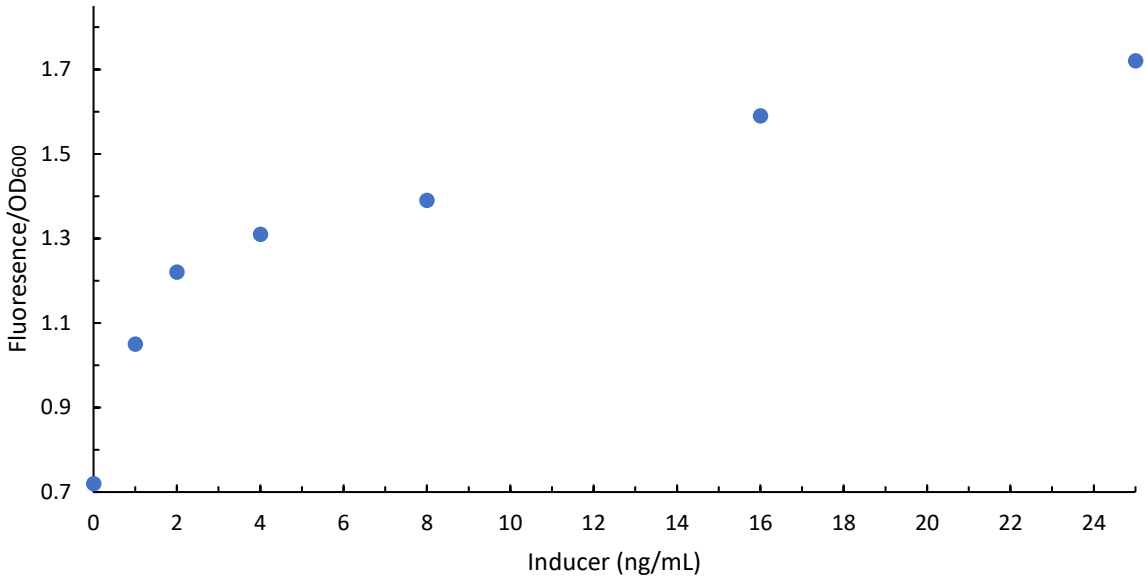

Figure 3.20. Dose-response with *L. plantarum* WCFS1 knock-in strain of mCherry. Dose-response of mCherry expressed from the genome 3 hours post induction. The presented results are an average of two parallel experiments with two technical replicas each.

4 Discussion

4.1 CRISPR/Cas9 knock-in systems in *L. plantarum* WCFS1

Genome editing is essential for probing genotype-phenotype relationships in industrial bacteria. Although CRISPR/Cas9 genome editing is successful in some model strains, CRISPR/Cas9-based genome editing has been slow to extend to the multitude of industrially relevant bacteria (Hsu et al., 2014; Vento et al., 2019; Zhang et al., 2018). Recent studies have successfully deleted and inserted small sequences in some bacteria (Hidalgo-Cantabrana et al., 2019; Jiang et al., 2017; Leenay et al., 2019). However, the efficiency of genome editing in bacterial strains are low (Leenay et al., 2019). Overexpression of the *Streptococcus pyogenes* Cas9 (SpCas9) to introduce double-stranded breaks (DSBs) have shown toxic and even lethal effects (Misra et al., 2019). E.g., in *Corynebacterium glutamicum* CRISPR/Cas9 results in a complete absence of transformants (Jiang et al., 2017). If the endogenous DSB repair system (HDR or NHEJ) in the bacteria is insufficient, the DSB is lethal (Amarh & Arthur, 2019). The present study aims to overcome the barriers of CRISPR/Cas9 genome editing by developing a tailored CRISPR/Cas9 system for integration of antigens into the genome of *L. plantarum* WCFS1. The ultimate goal was to develop a SARS-CoV-2 selection marker-free mucosal vaccine by knock-in of RBD into *L. plantarum* WCFS1. CRISPR/Cas9 editing in bacteria can be effective for smaller insertions and deletions. However, effective insertion and deletion size are generally less than 25 bp (Yoo et al., 2022), while large deletions and especially insertions of larger fragments like antigens are challenging (Ceasar et al., 2016; Vento et al., 2019). By developing and optimizing a fast and efficient CRISPR/Cas9 knock-in system in *L. plantarum* WCFS1, genes might be easily implemented into the bacteria.

There are many barriers to overcome for CRISPR/Cas9 genome editing in bacteria in order to be successful and efficient. Firstly, HDR which is necessary for knock-in, is not effective enough and shows low editing efficiency (Abdullah et al., 2020). Once DSBs occurs, most industrial bacteria prefer the NHEJ pathway over HDR, even when supplying an exogenous donor repair template which retards knock-in efficiency (Zhang et al., 2020). Secondly, successful CRISPR/Cas9 genome engineering in bacteria is limited by the widely varying target activity of the single guide RNA (sgRNA). Previous sgRNA activity prediction models that were trained on mammalian cells dataset is inadequate for genome editing in bacteria (Guo et al., 2018). A highly effective sgRNA for genome editing is important since it increases DSBs, thus also improves the negative selection caused by SpCas9, which further could increase the genome editing frequency. In addition, sgRNA DSB efficiency is dependent on a high level of

expression, thus the sgRNA should be inserted downstream a strong promoter. Unfortunately, finding suitable RNA pol III promoters is difficult (Zhang et al., 2020). Thirdly, high expression of SpCas9 affects the growth and recovery rate of the host bacteria after transformation and can often cause fatal damage to the cells even without the nuclease activity (Cui & Bikard, 2016; Jiang et al., 2017; Zhang et al., 2020).

A previous study indicated that CRISPR/Cas9 was unable to generate any recombinants in *L. plantarum* WCFS1 without overexpression of a recombinase (Huang et al., 2019). In the present study, a similar experiment was conducted to conclude whether overexpression of the recombinase machinery was necessary. By this mean, the pSgRNA_KI_RBD (Figure 3.7) was electroporated into *L. plantarum* WCFS1 already harbouring pCas_SH71 (Table 3.1). To ensure sufficient available SpCas9 in the cells, 25 ng/mL inducer pheromone was immediately added to the transformation mix to initiate expression of SpCas9. A few colonies appeared. Nevertheless, in accordance with Huang et al., (2019), CRISPR/Cas9 failed to achieve genome editing. The appearance of a few colonies might indicate that SpCas9 successfully managed to introduce DSBs and eliminate most of the unedited cells. In addition, these results reinforced the assumption that *L. plantarum* WCFS1 is unable to repair chromosomal breaks via native HDR. This might be due to low expression of the recombinase. Consequently, all following experiments included a recombinase machinery presented on either the pSIP_411_LpRec or the pSIP_411_Cas9_LpRec vector (Table 3.1, Figure 3.14), to increase HDR. To ensure high expression of the recombinase, the *L. plantarum* homologous *lp_0640-lp_0642* genes were expressed from the high-copy number pSIP_411 derivates. Next, the recombinase machinery was incorporated into this study's developed CRISPR/Cas9 knock-in systems.

To achieve knock-in of the receptor binding domain (RBD) of SARS-CoV-2 into *L. plantarum* WCFS1, four essential components were assembled onto a two-plasmid system, see system I (Figure 3.8) and system II (Figure 3.15). Both systems contained the SpCas9 nuclease, a sgRNA, a donor repair template and the overexpression of the *L. plantarum* homologous recombinase machinery. Due to the reported toxicity of SpCas9 in other species (Cui & Bikard, 2016; Jiang et al., 2017), SpCas9 was constructed to be expressed via an inducible promoter, P_{sppA}, where SpCas9 expression was strongly repressed without the inducer pheromone present (Figure 3.5). This might be most important for species where SpCas9 results in a complete lack of colonies, which is not the case for *L. plantarum* WCFS1.

To mediate knock-in, donor repair templates were constructed to facilitate HDR (Figure 3.6 and Figure 3.7). In a comparative genomics and phylogenetic study across 6000 genomes screened, only 22% of the bacteria included genes for NHEJ (Sharda et al., 2020), meaning that *L. plantarum* WCFS1 is most likely to repair the DSB by recombineering. To increase the low HDR efficiency, donor repair templates were made to facilitate HDR. The donor repair template for HDR was initially constructed both as a linear double-stranded (ds) PCR product (Figure 3.6), and as a circular donor repair template plasmid (Figure 3.7).

The construction of the donor repair template influences editing efficiency. However, the optimal construction of the donor repair template, varies as it is dependent on the cells preferred repair pathway (Song & Stieger, 2017). During electroporation nucleic acid can enter the cell both as a linearized and plasmid DNA. Nevertheless, linear DNA is more recombinogenic and more likely to be integrated into the host chromosome (Potter & Heller, 2003). Therefore, electroporation of a linearized donor repair template should be more efficient for insertion of targets gene into the genome. When electroporating the donor repair template as a PCR product together with pSgRNA_KI_Cas9 (Figure 3.5), no transformants emerged. The experiment was repeated two times and all the transformation mix (1 mL) was plated. The lack of colonies may be attributed to a highly efficient SpCas9 creating DSBs in all cells, or inefficient HDR due to the choice of donor repair template. The donor repair template constructed as a linearized ds PCR product may not be suitable for the over expressed recombinase machinery in *L. plantarum* WCFS1, thus hindering HDR. Another factor contributing to the absolute lack of colonies when electroporating the ds linear PCR product as a donor repair template could be the low transformation efficiency compared to plasmids. In addition, co-transformation decreases transformation efficiency (Goldsmith et al., 2007), which also could explain the lack of knock-ins.

By inserting the donor repair template and the gene encoding SpCas9 into the pSgRNA_KI vector (Table 3.1), the donor repair template was now available on a plasmid donor, pSgRNA_KI_Cas9_RBD_DC (Figure 3.9). The psgRNA_KI_Cas9_RBD_DC together with the pSIP411_LpRec make up the CRISPR/Cas9 knock-in system I, see Figure 3.8 for in-depth explanation. By transforming the donor repair template in a circular plasmid with CRISPR/Cas9 knock-in system I, one transformant emerged. The experiment was repeated six times with similar results, where two out of the six transformants were successful knock-ins of RBD. The survival of a few colonies and the successful knock-in when using a circular donor template vector might indicate that the overexpressed recombinase machinery from the *L. plantarum*

homologous *lp_0640-lp_0642* genes prefer a circular ds donor repair template to repair the DSB most effectively by recombineering. Other explanations for increased HDR efficiency using the plasmid donor repair template compared to the PCR donor repair template could be because linear DNA fragments are quickly degraded by exonucleases. By incorporating the donor repair template in a vector, the donor repair template is probably no longer prone to degradation from the exonucleases inside the bacterial cell. In addition, CRISPR/Cas9 knock-in system I, which takes advantage of the circular donor repair template is not co-transformed together with a vector containing the gene encoding SpCas9, because the gene is already inserted in the donor repair template vector (Figure 3.8). Thus, increasing transformation efficiency and possibly recombination efficiency. To sum up, although the PCR template is less laborious and in theory would have facilitated recombination, for knock-in in *L. plantarum* WCFS1 it might be beneficial to use a circular donor repair template.

Electrotransformation is the most efficient tool for plasmid DNA uptake, yet the efficiency is affected by many factors including electroporation DNA amount (Wu et al., 2010). In an attempt to increase the transformation efficiency of CRISPR/Cas9 knock-in system I, various quantities of pSgRNA_KI_Cas9_RBD (Figure 3.9) were transformed into the *L. plantarum* WCFS1 already harbouring the pSIP_411_LpRec (Figure 3.8). An initial test in this thesis, showed a linear connection between increased plasmid quantity with the increased number of transformants (Figure 3.11). Thus, to increase knock-in efficiency, instead of 1 µg pSgRNA_KI_Cas9_RBD, 5 µg pSgRNA_KI_Cas9_RBD was transformed in CRISPR/Cas9 knock-in system I. Nevertheless, a higher plasmid amount did not result in a positive mutant. This might indicate that increased plasmid amount does not correlate with increased knock-in efficiency. This may be because the vector containing SpCas9 could be unstable, consequently transforming less DNA amount might result in highest transformation efficiency. In total, plasmid amounts ranging from 0.3 to 5 µg were transformed, but knock-ins were only successful when transforming 1 and 1.5 µg pSgRNA_KI_Cas9_RBD.

In *E. coli*, knock-in efficiency drops sharply with increased fragment sizes. Studies from Tong et al., (2021) showed efficient insertion of small fragments in *E. coli* (<10 bp), while insertions of a sequence with 97 bp dropped below 2%. After successful knock-in of RBD_DC downstream of the inducible promoter P_{sppA} (~800 bp) by the CRISPR/Cas9 knock-in system I, larger fragments were attempted to be knocked-in. RBD_DC downstream of the inducible promoter and the lipo-protein anchor (~1050), and RBD_DC downstream of the constitutive promoter P_{SlpA} (~1200 bp). By using these two inserts, the CRISPR/Cas9 knock-in

system I failed to achieve new knock-ins (Table 3.3). This might be due to unfavourable conditions for HDR due to insert size and chromosomal arrangement. HDR rates decrease as the distance of homology deviations from the centre increase (Yang et al., 2013). If the insert length is too long, the homologous arms on the donor repair template might not fit alongside the complementary sequence on the chromosome. The distance between the homologous arms and the donor repair template may be too far away. In addition, a long insert sequence must probably be curved in order to be incorporated in the genome since the sequence is inserted and not exchanged with a sequence from the genome. Possible optimalization to achieve knock-in of larger fragments might be knock-in by exchange of a gene, instead of solely an insert, as this might ease the putative chromosomal bending problem. In addition, the donor repair template could be constructed with longer homologous arms (>1kb) possibly enhancing HDR by providing a longer template for the recombineering. Another reason might be that putatively knock-ins of RBD downstream the lipo-protein anchor were unable to grow due to stress from anchoring of RBD into the cell membrane. As shown in Figure 3.16, where plasmid-based expression of RBD with the lipo-protein anchor significantly reduces growth of the recombinant strain. Lastly, the sgRNA can be exchanged. The bacterial chromosome is folded into a variety of conformations that are supercoiled and wound around proteins (Dame et al., 2019). Consequently, one could speculate that not all sites at the genome are easily accessible for knock-ins. By exchanging the sgRNA, the insertion sequence might fit better into a different site at the genome, which could slightly increase knock-in size. In conclusion, inserts >800 bp might be too large to be inserted into the genome of *L. plantarum* WCFS1 via HDR, at least by targeting the genome between *lp_2071-lp_2074* by sgRNA_KI (Table 2.2).

Interestingly, by using the pSgRNA_KI_1261_RBD_DC_Cas9 and pSgRNA_KI_SlpA_RBD_DC_Cas9 vectors (Table 3.1) in the CRISPR/Cas9 knock-in system I, more than one transformant appeared (Table 3.3). The appearance of more transformants might be because the SpCas9:sgRNA complex fails to eliminate the unedited cells due to an out-of-frame mutation in SpCas9 or sgRNA. If the SpCas9:sgRNA complex is unable to cleave the genome, elimination would be unsuccessful. It is not known whether the DSB mediates the HDR or if SpCas9 eliminates the cells after HDR. If DSB mediates HDR and the SpCas9:sgRNA nuclease complex is inactivated due to an out-of-frame mutation, RBD would not be inserted in the genome. Nevertheless, the pSgRNA_KI_SlpA_RBD_DC_Cas9 vector and the SpCas9 encoded from one of the *L. plantarum* WCFS1 transformant were sequenced.

However, the sequencing did not reveal out-of-frame mutations that would have been responsible for SpCas9 inactivation.

In an attempt to make a less laborious knock-in system and increase the knock-in efficiency, CRISPR/Cas9 knock-in system II was constructed (Figure 3.15). Although, consisting of analogous components system II was unsuccessful in achieving knock-ins. In CRISPR/Cas9 knock-in system I, with pSgRNA_KI_Cas9_RBD_DC (Figure 3.8), the SpCas9 and the sgRNA were expressed from the same plasmid. However, in system II the sgRNA and the SpCas9 were delivered on opposite vectors. The arrangement of system I seemed to be efficient at introducing DSBs, as only one transformant emerged, while system II seemed to be inefficient in introducing DSBs. This spatial location of sgRNA and SpCas9 in system I and II may reveal an importance in the physical aspect of the sgRNA:SpCas9 complex. The findings from system I and system II might indicate that the spatial position of sgRNA and SpCas9 is important, and that these components should be physically close to each other. This might be because the sgRNA:SpCas9 needs to physically find each other in order to assemble. The SpCas9 cannot introduce the desired on-target cleavage without the sgRNA. This might be part of the reason why CRISPR/Cas9 knock-in system II failed.

To sum up, CRISPR/Cas9 knock-in system I was successfully developed for knock-in of RBD in *L. plantarum* WCFS1. The constructed sgRNA and SpCas9 complex managed to induce a DSB at the targeted site between *lp_2071* and *lp_2074*. The two-plasmid construction of system I seems to be an efficient model to achieve DSBs. This could be debated because of the high elimination of unedited cells (only one colony emerged). However, system I was ineffective and unsuitable for knock-ins of larger fragments (>800 kb) possibly due to unfavourable bending of the insert in order to be incorporated at the target site. System II was constructed to be less laborious than system I in order to prevent additional cloning of the unstable *spCas9* gene, to increase transformation efficiency by transforming a smaller vector, and to be more effective by increased expression of SpCas9 by using the high-copy-number replicon Rep_{SH71}. Nonetheless, System II was unsuccessful to achieve knock-in due to unknown reasons. It might be speculated that the sgRNA and SpCas9 should be expressed from the same vector to facilitate the assembly of the sgRNA:SpCas9 complex to achieve a more efficient elimination of the unedited cells. Overall, the CRISPR/Cas9 knock-in efficiency in *L. plantarum* WCFS1 is at a low level, this might be attributed to low efficiency of the HDR even though pSIP411_lpRec (Table 3.1) was overexpressed.

4.2 Characterization of RBD expressed from the genome of *L. plantarum* WCFS1

Growth curve analysis of cytoplasmatic expression of RBD in the recombinant strains did not show a significantly reduced growth rate compared to the wildtype strain (Figure 3.16). The expression of RBD appears not to be toxic as RBD at an intracellular location does not significantly impair growth. This might be because RBD is a small protein, and the cell does not need to use energy to translocate the antigen. As shown, anchoring of plasmid-based expression of RBD significantly reduces cell growth. This might be because anchoring of RBD requires additional energy usage, which takes away the ATP necessary for regular cell growth.

Western blot analysis confirmed the production of RBD expressed from the genome (Figure 3.17). The analysis indicated that the produced RBD was significantly lower from genome integrated RBD, compared to plasmid encoded RBD. This is probably due to the multiple plasmid-copy-number per cell, compared to the one genomic copy number. The plasmids replicate autonomously from the bacterial chromosome and are usually present in several copies per cell (Friehs, 2004). The copy number for Rep256 is estimated to be around 10-15 (Pers. med. Geir Mathiesen), while the knock-in strain of RBD only has one gene inserted in the chromosome. Thus, by using plasmid-based expression of RBD, the gene dose is higher, which might lead to the observed higher production of RBD compared to the genomic expression of RBD.

To analyze the RBD protein production over time, samples were harvested at different time-points after induction (Figure 3.18). Expression seemed to be highest 3 hours after induction. Interestingly, expression from the genome is only visible until 4 hours past induction. Expression of RBD from the plasmid also diminish 4 hours post induction, but remains visible until 18 hours past induction, probably due to a higher gene dose which leads to more production of RBD. In compliance with both samples, it seems the expression system stops expressing RBD around 4 hours after induction. This might be because the expression of RBD is inducible and relies on the presence of the inducer pheromone. The pSIP system is based on the quorum sensing mechanisms of *L. lactis* (Eijsink et al., 1996; Sørvig et al., 2005). Consequently, when the concentration of inducer pheromone diminish, expression of RBD might stop. A decreased concentration of SppIP in the cultures might result from degradation of the pheromone.

The pSIP expression system has shown a clear dose-response effect for the SppIP concentration with optimum at about 40 ng/mL (Nguyen et al., 2015). Further characterization of expression

with western blot, did not show a gene dose expression pattern, unlike the pSIP expression system (Figure 3.19). This is probably due to the low expression of RBD, which make it difficult to detect the dose-response from the Western blot. In contrast to the western blot analysis, quantitative dose-response analysis of the knock-in strain with the fluorescent reporter gene mCherry revealed a dose-response effect, as expected (Figure 3.21). The dose-response tested with 0-25 ng/mL SppIP shows an increasing response to SppIP concentration up to 25 ng/mL, although the expression is significantly lower than mCherry expression from plasmid (data not shown). The expression was shown to be very sensitive. Addition of 1 ng/mL SppIP initiated expression of mCherry, thus addition of >1 ng/mL inducer pheromone may not be necessary.

In summary, analysis of genomic expression indicated low expression. Genomic expression under the P_{sppA} promoter initiated by structural genes from the pEV might not be optimal for genomic expression. To solve the low expression, a pEV with the high copy-number replicon Rep_{SH71} might increase the number of structural genes to increase transcription of the target gene. Other options might be to exchange the P_{sppA} promoter.

4.3 Concluding remarks and future prospect

This study presents a proof-of-concept for CRISPR/Cas9 knock-in in *L. plantarum* WCFS1. The knock-in is a scarless and marker less approach which could potentially one day outcompete previously used genome editing methods that leaves a scar and rely on selection markers. Nevertheless, several challenges must be addressed before CRISPR/Cas9 genome editing can be efficiently used in bacteria. In this study, the developed CRISPR/Cas9 knock-in systems have encountered many problems and is still laborious and inefficient. In system II there was a deficiency in the elimination of unedited cells which was speculated to be due to inefficient assembly of the sgRNA:SpCas9. A similar decrease in DSB occurred in system I after additional cloning of the pSgRNA_KI_RBD_DC_Cas9 vector (Table 3.1). Although the gene encoding SpCas9 was free from mutations, out-of-frame mutations in the sgRNA could be a reason for the decreased elimination. In this thesis, it is speculated that the low frequency of knock-ins is due to HDR inefficiency in *L. plantarum* WCFS1 even when overexpression the homologous *lp_0640-lp_0642* genes. Consequently, finding a host where the HDR is natively more effective could potentially increase the knock-in frequency. Huang et al., (2019) showed that RecE/T-assisted HDR in *Lactobacillus brevis* ATCC367 increased editing frequencies six- to tenfold compared to CRISPR/Cas9 editing in *L. plantarum* WCFS1. Consequently, further knock-in experiments could be attempted in other strains e.g., *L. brevis* ATCC367.

The main goal was to insert the RBD_DC into the genome of *L. plantarum* WCFS1 with a constitutive expression of RBD and to anchor the antigen to the cell membrane. The anchoring of the antigen to the cell membrane could have offered protection from the mucosal milieu (Michon et al., 2016). In addition, display of the antigen on the cell membrane and the DC-specific peptide downstream of RBD might increase specific affinity to the dendritic cells, to provoke a stronger immune response (Cohn & Delamarre, 2014). This study managed to insert RBD_DC fused downstream of the inducible promoter P_{sppA} into the genome of *L. plantarum* WCFS1. However, the inducible promoter is dependent on structural genes, *sppR* and *sppK*, from the pSIP system in order to express the target gene. In addition, expression is dependent on activation by the inducer pheromone, SppIP. Characterization of cytoplasmatic RBD expression indicated low expression from the genome, which could possibly be too low to generate an immune response (Billeskov et al., 2019). Still, optimalization of the promoter, the display of the antigen, the DC-peptide sequence, or the adjuvant effect of the *L. plantarum* in accumulation might be enough to provoke immunity against SARS-CoV-2. In conclusion, the CRISPR/Cas9 knock-in system should be further optimized to knock-in a constitutive promoter and the *lp_1261* gene. Since the current CRISPR/Cas9 knock-in system has the ability to precisely knock-in inserts less than 800 bp, the system can be used to individually insert the constitutive promoter and lipo-protein anchor at the genome in front of the RBD in the knock-in strain.

5 References

Abdullah, Jiang, Z., Hong, X., Zhang, S., Yao, R., & Xiao, Y. (2020). CRISPR base editing and prime editing: DSB and template-free editing systems for bacteria and plants. *Synthetic and Systems Biotechnology*, *5*(4), 277–292. https://doi.org/10.1016/J.SYNBIO.2020.08.003

Adli, M. (2018). The CRISPR tool kit for genome editing and beyond. In *Nature Communications* (Vol. 9, Issue 1). Nature Publishing Group. https://doi.org/10.1038/s41467-018-04252-2

Amarh, V., & Arthur, P. K. (2019). DNA double-strand break formation and repair as targets for novel antibiotic combination chemotherapy. *Future Science OA*, *5*(8). https://doi.org/10.2144/FSOA-2019-0034

Arroyo-Olarte, R. D., Bravo Rodríguez, R., & Morales-Ríos, E. (2021a). Genome Editing in Bacteria: CRISPR-Cas and Beyond. *Microorganisms*, *9*(4). https://doi.org/10.3390/MICROORGANISMS9040844

Aukrust, T. W., Brurberg, M. B., & Nes, I. F. (1995). Transformation of *Lactobacillus* by electroporation. *Methods in Molecular Biology (Clifton, N.J.)*, *47*, 201–208. https://doi.org/10.1385/0-89603-310-4:201

Barrangou, R., Fremaux, C., Deveau, H., Richards, M., Boyaval, P., Moineau, S., Romero, D. A., & Horvath, P. (2007). CRISPR provides acquired resistance against viruses in prokaryotes. *Science*, *315*(5819), 1709–1712. https://doi.org/10.1126/SCIENCE.1138140/SUPPL_FILE/BARRANGOU.SOM.PDF

Berg, K. H., Biørnstad, T. J., Straume, D., & Håvarstein, L. S. (2011). Peptide-Regulated Gene Depletion System Developed for Use in *Streptococcus pneumoniae*. *Journal of Bacteriology*, *193*(19), 5207. https://doi.org/10.1128/JB.05170-11

Billeskov, R., Beikzadeh, B., & Berzofsky, J. A. (2019). The effect of antigen dose on T cell-targeting vaccine outcome. *Human Vaccines & Immunotherapeutics*, *15*(2), 407. https://doi.org/10.1080/21645515.2018.1527496

Carr, F. J., Maida, N., & Chill, D. (2002). The Lactic Acid Bacteria: A Literature Survey. *Critical Reviews in Microbiology*, *28*(4), 281–370. https://doi.org/10.1080/1040-840291046759

Ceasar, S. A., Rajan, V., Prykhozhij, S. v., Berman, J. N., & Ignacimuthu, S. (2016). Insert, remove or replace: A highly advanced genome editing system using CRISPR/Cas9. *Biochimica et Biophysica Acta (BBA) - Molecular Cell Research*, *1863*(9), 2333–2344. https://doi.org/10.1016/J.BBAMCR.2016.06.009

Choudhury, A., Fenster, J. A., Fankhauser, R. G., Kaar, J. L., Tenaillon, O., & Gill, R. T. (2020). CRISPR/Cas9 recombineering-mediated deep mutational scanning of essential genes in Escherichia coli. *Molecular Systems Biology*, *16*(3), e9265. https://doi.org/10.15252/MSB.20199265

Cohn, L., & Delamarre, L. (2014). Dendritic cell-targeted vaccines. *Frontiers in Immunology*, *5*(MAY), 255. https://doi.org/10.3389/FIMMU.2014.00255/BIBTEX

Cui, L., & Bikard, D. (2016). Consequences of Cas9 cleavage in the chromosome of *Escherichia coli*. *Nucleic Acids Research*, *44*(9), 4243–4251. https://doi.org/10.1093/NAR/GKW223

Dalvie, N. C., Rodriguez-Aponte, S. A., Hartwell, B. L., Tostanoski, L. H., Biedermann, A. M., Crowell, L. E., Kaur, K., Kumru, O. S., Carter, L., Yu, J., Chang, A., McMahan, K., Courant, T., Lebas, C., Lemnios, A. A., Rodrigues, K. A., Silva, M., Johnston, R. S., Naranjo, C. A., … Love, J. C. (2021). Engineered SARS-CoV-2 receptor binding domain improves manufacturability in yeast and immunogenicity in mice. *Proceedings of the National Academy of Sciences of the United States of America*, *118*(38). https://doi.org/10.1073/PNAS.2106845118/SUPPL_FILE/PNAS.2106845118.SAPP.PDF

Dame, R. T., Rashid, F. Z. M., & Grainger, D. C. (2019). Chromosome organization in bacteria: mechanistic insights into genome structure and function. *Nature Reviews Genetics 2019 21:4*, *21*(4), 227–242. https://doi.org/10.1038/s41576-019-0185-4

Dhar, J., Samanta, J., & Kochhar, R. (2020). Corona Virus Disease-19 pandemic: The gastroenterologists' perspective. *Indian Journal of Gastroenterology 2020 39:3*, *39*(3), 220–231. https://doi.org/10.1007/S12664-020-01075-2

Doudna, J. A., & Charpentier, E. (2014). The new frontier of genome engineering with CRISPR-Cas9. In *Science* (Vol. 346, Issue 6213). American Association for the Advancement of Science. https://doi.org/10.1126/science.1258096

Eijsink, V. G. H., Brurberg, M. B., Middelhoven, P. H., & Nes, I. F. (1996). Induction of bacteriocin production in *Lactobacillus* sake by a secreted peptide. *Journal of Bacteriology*, *178*(8), 2232–2237. https://doi.org/10.1128/JB.178.8.2232-2237.1996

Fredriksen, L., Kleiveland, C. R., Olsen Hult, L. T., Lea, T., Nygaard, C. S., Eijsink, V. G. H., & Mathiesen, G. (2012a). Surface display of N-terminally anchored invasin by Lactobacillus plantarum activates NF-κB in monocytes. *Applied and Environmental Microbiology*, *78*(16), 5864–5871. https://doi.org/10.1128/AEM.01227-12

Gareau, M. G., Sherman, P. M., & Walker, W. A. (2010). Probiotics and the gut microbiota in intestinal health and disease. *Nature Reviews Gastroenterology & Hepatology 2010 7:9*, *7*(9), 503–514. https://doi.org/10.1038/nrgastro.2010.117

Ghavami, S., & Pandi, A. (2021). CRISPR interference and its applications. *Progress in Molecular Biology and Translational Science*, *180*, 123–140. https://doi.org/10.1016/BS.PMBTS.2021.01.007

Goldsmith, M., Kiss, C., Bradbury, A. R. M., & Tawfik, D. S. (2007). Avoiding and controlling double transformation artifacts. *Protein Engineering, Design and Selection*, *20*(7), 315–318. https://doi.org/10.1093/PROTEIN/GZM026

Goldstein, E. J. C., Tyrrell, K. L., & Citron, D. M. (2015). *Lactobacillus* Species: Taxonomic Complexity and Controversial Susceptibilities. *Clinical Infectious Diseases*, *60*(suppl_2), S98–S107. https://doi.org/10.1093/CID/CIV072

Guo, J., Wang, T., Guan, C., Liu, B., Luo, C., Xie, Z., Zhang, C., & Xing, X. H. (2018). Improved sgRNA design in bacteria via genome-wide activity profiling. *Nucleic Acids Research*, *46*(14), 7052. https://doi.org/10.1093/NAR/GKY572

Hammes, W. P., & Tichaczek, P. S. (1994). ef N elh e] The potential of lactic acid bacteria for the production of safe and wholesome food. In *Z Lebensm Unters Forsch* (Vol. 198).

Hidalgo-Cantabrana, C., Goh, Y. J., Pan, M., Sanozky-Dawes, R., & Barrangou, R. (2019). Genome editing using the endogenous type I CRISPR-Cas system in *Lactobacillus* crispatus. *Proceedings of the National Academy of Sciences of the United States of America*, *116*(32), 15774–15783. https://doi.org/10.1073/PNAS.1905421116/SUPPL_FILE/PNAS.1905421116.SAPP.PDF

Hsu, P. D., Lander, E. S., & Zhang, F. (2014). Development and applications of CRISPR-Cas9 for genome engineering. *Cell*, *157*(6), 1262–1278. https://doi.org/10.1016/J.CELL.2014.05.010

Huang, H., Song, X., & Yang, S. (2019). Development of a RecE/T-Assisted CRISPR–Cas9 Toolbox for *Lactobacillus*. *Biotechnology Journal*, *14*(7), 1800690. https://doi.org/10.1002/biot.201800690

Jiang, Y., Qian, F., Yang, J., Liu, Y., Dong, F., Xu, C., Sun, B., Chen, B., Xu, X., Li, Y., Wang, R., & Yang, S. (2017). CRISPR-Cpf1 assisted genome editing of Corynebacterium glutamicum. *Nature Communications*, *8*. https://doi.org/10.1038/NCOMMS15179

Jinek, M., Chylinski, K., Fonfara, I., Hauer, M., Doudna, J. A., & Charpentier, E. (2012). A programmable dual-RNA-guided DNA endonuclease in adaptive bacterial immunity. *Science*, *337*(6096), 816–821. https://doi.org/10.1126/science.1225829

Kandler, O. (1983). Carbohydrate metabolism in lactic acid bacteria. *An Tonie van Leeuwenhoek*, *49*, 209–224.

Klaenhammer, T. R., Altermann, E., Pfeiler, E., Buck, B. L., Goh, Y. J., O'Flaherty, S., Barrangou, R., & Duong, T. (2008). Functional genomics of probiotic *Lactobacilli*. *Journal of Clinical Gastroenterology*, *42 Suppl 3 Pt 2*. https://doi.org/10.1097/MCG.0B013E31817DA140

Kleerebezem, M., Boekhorst, J., Van Kranenburg, R., Molenaar, D., Kuipers, O. P., Leer, R., Tarchini, R., Peters, S. A., Sandbrink, H. M., Fiers, M. W. E. J., Stiekema, W., Klein Lankhorst, R. M., Bron, P. A., Hoffer, S. M., Nierop Groot, M. N., Kerkhoven, R., De Vries, M., Ursing, B., De Vos, W. M., & Siezen, R. J. (2003). Complete genome sequence of *Lactobacillus plantarum* WCFS1. *Proceedings of the National Academy of Sciences of the United States of America*, *100*(4), 1990–1995. https://doi.org/10.1073/PNAS.0337704100/ASSET/4CBF5592-3686-48CB-B1EF-D9D451ACA4EA/ASSETS/GRAPHIC/PQ0337704002.JPEG

Kleerebezem, M., Hols, P., Bernard, E., Rolain, T., Zhou, M., Siezen, R. J., & Bron, P. A. (2010). The extracellular biology of the lactobacilli. *FEMS Microbiology Reviews*, *34*(2), 199–230. https://doi.org/10.1111/J.1574-6976.2009.00208.X

König, H., & Fröhlich, J. (2009). Lactic Acid Bacteria. *Biology of Microorganisms on Grapes, in Must and in Wine*, 3–29. https://doi.org/10.1007/978-3-540-85463-0_1

Kuczkowska, K., Kleiveland, C. R., Minic, R., Moen, L. F., Øverland, L., Tjåland, R., Carlsen, H., Lea, T., Mathiesen, G., & Eijsink, V. G. H. (2016). Immunogenic Properties of Lactobacillus plantarum Producing Surface-Displayed *Mycobacterium tuberculosis* Antigens. *Applied and Environmental Microbiology*, *83*(2). https://doi.org/10.1128/AEM.02782-16

Kuipers, O. P., De Ruyter, P. G. G. A., Kleerebezem, M., & De Vos, W. M. (1997). Controlled overproduction of proteins by lactic acid bacteria. *Trends in Biotechnology*, *15*(4), 135–140. https://doi.org/10.1016/S0167-7799(97)01029-9

Kwok, L. (2014). Lactic Acid Bacteria and the Human Gastrointestinal Tract. *Lactic Acid Bacteria: Fundamentals and Practice*, 375–441. https://doi.org/10.1007/978-94-017-8841-0_6

Leenay, R. T., & Beisel, C. L. (2017). Deciphering, Communicating, and Engineering the CRISPR PAM. *Journal of Molecular Biology*, *429*(2), 177–191. https://doi.org/10.1016/J.JMB.2016.11.024

Leenay, R. T., Vento, J. M., Shah, M., Martino, M. E., Leulier, F., & Beisel, C. L. (2019). Genome Editing with CRISPR-Cas9 in *Lactobacillus plantarum* Revealed That Editing Outcomes Can Vary Across Strains and Between Methods. *Biotechnology Journal*, *14*(3). https://doi.org/10.1002/biot.201700583

Li, X. T., Thomason, L. C., Sawitzke, J. A., Costantino, N., & Court, D. L. (2013). Positive and negative selection using the tetA-sacB cassette: recombineering and P1 transduction in Escherichia coli. *Nucleic Acids Research*, *41*(22). https://doi.org/10.1093/NAR/GKT1075

Lieber, M. R. (2010). The Mechanism of Double-Strand DNA Break Repair by the Nonhomologous DNA End Joining Pathway. *Annual Review of Biochemistry*, *79*, 181. https://doi.org/10.1146/ANNUREV.BIOCHEM.052308.093131

Liu, P., Jenkins, N. A., & Copeland, N. G. (2003). A highly efficient recombineering-based method for generating conditional knockout mutations. *Genome Research*, *13*(3), 476–484. https://doi.org/10.1101/GR.749203

Lone, B. A., Karna, S. K. L., Ahmad, F., Shahi, N., & Pokharel, Y. R. (2018). CRISPR/Cas9 System: A bacterial tailor for genomic engineering. In *Genetics Research International* (Vol. 2018). Hindawi Limited. https://doi.org/10.1155/2018/3797214

Lozupone, C. A., Stombaugh, J. I., Gordon, J. I., Jansson, J. K., & Knight, R. (2012). Diversity, stability and resilience of the human gut microbiota. *Nature*, *489*(7415), 220. https://doi.org/10.1038/NATURE11550

Makarova, K., Slesarev, A., Wolf, Y., Sorokin, A., Mirkin, B., Koonin, E., Pavlov, A., Pavlova, N., Karamychev, V., Polouchine, M., Shakhova, V., Grigoriev, I., Lou, Y., Rohksar, D., Lucas, S., Huang, K., Goodstein, D. M., Hawkins, T., Plengvidhya, V., … Mills, D. (2006). Comparative genomics of the lactic acid bacteria. *Proceedings of the National Academy of Sciences of the United States of America*, *103*(42), 15611–15616. https://doi.org/10.1073/PNAS.0607117103/SUPPL_FILE/07117TABLE1.DOC

Markowiak, P., & Ślizewska, K. (2017). Effects of Probiotics, Prebiotics, and Synbiotics on Human Health. *Nutrients 2017, Vol. 9, Page 1021*, *9*(9), 1021. https://doi.org/10.3390/NU9091021

Mathiesen, G., Sørvig, E., Blatny, J., Naterstad, K., Axelsson, L., & Eijsink, V. G. H. (2004). High-level gene expression in *Lactobacillus plantarum* using a pheromone-regulated bacteriocin promoter. *Letters in Applied Microbiology*, *39*(2), 137–143. https://doi.org/10.1111/J.1472-765X.2004.01551.X

Mathiesen, G., Sveen, A., Brurberg, M. B., Fredriksen, L., Axelsson, L., & Eijsink, V. G. H. (2009). Genome-wide analysis of signal peptide functionality in Lactobacillus plantarum WCFS1. *BMC Genomics*, *10*(1), 425. https://doi.org/10.1186/1471-2164-10-425/TABLES/4

Medina, M., Vintiñi, E., Villena, J., Raya, R., & Alvarez, S. (2010). *Lactococcus lactis* as an adjuvant and delivery vehicle of antigens against pneumococcal respiratory infections. *Bioengineered Bugs*, *1*(5), 313. https://doi.org/10.4161/BBUG.1.5.12086

Michon, C., Langella, P., Eijsink, V. G. H., Mathiesen, G., & Chatel, J. M. (2016). Display of recombinant proteins at the surface of lactic acid bacteria: strategies and applications. *Microbial Cell Factories 2016 15:1*, *15*(1), 1–16. https://doi.org/10.1186/S12934-016-0468-9

Milani, C., Duranti, S., Bottacini, F., Casey, E., Turroni, F., Mahony, J., Belzer, C., Delgado Palacio, S., Arboleya Montes, S., Mancabelli, L., Lugli, G. A., Rodriguez, J. M., Bode, L., de Vos, W., Gueimonde, M., Margolles, A., van Sinderen, D., & Ventura, M. (2017). The First Microbial Colonizers of the Human Gut: Composition, Activities, and Health Implications of the Infant Gut Microbiota. *Microbiology and Molecular Biology Reviews : MMBR*, *81*(4). https://doi.org/10.1128/MMBR.00036-17

Misra, C. S., Bindal, G., Sodani, M., Wadhawan, S., Kulkarni, S., Gautam, S., Mukhopadhyaya, R., & Rath, D. (2019). Determination of Cas9/dCas9 associated toxicity in microbes. *BioRxiv*, 848135. https://doi.org/10.1101/848135

Mohamadzadeh, M., Olson, S., Kalina, W. V., Ruthel, G., Demmin, G. L., Warfield, K. L., Bavari, S., & Klaenhammer, T. R. (2005). *Lactobacilli* active human dendritic cells that skew T cells toward T helper 1 polarization. *Proceedings of the National Academy of Sciences of the United States of America*, *102*(8), 2880–2885. https://doi.org/10.1073/pnas.0500098102

Mojica, F. J. M., Díez-Villaseñor, C., García-Martínez, J., & Soria, E. (2005). Intervening sequences of regularly spaced prokaryotic repeats derive from foreign genetic elements. *Journal of Molecular Evolution*, *60*(2), 174–182. https://doi.org/10.1007/S00239-004-0046-3/TABLES/6

Morel, P. A., & Butterfield, L. H. (2015). Dendritic cell control of immune responses. *Frontiers in Immunology*, *6*(FEB), 42. https://doi.org/10.3389/FIMMU.2015.00042/BIBTEX

Mosberg, J. A., Lajoie, M. J., & Church, G. M. (2010). Lambda Red Recombineering in Escherichia coli Occurs Through a Fully Single-Stranded Intermediate. *Genetics*, *186*(3), 791–799. https://doi.org/10.1534/GENETICS.110.120782

Neutra, M. R., & Kozlowski, P. A. (2006). Mucosal vaccines: the promise and the challenge. *Nature Reviews Immunology 2006 6:2*, *6*(2), 148–158. https://doi.org/10.1038/nri1777

Oozeer, R., Leplingard, A., Mater, D. D. G., Mogenet, A., Michelin, R., Seksek, I., Marteau, P., Doré, J., Bresson, J. L., & Corthier, G. (2006). Survival of Lactobacillus casei in the human digestive tract after consumption of fermented milk. *Applied and Environmental Microbiology*, *72*(8), 5615–5617. https://doi.org/10.1128/AEM.00722-06

Paix, A., Folkmann, A., Goldman, D. H., Kulaga, H., Grzelak, M. J., Rasoloson, D., Paidemarry, S., Green, R., Reed, R. R., & Seydoux, G. (2017). Precision genome editing using synthesis-dependent repair of Cas9-induced DNA breaks. *Proceedings of the National Academy of Sciences of the United States of America*, *114*(50), E10745–E10754. https://doi.org/10.1073/PNAS.1711979114/SUPPL_FILE/PNAS.1711979114.SAPP.PDF

Paques, F., & Duchateau, P. (2007). Meganucleases and DNA Double-Strand Break-Induced Recombination: Perspectives for Gene Therapy. *Current Gene Therapy*, *7*(1), 49–66. https://doi.org/10.2174/156652307779940216

Potter, H., & Heller, R. (2003). Transfection by Electroporation. *Current Protocols in Molecular Biology / Edited by Frederick M. Ausubel ... [et Al.]*, *CHAPTER*(SUPPL. 92), Unit. https://doi.org/10.1002/0471142727.MB0903S62

Ramachandran, G., & Bikard, D. (2019). Editing the microbiome the CRISPR way. In *Philosophical Transactions of the Royal Society B: Biological Sciences* (Vol. 374, Issue 1772). Royal Society Publishing. https://doi.org/10.1098/rstb.2018.0103

Rath, D., Amlinger, L., Rath, A., & Lundgren, M. (2015). The CRISPR-Cas immune system: Biology, mechanisms and applications. In *Biochimie* (Vol. 117, pp. 119–128). Elsevier B.V. https://doi.org/10.1016/j.biochi.2015.03.025

Rud, I., Jensen, P. R., Naterstad, K., & Axelsson, L. (2006). A synthetic promoter library for constitutive gene expression in *Lactobacillus plantarum*. *Microbiology*, *152*(4), 1011–1019. https://doi.org/10.1099/MIC.0.28599-0/CITE/REFWORKS

Ruiz-Barba, J. L., Piard, J. C., & Jiménez-Díaz, R. (1991). Plasmid profiles and curing of plasmids in Lactobacillus plantarum strains isolated from green olive fermentations. *Journal of Applied Bacteriology*, *71*(5), 417–421. https://doi.org/10.1111/J.1365-2672.1991.TB03810.X

Sander, J. D., & Keith Joung, J. (2014). r e v i e w CriSPr-Cas systems for editing, regulating and targeting genomes. *Nature Biotechnology*, *32*(4). https://doi.org/10.1038/nbt.2842

Schneewind, O., & Missiakas, D. (2014). Sec-Secretion and Sortase-Mediated Anchoring of Proteins in Gram-Postive Bacteria. *Biochimica et Biophysica Acta*, *1843*(8), 1687. https://doi.org/10.1016/J.BBAMCR.2013.11.009

Sharda, M., Badrinarayanan, A., & Seshasayee, A. S. N. (2020). Evolutionary and Comparative Analysis of Bacterial Nonhomologous End Joining Repair. *Genome Biology and Evolution*, *12*(12), 2450–2466. https://doi.org/10.1093/GBE/EVAA223

Song, F., & Stieger, K. (2017). Optimizing the DNA Donor Template for Homology-Directed Repair of Double-Strand Breaks. *Molecular Therapy - Nucleic Acids*, *7*, 53–60. https://doi.org/10.1016/J.OMTN.2017.02.006

Sørvig, E., Grönqvist, S., Naterstad, K., Mathiesen, G., Eijsink, V. G. H., & Axelsson, L. (2003). Construction of vectors for inducible gene expression in Lactobacillus sakei and L plantarum. *FEMS Microbiology Letters*, *229*(1), 119–126. https://doi.org/10.1016/S0378-1097(03)00798-5

Sørvig, E., Mathiesen, G., Naterstad, K., Eijsink, V. G. H., & Axelsson, L. (2005a). High-level, inducible gene expression in Lactobacillus sakei and Lactobacillus plantarum using versatile expression vectors. *Microbiology*, *151*(7), 2439–2449. https://doi.org/10.1099/MIC.0.28084-0/CITE/REFWORKS

Sun, Z., Yu, J., Dan, T., Zhang, W., & Zhang, H. (2014). Phylogenesis and Evolution of Lactic Acid Bacteria. *Lactic Acid Bacteria: Fundamentals and Practice*, 1–101. https://doi.org/10.1007/978-94-017-8841-0_1

Tauer, C., Heinl, S., Egger, E., Heiss, S., & Grabherr, R. (2014). Tuning constitutive recombinant gene expression in *Lactobacillus plantarum*. *Microbial Cell Factories*, *13*(1), 1–11. https://doi.org/10.1186/S12934-014-0150-Z/FIGURES/9

Tjalsma, H., Antelmann, H., Jongbloed, J. D. H., Braun, P. G., Darmon, E., Dorenbos, R., Dubois, J.-Y. F., Westers, H., Zanen, G., Quax, W. J., Kuipers, O. P., Bron, S., Hecker, M., & van Dijl, J. M. (2004). Proteomics of Protein Secretion by *Bacillus subtilis* : Separating the “Secrets” of the Secretome . *Microbiology and Molecular Biology Reviews*, *68*(2), 207–233. https://doi.org/10.1128/MMBR.68.2.207-233.2004/ASSET/0BAF08DC-0A9C-4563-A1D7-952B78448BE7/ASSETS/GRAPHIC/ZMR0020420490007.JPEG

Tong, Y., Jørgensen, T. S., Whitford, C. M., Weber, T., & Lee, S. Y. (2021). A versatile genetic engineering toolkit for E. coli based on CRISPR-prime editing. *Nature Communications 2021 12:1*, *12*(1), 1–11. https://doi.org/10.1038/s41467-021-25541-3

Trondsen, L. (2021). *Production and surface anchoring of Mycobacterium tuberculosis and SARS-CoV-2 antigens in Lactobacillus plantarum*.

Vento, J. M., Crook, N., & Beisel, C. L. (2019). Barriers to genome editing with CRISPR in bacteria. *Journal of Industrial Microbiology and Biotechnology*, *46*(9–10), 1327–1341. https://doi.org/10.1007/S10295-019-02195-1/FIGURES/3

Verdú, C., Sanchez, E., Ortega, C., Hidalgo, A., Berenguer, J., & Mencía, M. (2019). A Modular Vector Toolkit with a Tailored Set of Thermosensors to Regulate Gene Expression in Thermus thermophilus. *ACS Omega*, *4*(11), 14626. https://doi.org/10.1021/ACSOMEGA.9B02107/SUPPL_FILE/AO9B02107_SI_001.PDF

Villena, J., Li, C., Vizoso-Pinto, M. G., Sacur, J., Ren, L., & Kitazawa, H. (2021). *Lactiplantibacillus plantarum* as a Potential Adjuvant and Delivery System for the Development of SARS-CoV-2 Oral Vaccines. *Microorganisms 2021, Vol. 9, Page 683*, *9*(4), 683. https://doi.org/10.3390/MICROORGANISMS9040683

Wiig, S. B. (2020). *Constitutive expression and anchoring of Mycobacterium tuberculosis antigens in Lactobacillus plantarum*.

Wiull, K. (2018). *Implementation of a two-plasmid CRISPR/Cas9 system in Lactobacillus plantarum: A new approach in the development of a novel vaccine against Mycobacterium tuberculosis*.

Wu, N., Matand, K., Kebede, B., Acquaah, G., & Williams, S. (2010). Enhancing DNA electrotransformation efficiency in *Escherichia coli* DH10B electrocompetent cells. *Electronic Journal of Biotechnology*, *13*(5), 0–0. https://doi.org/10.2225/VOL13-ISSUE5-FULLTEXT-11

Xiong, L., Zeng, Y., Tang, R. Q., Alper, H. S., Bai, F. W., & Zhao, X. Q. (2018). Condition-specific promoter activities in Saccharomyces cerevisiae. *Microbial Cell Factories*, *17*(1), 58. https://doi.org/10.1186/S12934-018-0899-6

Xu, H., Zhong, L., Deng, J., Peng, J., Dan, H., Zeng, X., Li, T., & Chen, Q. (2020). High expression of ACE2 receptor of 2019-nCoV on the epithelial cells of oral mucosa.

International Journal of Oral Science 2020 12:1, 12(1), 1–5. https://doi.org/10.1038/s41368-020-0074-x

Yang, L., Guell, M., Byrne, S., Yang, J. L., de Los Angeles, A., Mali, P., Aach, J., Kim-Kiselak, C., Briggs, A. W., Rios, X., Huang, P. Y., Daley, G., & Church, G. (2013). Optimization of scarless human stem cell genome editing. *Nucleic Acids Research*, *41*(19), 9049–9061. https://doi.org/10.1093/NAR/GKT555

Yoo, K. W., Yadav, M. K., Song, Q., Atala, A., & Lu, B. (2022). Targeting DNA polymerase to DNA double-strand breaks reduces DNA deletion size and increases templated insertions generated by CRISPR/Cas9. *Nucleic Acids Research*, *50*(7), 3944–3957. https://doi.org/10.1093/NAR/GKAC186

Zhang, D., Hussain, A., Manghwar, H., Xie, K., Xie, S., Zhao, S., Larkin, R. M., Qing, P., Jin, S., & Ding, F. (2020). Genome editing with the CRISPR-Cas system: an art, ethics and global regulatory perspective. In *Plant Biotechnology Journal* (Vol. 18, Issue 8, pp. 1651–1669). Blackwell Publishing Ltd. https://doi.org/10.1111/pbi.13383

Zhang, S., Guo, F., Yan, W., Dai, Z., Dong, W., Zhou, J., Zhang, W., Xin, F., & Jiang, M. (2020). Recent Advances of CRISPR/Cas9-Based Genetic Engineering and Transcriptional Regulation in Industrial Biology. *Frontiers in Bioengineering and Biotechnology*, *7*, 459. https://doi.org/10.3389/FBIOE.2019.00459/BIBTEX

Zhang, W., & Zhang, H. (2014). Genomics of Lactic Acid Bacteria. *Lactic Acid Bacteria: Fundamentals and Practice*, 205–247. https://doi.org/10.1007/978-94-017-8841-0_3

Zhang, Z. T., Jiménez-Bonilla, P., Seo, S. O., Lu, T., Jin, Y. S., Blaschek, H. P., & Wang, Y. (2018). Bacterial Genome Editing with CRISPR-Cas9: Taking *Clostridium beijerinckii* as an Example. *Methods in Molecular Biology (Clifton, N.J.)*, *1772*, 297–325. https://doi.org/10.1007/978-1-4939-7795-6_17

Zhao, D., Yuan, S., Xiong, B., Sun, H., Ye, L., Li, J., Zhang, X., & Bi, C. (2016). Development of a fast and easy method for *Escherichia coli* genome editing with CRISPR/Cas9. *Microbial Cell Factories*, *15*(1), 1–9. https://doi.org/10.1186/S12934-016-0605-5/TABLES/4

Zhao, J., Fang, H., & Zhang, D. (2020). Expanding application of CRISPR-Cas9 system in microorganisms. *Synthetic and Systems Biotechnology*, *5*(4), 269–276. https://doi.org/10.1016/J.SYNBIO.2020.08.001

Zhou, P., Yang, X.-L., Wang, X.-G., Hu, B., Zhang, L., Zhang, W., Si, H.-R., Zhu, Y., Li, B., Huang, C.-L., Chen, H.-D., Chen, J., Luo, Y., Guo, H., Jiang, R.-D., Liu, M.-Q., Chen, Y., Shen, X.-R., Wang, X., … Shi, Z.-L. (2020). A pneumonia outbreak associated with a new coronavirus of probable bat origin. *Nature 2020 579:7798*, *579*(7798), 270–273. https://doi.org/10.1038/s41586-020-2012-7

6 Appendix

A-1 Construction of the pSgRNA_KI_1261_RBD_DC_Cas9 and pSgRNA_KI_SlpA_RBD_DC_Cas9 vector for the CRISPR/Cas9 knock-in system I

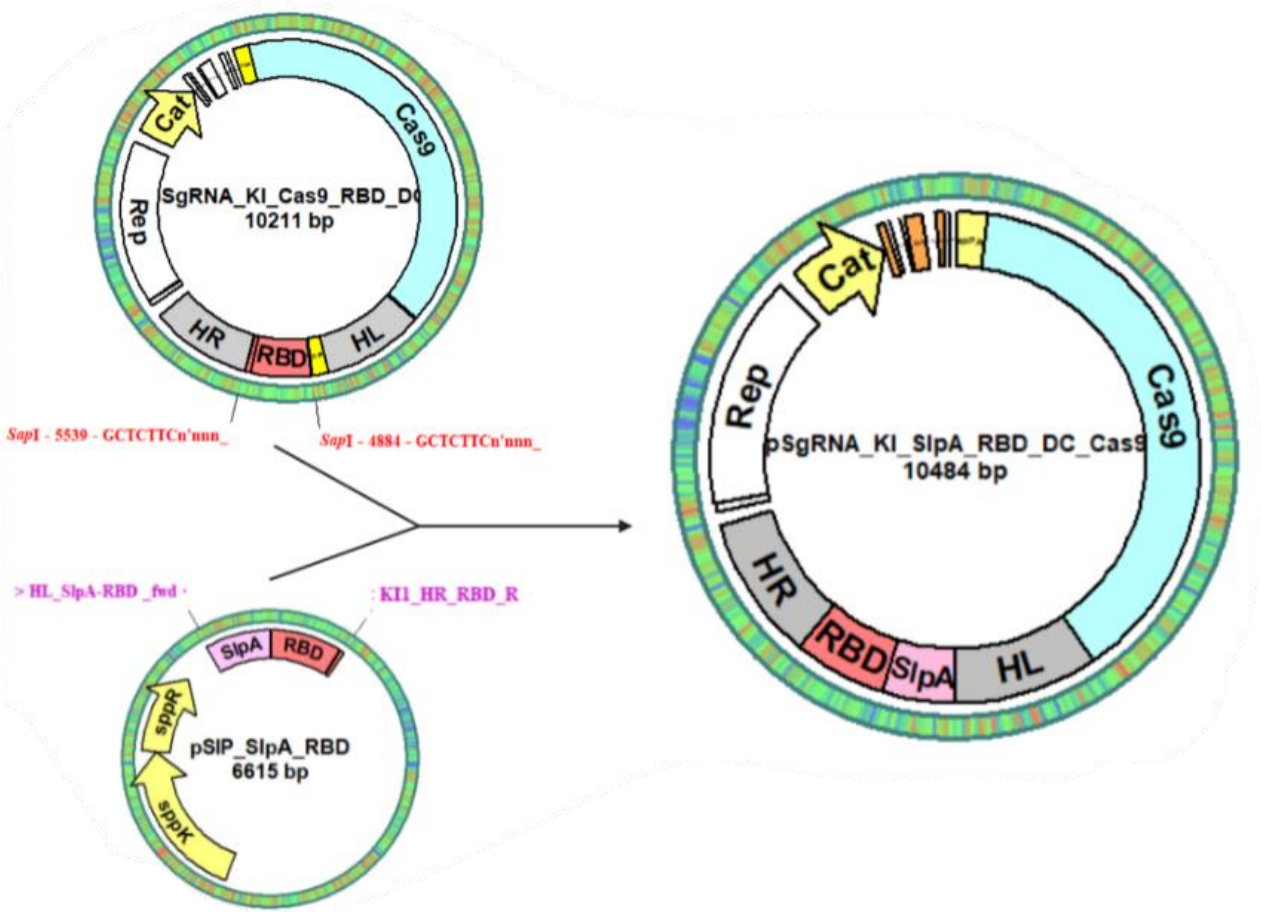

Figure A-1. Strategy for constructing the CRISP/Cas9 vectors for system I. pSgRNA_KI_Cas9_RBD_DC was digested with restriction enzyme SapI to remove the knock-in sequence. The insertion sequence was exchanged by the sequence for lipoprotein anchored RBD_DC and constitutive promoter P_{SlpA} fused upstream of RBD_DC. For PCR amplification of the insertion sequence, pSIP_RBD_DC, pLp1261_RBD_DC and pSIP_SlpA_RBD_DC were used as templates. For construction of pSgRNA_KI_RBD_DC_Cas9 and pSgRNA_KI_1261_RBD_DC_Cas9 In-Fusion primer Psppa_RBD_fwd and KI1_HR_RBD_R were used. For construction of pSgRNA_KI__SlpA_RBD_DC_Cas9, as shown in the figure, In-Fusion primer HL_SlpA-RBD _fwd and KI1_HR_RBD_R were used.

Norges miljø- og biovitenskapelige universitet
Noregs miljø- og biovitskapelege universitet
Norwegian University of Life Sciences

Postboks 5003
NO-1432 Ås
Norway